Southeastern Geology: Volume 47, No. 3 August 2010

Editor in Chief: S. Duncan Heron, Jr.

Abstract

Academic journal published quarterly by the Department of Geology, Duke University.

SOUTHEASTERN GEOLOGY

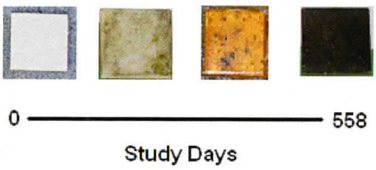

Vol. 47, No. 3

August 2010

SOUTHEASTERN GEOLOGY

PUBLISHED

at

DUKE UNIVERSITY

Duncan Heron

Editor-in-Chief

David M. Bush

Editor

This journal publishes the results of original research on all phases of geology, geophysics, geochemistry and environmental geology as related to the Southeast. Send manuscripts to **David Bush, Department of Geosciences, University of West Georgia, Carrollton, Georgia 30118, for Fed-X, etc. 1601 Maple St.,** Phone: 678-839-4057, Fax: 678-839-4071, Email: dbush@westga.edu. Please observe the following:

1) Type the manuscript with double space lines and submit in duplicate, or submit as an Acrobat file attached to an email.
2) Cite references and prepare bibliographic lists in accordance with the method found within the pages of this journal. Data citations examples can be found at http://www.geoinfo.org/TFGeosciData.htm
3) Submit line drawings and complex tables reduced to final publication size (no bigger than 8 x 5 3/8 inches).
4) Make certain that all photographs are sharp, clear, and of good contrast.
5) Stratigraphic terminology should abide by the North American Stratigraphic Code (American Association Petroleum Geologists Bulletin, v. 67, p. 841-875).
6) Email Acrobat (pdf) submissions are encouraged.

Subscriptions to *Southeastern Geology* for volume 47 are: individuals - $26.00 (paid by personal check); corporations and libraries - $40.00; foreign $55. Inquiries should be sent to: **SOUTHEASTERN GEOLOGY, DUKE UNIVERSITY, DIVISION OF EARTH & OCEAN SCIENCES, BOX 90233, DURHAM, NORTH CAROLINA 27708-0233**. Make checks payable to: *Southeastern Geology*.

Information about **SOUTHEASTERN GEOLOGY** is on the World Wide Web including a searchable author-title index 1958-2010 (Acrobat format). The URL for the Web site is: http://www.southeasterngeology.org

SOUTHEASTERN GEOLOGY is a peer review journal.

ISSN 0038-3678

SOUTHEASTERN GEOLOGY

Table of Contents

Volume 47, No. 3 August 2010

SOUTHEASTERN GEOLOGY
V. 47, No.3, August 2010, p. 117-122

ARSENIC IN GROUNDWATER IN THE NORTH CAROLINA EASTERN SLATE BELT (ESB): NASH AND HALIFAX COUNTIES, NORTH CAROLINA

JEFFREY C. REID

North Carolina Geological Survey
Raleigh, North Carolina 27699-1612

WALTER T. HAVEN

DAVID D. EUDY

North Carolina Division of Environmental Health
Raleigh, North Carolina 27699-1630

RAYMOND M. MILOSH

ELLEN G. STAFFORD

North Carolina Division of Water Quality
Raleigh, North Carolina 27699-1623

ABSTRACT

Naturally occurring arsenic-contaminated groundwater is present within the Eastern Slate Belt (ESB) of North Carolina. Long-term, integrated geologic and geochemical investigations have determined the presence of arsenic by analyzing precipitates from first and second order streams under base flow conditions. When groundwater discharges into streams, arsenic and other metals are precipitated from solution, due to redox changes between the subsurface and surface environments. Analyses (As, base metals, Fe and Mn) were determined following chemical extraction of naturally occurring manganese-iron oxide-coatings, which had precipitated from solution onto streambed cobbles. Additionally, artificial redox fronts were produced by placing ceramic tiles in streambeds to collect and analyze oxide precipitates. Thermochemical plots from these data, as well as information from respective stream water measurements (pH and Eh), water sampling, and rock chemical analyses indicate mobile arsenic in predicted stability fields. Initial results show that naturally occurring arsenic-contaminated groundwater is present within the study area. However, the resulting oxidation and precipitation within streams appreciably removes this contaminant from surface water solution.

INTRODUCTION

We report, herein, the results of long-term time-integrated field geologic and geochemical investigations of naturally occurring arsenic in the Eastern Slate Belt (ESB), Nash and Halifax Counties, North Carolina. An initial report was presented in 2007 (Reid and others). The Eastern Slate Belt (ESB) of North Carolina is characterized by mafic and felsic meta-volcanic rock, interbedded with meta-mudstones and meta-argillites (Stoddard and others, 1991). These units are contiguous with metamorphosed plutons of granitic and dioritic rock (North Carolina Geological Survey, 1985). According to Carpenter, gold exploration and mining operated in the ESB (Figure 1), from 1835 to 1988, along the Nash and Halifax County border (1999).

Arsenic has been used in pesticides, rodenticides, chemical warfare agents, medicines, and as leather and wood preservatives (USGS, 2010), and typically occurs in natural waters as either oxidized or reduced, As(V) and As(III), respectively (Inskeep and others, 2002). As(III) is generally more toxic than As(V), although

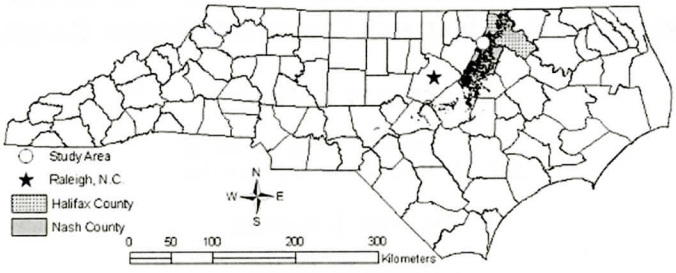

Figure 1. Eastern Slate Belt (shown in black), with respective study area.

the ingestion of inorganic, oxidized arsenic compounds can ultimately lead to arsenic reduction within the body (Manahan, 1992). Exposure to hazardous levels of arsenic can result in damage to the lungs, liver, kidneys, intestines, and the skin (Manahan, 1992).

Arsenic-bearing minerals have long been linked to gold exploration and recovery operations (Agricola, 1556). Arsenic typically occurs as a constituent element of various sulfide minerals and therefore, is commonly associated with in-situ gold occurrences (Fetter, 1993).

Groundwater studies concerning naturally occurring arsenic and resulting human health impacts are well documented (e.g., Bangladesh and South India; Anawar and others, 2003). Additionally, previous studies by Reid, and others (2005) of the Carolina Slate Belt, which is geologically similar to the ESB (Butler, 1991), indicate the presence of naturally occurring arsenic in groundwater. Prior to the study presented in this paper, no known research to specifically address naturally occurring arsenic-contaminated groundwater in the ESB had been conducted.

SITE SELECTION AND METHODS

In order to maximize opportunity for detecting naturally occurring arsenic-contaminated groundwater, a reconnaissance study of the "House Mine" property, in Halifax County, was conducted. This area had been sporadically mined for gold, and other metals from 1940 to 1957 (Carpenter, 1999) and intersects a second order stream known as "Powell's Creek." Sulfide-bearing rock samples were collected from the mine property for chemical analysis. Additionally, cobble-sized rocks were collected from the streambed of Powell's Creek, in areas down flow from the old mine. These samples were coated with a precipitated dark-colored oxide material, which was chemically digested with an acid mixture, filtered, and analyzed. We also deployed acid-cleaned ceramic tiles to serve as oxide precipitation sites as part of this long term field experiment as described below.

The summary of our digestion procedure for the tiles follows. Tiles were placed exposed surface pointing downward in a 150 ml beaker along with aliquots of 2 different acids (66.6% HNO_3 and 33.3% HCL). The beaker was covered with a watch glass and gently heated on a hot plate allowing the acid to reflux for 30 minutes. The tiles were then allowed to cool and the tiles and beaker were both rinsed with double deionized water through quantitative filter paper into a 100 ml graduated cylinder. The rinse was repeated three times and then the digestate was brought to a volume of 100 ml with DD water and mixed thoroughly. The digestate was then analyzed for metals by EPA Methods 200.7 (ICP) and 200.8(ICP-MS). Rock sample digestion followed a similar procedure.

Results from the House Mine rock samples (Table 1) and the Powell's Creek rock coating samples (Figure 2) indicated the presence of arsenic, as well as other base metals, such as iron and manganese.

At the completion of this reconnaissance phase, four primary data collection stations were established, for the seasonal analysis of stream water quality and precipitated sediment. Two stations (PC-1 and PC-2) were located along Powell's Creek, down flow from the House Mine property. Another station (PC-3)

Table 1. Hard Rock Chemistry Results. The House Mine-3 sample was not chemically analyzed, but has been archived for reference. Arsenic was analyzed by both the "HAS" (arsenic by hydride extraction) and via ICP (induced coupled plasma instrument) to help ensure all detectable arsenic could be resolved.

Rock Sample	Arsenic (ICP)	Arsenic (HAS)	Iron (ICP)	Manganese (ICP)
House Mine-1	Not Detected	6,200 µg/l	5,600 µg/l	163,000 µg/l
House Mine-2	3,000 µg/l	5,400 µg/l	4,180 µg/l	260,000 µg/l
House Mine-4	11,000 µg/l	25,700 µg/l	7,530 µg/l	1,140,000 µg/l
House Mine-5	Not Detected	1,800 µg/l	7,010 µg/l	1,570,000 µg/l

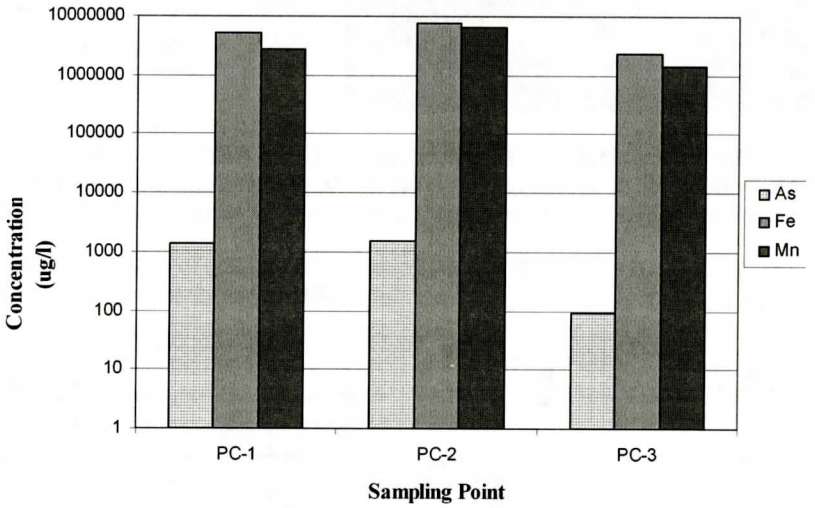

Figure 2. Rock Coating Results. Analysis results from metal oxides on stream rocks. Data are not area normalized.

was located along a second order tributary to Powell's Creek and does not drain any known mine property. Powell's Creek and the tributary are characterized by sandy to rocky streambeds, with outcropping of fractured meta-volcanic rock.

Finally, a fourth station (Portis) was located on a first order stream, incising the "Portis Mine" property. The Portis Mine, which sporadically produced gold ore from 1835 to 1988 (Carpenter, 1999), was discovered after the reconnaissance phase of the study. However, based on initial House Mine and Powell's Creek data (Table 1 and Figure 2), the Portis site was considered to be an appropriate sampling location. The stream draining the Portis property is characterized by a clayey bed, with a few exposures of quartz dikes and saprolite.

Watersheds within the study area are forested and are approximately 8 km^2 (PC-1 and PC-2), 6 km^2 (PC-3), and 2 km^2 (Portis). These drainage basins are not known to have supported agricultural or other operations, which would have required the land application of arsenic-based pesticides. The only known anthropogenic activities are a borrow pit, located near station PC-1 and previous gold mining activities. All respective streams are perennial and recharged by base flow, with contribution from surface runoff, apparently being sporadic.

To address stream water quality, filtered stream water samples were periodically collected from each station, preserved with HNO_3, and analyzed for metals. Ambient stream measurements of pH and Eh were also collected, during each water-sampling event.

To analyze oxide precipitation, eight white unglazed porcelain tiles were glued to a cement

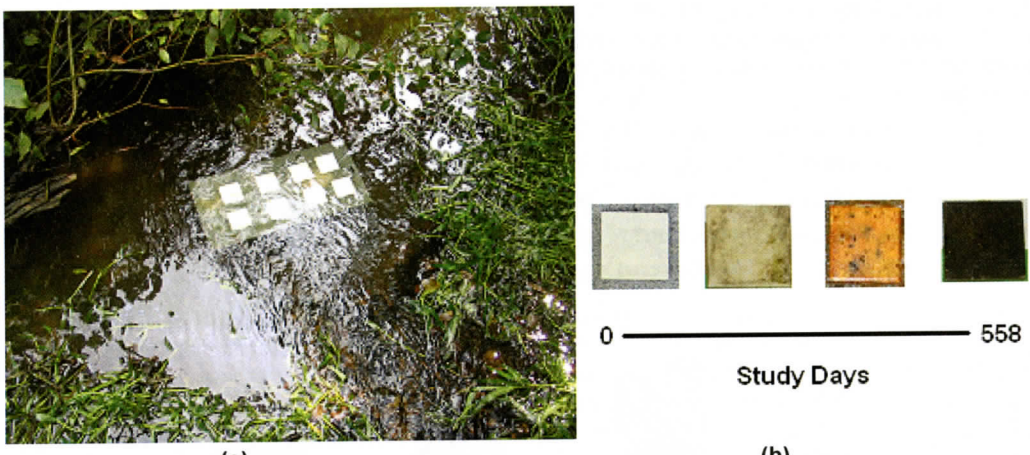

(a) (b)

Figures 3a and 3b. Tile Deployment. Tiles adhered to cement block and stationed on streambed (3a left) and change of tile appearance over time, due to precipitation of metal oxides (3b - right). The study extended for 558 days, from August 2005 through February 2007.

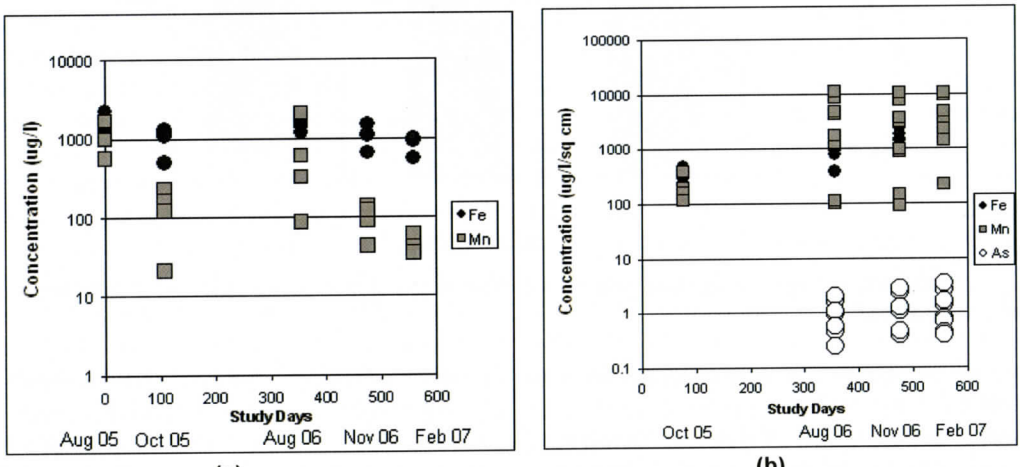

(a) (b)

Figures 4a and 4b. ESB Stream Water Results (4a - left), with concentrations of iron and manganese, but no detected arsenic (lab detection limit of 5.0 µg/l). ESB Stream Tile Results (4b - right), with detected arsenic, as well as increasing metals concentrations over time.

block with silicone caulk, leaving each tile with an exposed surface area of about 32.5 cm^2. One cement block, with the glued tiles was then placed into the water at each stream station, so that the tiles were about 5 to 10 centimeters beneath the stream surface (Figure 3a). Despite periodic water level fluctuations, this placement helped to produce a Redox front as water flowed over the tiles and induced oxide precipitation. Thus, the tiles served as time and area integrated collection sites for precipitated sediments, mimicking the natural oxide coating of stream rocks (Figure 3b). Beginning in October 2005, two tiles were taken from each sampling station for oxide coating digestion, filtering, and analysis. All other tiles remained on site for the continued collection of precipitates, until the next sampling round.

RESULTS

Stream water sampling (Figure 4a) revealed iron ranging from 550 µg/l to 2,300 µg/l, with manganese ranging from 21 µg/l to 2,100 µg/l.

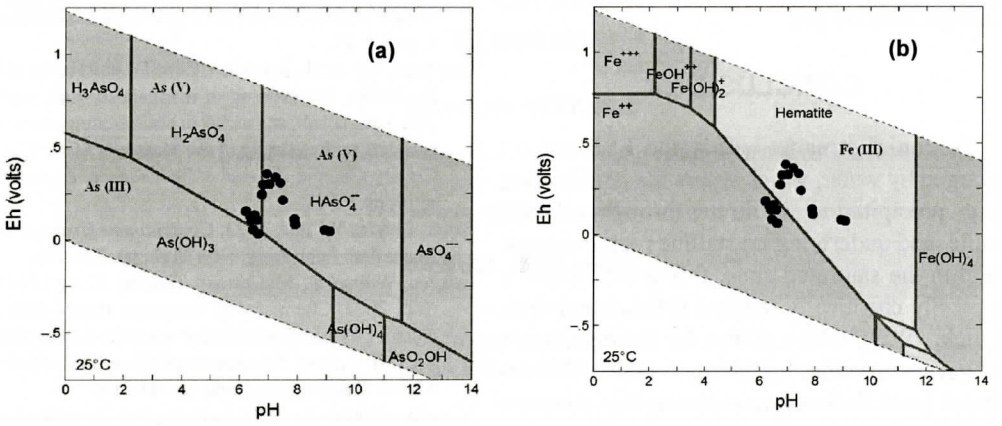

Figures 5a and 5b. Arsenic Phase Diagram (5a - left) and Iron Phase Diagram (5b - right) with Eh and pH plots from stream measurements. Shaded areas represent the boundaries of surface water stability at 25°C.

However, detectable levels of arsenic (detection limit of 5.0 µg/l) were not found. Stream tile sampling of precipitated oxide coatings show an overall trend of increasing metals concentrations over time deployed. Specifically, tile analysis (Figure 4b) revealed iron ranging from 237 µg/l/cm^2 to 9,231 µg/l/cm^2, manganese ranging from 89 µg/l/cm^2 to 11,077 µg/l/cm^2. Arsenic concentrations ranged from non-detectable (October 2005) to 3 µg/l/cm^2. Results of on-site stream water pH measurements typically ranged between 6 and 7.5 for all sampling stations. However, measurements from November 30, 2006, yielded pH ranging from 8 to 9.8. Despite regular instrument calibration, this is likely due to equipment error, as on-site conditions are not known to induce water alkalinity of this magnitude. Eh measurements ranged from 52 mv to 558 mv.

DISCUSSION

Open channel, exposed surfaces of ESB stream rocks are coated with a veneer of metal oxides. However, cobble surfaces recessed into the streambed show no evidence of oxide accumulation, indicating precipitation occurs at or above the streambed. Surface areas of cobbles and respective oxide accumulation are difficult to determine. Therefore, the deployment of unglazed stream tiles is a cost effective and labor efficient method of mimicking natural precipitation of dissolved metals onto streambed material (Carpenter and Hayes, 1978a; Carpenter and others, 1978b). This also allows for time and area integrated assessments of metal oxide precipitation.

Naturally occurring base metals, such as iron and manganese, are in the rocks, stream water, streambed rock coatings, and in stream tile oxide coatings. Naturally occurring arsenic is also in the rocks, streambed rock coatings, and in the stream tile oxide coatings, but is not above detectable limits in stream water. The absence of arsenic in stream water can be explained by the by plotting stream water Eh and pH field data onto a typical phase diagram (Figure 5a) for arsenic, as described by Bethke (2004). Data indicate that Eh and pH values are consistent with stream water oxidizing conditions, which would induce the precipitation of As(V) from the water column. This assertion is somewhat reinforced by plotting these data onto a phase diagram for iron (Figure 5b), as described by Bethke (2004). In this diagram, Eh and pH values fall either within or close to the Fe(III) or oxidized phase. The reader is reminded that Figures 5a and 5b are based on water stability at 25°C, which is not typical of sustained field conditions, and that temperature, as well as microbial activity can influence phase boundaries. Regardless, these diagrams also indicate that ar-

senic solubility is more affected by typical Eh changes than by pH.

CONCLUSIONS

Perennial streams within the ESB are recharged by water, which enters the land surface (e.g., precipitation), infiltrates through soil, saprolite, and underlying crystalline rock fractures. Within the saturated zone, this groundwater is typically chemically reduced (Mitsch and Gosselink, 1993), which allows for the dissolution of various metals, including arsenic. This reduced groundwater then enters stream channels via base flow, crossing a redox boundary (the streambed), and precipitates dissolved metal oxides onto streambed cobbles. It is through this process that arsenic is transported into stream channels as As(III), but is naturally removed from solution and precipitated as As(V).

ACKNOWLEDGEMENTS

The authors thank Amy Keyworth and K. Randy Prillaman of the North Carolina Department of Environment and Natural Resources, as well as Jeff Wyers and James I. Richardson of Nash Brick Company for their support.

REFERENCES CITED

Anawar, Hossain M., Akai Junji, Komaki K Kaori, Terao Hiroshi, Yoshioka, Ishizuka Toshio, Safiullah Safiullah, and Kato, Kikuo, 2003, Geochemical occurrence of arsenic in groundwater of Bangladesh: sources and mobilization processes, *Journal of Geochemical Exploration*, vol. 77, pp. 109-131.

Agricola, Georgius, 1556, *De Re Metallica*, translated by Hoover, H.C. and Hoover, L.H.,1950, Dover Publications, Mineola, New York, 630p.

Bethke, C. M., 2004, *The Geochemist's Workbench GWB Essentials Guide*, RockWare, Inc: Golden, Colorado (software and manual).

Butler, J. Robert, 1991, 8. Metamorphism, *in* Horton, J. Wright Jr., and Zullo, Victor. A. (*editors*), *The Geology of the Carolinas – Carolina Geological Society, Fiftieth Anniversary Volume*: The University of Tennessee Press: Knoxville, Tennessee, pp. 127-141.

Carpenter, P. Albert III, 1999, *Gold in North Carolina*, North Carolina Geological Survey Information Circular 29, North Carolina Geological Survey: Raleigh, North Carolina, 51p.

Carpenter, Robert H. and Hayes, Willis B., 1978a, Precipitation of iron, manganese, zinc, and copper on clean, ceramic surfaces in a stream draining a polymetallic sulfide deposit, *Journal of Geochemical Exploration*, v. 9, pp. 31-37.

Carpenter, Robert H., Robinson, Gene D., and Hayes, Willis B., 1978b, Partitioning of manganese, iron, copper, zinc, lead, cobalt, and nickel in black coatings on stream boulders in the vicinity of the Magruder Mine, Lincoln County, Georgia, *Journal of Geochemical Exploration*, v. 10, pp. 75-89.

Fetter, Charles Willard, 1993, *Contaminant Hydrogeology*, Macmillan Publishing: New York, pp. 274-276.

Inskeep, William P., McDermott Timothy R., and Fendorf Sott, 2002, Chemistry of inorganic arsenic (III) and arsenic (V) in soils and natural waters, *in* Frankenberger W. T. Jr. (*editor*), *Environmental Chemistry of Arsenic*, Marcel Dekker: New York, pp.185-215.

Manahan, Stanley E., 1992, *Toxicological Chemistry*, Lewis Publishers: Chelsea, Michigan, pp. 260-261, 282-284.

Mitsch, William J., and Gosselink James G., 1993, *Wetlands*, Van Nostrand Reinhold Publishers: New York, pp. 120-126.

North Carolina Geological Survey, 1985, *Geologic Map of North Carolina*, North Carolina Geological Survey, Raleigh, North Carolina, in color, scale 1:500,000.

Reid, Jeffrey C., Pippen, C.G., Haven, Walter T., and Wooten, Richard M., 2005, *Assessing the Source for Arsenic in Groundwater, North Carolina Piedmont*, Proceeding of the 2005 National Groundwater Association, Naturally Occurring Contaminants Conference: Arsenic, Radium, Radon, and Uranium, pp. 103-109.

Reid, Jeffrey C., Haven, Walter T., Eudy, David D., Milosh, Raymond M., and Stafford, Ellen G., 2007, Arsenic groundwater investigations – Eastern Slate Belt (ESB): Nash and Wilson Counties, North Carolina, Abstract, Southeastern Section Meeting, Geological Society of America Abstracts with Programs, Vol. 39, No. 2, p. 76: Charleston, South Carolina.

Stoddard, Edwin F., Farrar, Stuart S., Horton J. Wright Jr., Butler J. Robert, and Druhan Robert M., 1991, 5. The Eastern Piedmont in North Carolina, *in* Horton, J. Wright Jr., and Zullo, Victor. A. (*editors*), *The Geology of the Carolinas – Carolina Geological Society, Fiftieth Anniversary Volume*: The University of Tennessee Press: Knoxville, Tennessee, pp.79-92.

USGS, 2010, Arsenic Statistics and Information, viewed March 5, 2010 at URL http://minerals.usgs.gov/minerals/pubs/commodity/arsenic/.

SOUTHEASTERN GEOLOGY
V. 47, No.3, August 2010, p. 123-145

METAMORPHISM OF CPX-RICH ROCKS FROM WEBSTER-ADDIE ULTRAMAFIC COMPLEX

RICHARD WARNER

Department of Environmental Engineering and Earth Sciences
Clemson University, Clemson, SC 29634-0919
wrichar@clemson.edu

SAMUEL SWANSON

Department of Geology
University of Georgia
Athens, GA 30602-2501

ABSTRACT

Clinopyroxene-rich rocks, chiefly metawebsterite and olivine metaclinopyroxenite, are an important constituent of the Webster-Addie ultramafic complex, but are rare elsewhere in Blue Ridge metaultramafic bodies. They occur as layers and lenses in metadunite, ranging in thickness from a few millimeters to tens of meters. Compositional and structural (layering) characteristics are similar to, and suggest derivation from, the ultramafic cumulate portion of an ophiolite.

Metamorphism of the clinopyroxene-rich rocks has produced the assemblage clinopyroxene (Cpx) + orthopyroxene (Opx) + olivine + calcic amphibole + Al-rich spinel, characteristic of the amphibolite-granulite facies transition. Application of two-pyroxene geothermometry to exsolution lamellae formed in the pyroxenes yields peak metamorphic temperatures of 795-835°C. The absence of anthophyllite in associated metadunites indicates that pressure during metamorphism was at least 11 kb.

A major feature of the metamorphism at Webster-Addie is the growth of calcic amphibole at the expense of pyroxene. Initially, this produced an aluminous hornblende, edenite. Later, edenite was, in part, retrograde metamorphosed to tremolite, resulting in composite crystals with edenite cores mantled by tremolite. Depending on the extent to which pyroxene was replaced by calcic amphibole, rocks grade from pyroxene-rich with minor amphibole to nearly pure amphibole rocks. Calcic amphiboles similar to those found replacing pyroxene at Webster-Addie are a minor, but widespread, constituent in Blue Ridge metaultramafic bodies, and may reflect origin from a Cpx-bearing protolith.

INTRODUCTION

Numerous small bodies of metamorphosed ultramafic rocks are distributed along the Blue Ridge Belt of the Southern Appalachians (Hess, 1955; Larrabee, 1966). Although their cumulative volume constitutes just a small fraction of the entire Blue Ridge, they have been the focus of many studies aimed at deciphering the formation and metamorphic history of the southern Appalachians (Misra and Keller, 1978; McElhaney and McSween, 1983; Hatcher and others, 1984; Raymond and Abbott, 1997; Berger and others, 2001; Raymond and others, 2001, 2003; Swanson, 2001; Warner, 2001; Warner and Hepler, 2005). These studies have indicated that the ultramafic rocks were variously hydrated during multiple episodes of metamorphism, and that most protoliths were olivine-rich. Metadunite is the dominant rock type and grades from nearly anhydrous recrystallized olivine with granoblastic polygonal texture to hydrated rocks containing olivine plus varying amounts of chlorite, calcic amphibole, talc, and serpentine, and ultimately to serpentinites and talc-amphibole-chlorite schists (Raymond and Abbott, 1997; Swanson, 2001). Metaharzburgite is often a minor component (except at Dark Ridge, where steatitized metaharzburgite forms

a significant portion of the metaultramafic body (Warner and Hepler, 2005)). Metaorthopyroxenite is present in a few metadunite bodies (Swanson, 1980, 2001; Raymond and others, 2001); however, metaultramafic rocks containing clinopyroxene (Cpx) are rare.

The only confirmed clinopyroxene-bearing metaultramafic rocks in the Blue Ridge Belt occur in the Webster-Addie complex of western North Carolina. The latter consists of a discontinuous sheet of metaultramafic rocks that has been folded into a dome shape (Madison, 1968; Quinn, 1991). Metadunite is the principal lithology, but pyroxene-rich rocks (metawebsterite, metaclinopyroxenite, metaorthopyroxenite) are locally abundant as lenses ranging in thickness from a few millimeters to tens of meters. Small lenses of massive chromitite also occur in the Webster-Addie complex, some of which (particularly those near the town of Webster) were mined in the early 1900s (Hunter and others, 1942).

The realization that the metaultramafic bodies of the Blue Ridge Belt are probably scattered fragments of dismembered ophiolites (McSween and Hatcher, 1985) has led to attempts to interpret their origin within the framework of current ophiolite classification schemes (Swanson and others, 2005). For example, Boudier and Nicolas (1985) divided ophiolites into two petrologic subtypes: lherzolite ophiolite type (LOT) and harzburgite ophiolite type (HOT); a third, intermediate type – lherzolite-harzburgite ophiolite type (LHOT) – was later added (Nicolas and Boudier, 2003). Based on the presence of chromitite and metawebsterite, as well as the nature of associated amphibolites (Ryan and others, 2005), a LHOT designation is inferred for the Webster-Addie complex (Swanson and others, 2005).

Whatever the original igneous protoliths, the Blue Ridge ultramafic rocks were subjected to a complex polymetamorphic history (Raymond and Warner, 2001). Our purpose in this paper is to describe the metamorphic petrology of the Cpx-rich metaultramafic rocks from the Webster-Addie complex. Although our main focus is on the pyroxene-bearing rocks at Webster-Addie, we include a representative sampling of olivine-rich metaultramafic rocks in our synthesis to allow comparison to the other olivine-rich rocks of the Blue Ridge belt (e.g., Swanson and others, 2005).

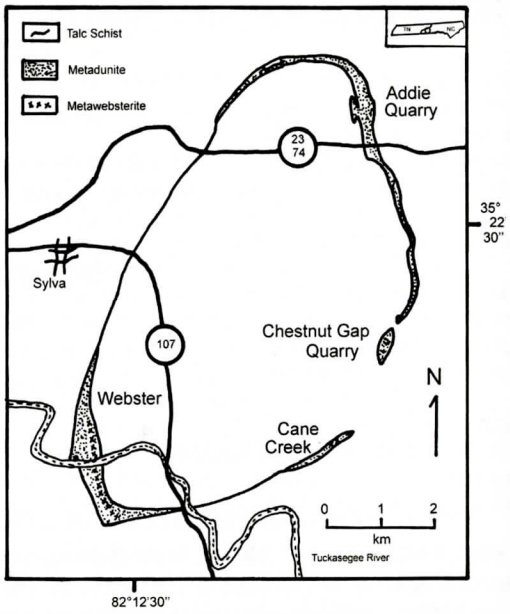

Figure 1. Distribution of rock types in the Webster-Addie ultramafic complex based on the map by Pratt and Lewis (1905). The term "meta" was added to the ultramafic rock names by the authors. The presence of talc schist, shown by Pratt and Lewis, was confirmed along the margins of the larger outcrops, but was not noted in other locations.

PREVIOUS WORK

The earliest reference in the literature to pyroxene-rich rocks from the Webster-Addie body (Williams, 1890) described the occurrence of two-pyroxene rocks outcropping in the vicinity of Webster in Jackson County, North Carolina, to which the name websterite was applied. At this type locality, websterite consists dominantly of bright green diopside (Cpx) with subordinate amounts of brown bronzite (orthopyroxene, Opx) and variable amounts of pleonaste (Cr-poor spinel) (Pratt and Lewis, 1905). The Pratt and Lewis treatise (1905) on "Corundum and the peridotites of North Carolina" contained the first published field map of the Webster-Addie complex and showed its dis-

tinctive ring-like outcrop pattern (Figure 1). These authors noted that the main occurrence of websterite was just north of the Tuckasegee River in "a mass about 550 feet wide entirely enclosed in dunite" (p. 45). Smaller outcrops were traced north and south for a distance of about 1.5 km, and a satellite websterite body was found along Cane Creek, 5 km east of Webster.

For the next half century research concentrated on the origin and economic aspects of the mineral deposits associated with the Webster-Addie complex (Ross and Shannon, 1926; Ross and others, 1928, 1929; Hunter, 1941; Hunter and others, 1942; Murdock and Hunter, 1946). With regard to the various olivine deposits described by Hunter (1941), it is noted that olivine was subsequently mined at two locations within the Webster-Addie complex: (1) just southeast of Addie, on the slopes above Ochre Hill Creek, and (2) at a quarry south of Chestnut Gap (and about 5 km south of Addie). Both quarries are now closed. Small amounts of chromite were removed from the vicinity of the Addie olivine quarry and from chromite lenses southeast of Webster (Hunter and others, 1942).

Since 1950 a number of doctoral dissertations and master's theses have been completed dealing with the petrology, structure and origin of the Webster-Addie complex (Miller, 1951; Madison, 1968; Pike, 1968; Cronin, 1983). Miller (1951; 1953) concluded that the ultramafic rocks at Webster-Addie were intruded as a sheet-like mass that was subsequently deformed. Madison (1968), based on a combination of paleomagnetic and structural evidence, reached a similar conclusion and attributed the present domal structure to post-emplacement deformation. Pike (1968) argued for tectonic emplacement of the body as a solid mass, a view shared by Cronin (1983). All agree that later deformation folded the body into its domal configuration. Recent detailed (1:24,000 scale) geologic mapping of the area surrounding Sylva, NC by Quinn (1991) has corroborated a post-emplacement origin for the "Webster-Addie dome".

Post-emplacement deformation of ultramafic bodies in the Blue Ridge Belt was accompanied by multiple episodes of metamorphism and recrystallization (Raymond and Warner, 2001; Raymond and others, 2003). Hence, the present rocks at Webster-Addie are metamorphic rocks (metaultramafics), and metamorphic rock names are appropriate, to which we adhere for the remainder of this paper. A brief overview of the metamorphic mineral assemblages observed in the Webster-Addie complex was presented in Raymond (2002, p. 654), and a preliminary report on mineral compositions was given by Warner and Swanson (2000) (see also Raymond, 2002). Warner and Swanson (2000) noted that mafic minerals in metawebsterites were distinctly less Mg-rich than in associated metadunites, that chromite exhibited a large compositional variation, and that there is a widespread occurrence of calcic amphibole (both edenite and tremolite) in the metaultramafic rocks. Swanson and Warner (2001) emphasized the metamorphic character of the pyroxene-rich rocks at Webster-Addie. Some geochemical data on the Webster-Addie rocks was published in Berger and others (2001) and in two recent field trip guidebook articles (Ryan and others, 2005; Peterson and others, 2006).

FIELD SAMPLING AND ANALYTICAL METHODS

Samples utilized in this study were collected mainly from the area south and east of Webster, which is the largest surficial exposure of the Webster-Addie complex (Hunter, 1941), and from the Chestnut Gap quarry (Figure 1). Additional samples were obtained along Cane Creek, where a smaller, lens-shaped portion of the body outcrops for about 500 m (Hunter, 1941), and from the Addie area in the northern part of the complex, both at the old Addie quarry and from outcrops along Blanton Branch Road at its intersection with US 23-74. Sample numbers with "WA" are from the Webster area, those designated "CG" are from Chestnut Gap quarry, "CC" refers to Cane Creek, and "AD" indicates Addie area samples. The only departure from this numbering scheme is that samples WA-1A and WA-1B are from the Blanton Branch Road outcrop, not the Webster area.

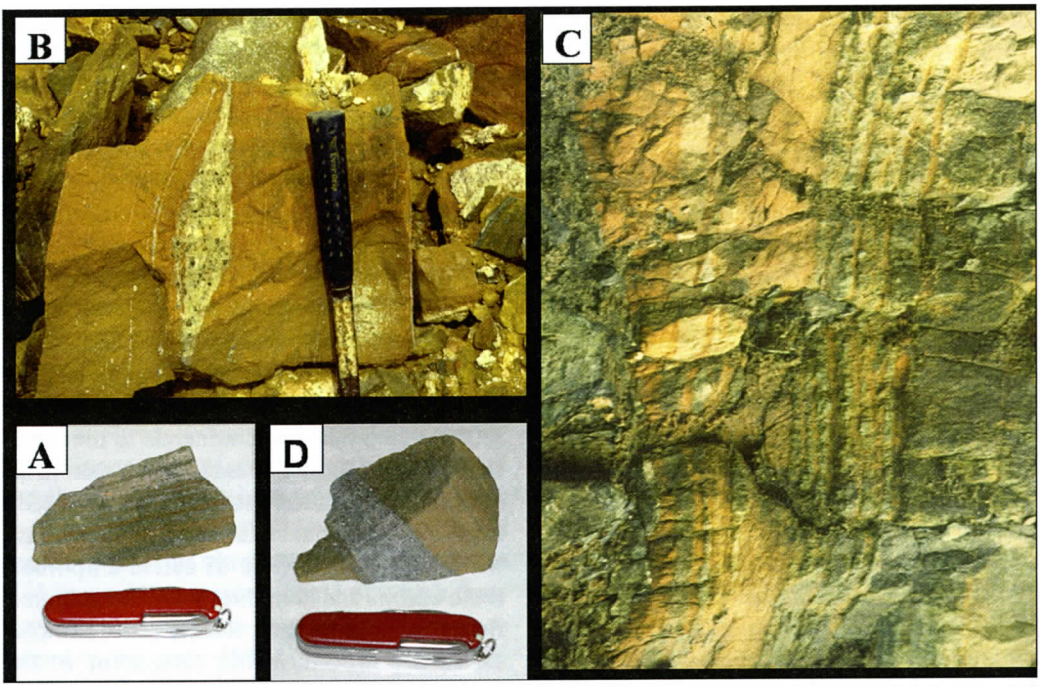

Figure 2. Chestnut Gap quarry exposures. Clockwise from lower left: A) Hand sample (CG-3) showing fine-scale layering. Darker (brown) layers are metadunite; lighter (greenish) layers are Cpx-rich metaultramafic cumulates. B) Metaorthopyroxenite boudin in metadunite. Disaggregation of boudin has introduced laminations and coarse crystals of Opx into adjacent metadunite. C) Layers of amphibole-rich rock (edenite-tremolite metapyroxenite) in metadunite exposed along quarry wall. D) Hand sample (CG-3B) with amphibole-rich metaclinopyroxenite layer in metadunite.

Metadunite (often serpentinized) and subordinate metaharzburgite are the most abundant metaultramafic rock types in the Webster-Addie complex, and samples of these olivine-rich rocks were collected at all the afore-mentioned localities. The distribution of pyroxene-rich rocks is non-uniform, and their sampling was as described below.

The largest outcrop of metawebsterite is just east of Webster, on the hill slopes north of the Tuckasegee River (Pratt and Lewis, 1905). Samples of metawebsterite (WA-16B, WA-16C) were collected from this type locality. Metawebsterite was also sampled at two localities (WA-12, WA-13) about 1 km south of the Tuckasegee River. Both metawebsterite and metaclinopyroxenite were recovered from Chestnut Gap quarry. At the latter site, Cpx-rich rocks locally are finely interlayered with metadunite, often on a scale of millimeters to a few centimeters (Figure 2A). Two Cpx-rich samples (AD-7, AD-21) were recovered from the Addie quarry, but it should be noted that pyroxene-bearing rocks are extremely rare in the northern portion of the Webster-Addie complex.

Metaorthopyroxenite occurs chiefly as narrow lenses or boudins enclosed by metadunite (Figure 2B). It is most common and best exposed at Chestnut Gap quarry (McIlmoil and others, 2002; Ryan and others, 2005; Peterson and others, 2006). Samples of metaorthopyroxenite (WA-8B, WA-8D) were also obtained from a large outcrop of serpentinized metadunite at Webster.

Rocks dominantly composed of calcic amphibole are a minor but important component of the metaultramafic suite exposed in the Addie and Chestnut Gap quarries. They occur as irregular bands, typically less than 10 cm thick, that are interlayered with metadunite (Figure 2C,D).

Veins with comparable mineralogy were observed to crisscross massive metawebsterite at the "websterite" type locality, but were not found elsewhere in the Webster-Addie complex.

Polished thin sections were commercially prepared from field samples collected in this study. These were examined with a Jenapol U polarizing microscope, using both transmitted and incident light. Modal abundances were obtained with a Swift Model F automatic point counter (average number of points counted per section was slightly less than 500). For some Cpx-rich samples, where it was difficult to optically distinguish Cpx from olivine, modes were determined with a JEOL JXA-8600 scanning electron microprobe at the University of Georgia, using energy dispersive spectra (EDS) of the individual points. This instrument was also utilized to obtain mineral compositions using wavelength dispersive spectrometers. The analyses were made using a 15 nanoamp beam current at an accelerating voltage of 15 KV, and were corrected for differential matrix effects following the procedure of Bence and Albee (1968). Chromite analyses were recalculated on the basis of stoichiometry to determine Fe^{3+} and Fe^{2+} from total Fe.

Ten representative samples were selected for whole rock geochemical analyses. The analyses were performed at Acme Analytical Laboratories Ltd. in Vancouver, British Columbia. The procedure utilized inductively coupled plasma emission spectrometry (ICP-es) on 0.2 g samples following a $LiBO_2$ fusion and dilute nitric acid digestion. Loss on ignition (LOI) was determined by weight difference after ignition to 1000°C.

MODAL MINERALOGY

Table 1 gives mineral modes for Webster-Addie metaultramafic rocks. Because the pyroxene-rich rocks (and amphibole-rich rocks derived from them) are the main focus of this paper, only a limited number of olivine-rich rocks are included in Table 1. These typically contain 1-2% chromite. Cpx is present in only trace amounts, or is lacking altogether; however, calcic amphibole is common in amounts up to 5%. Talc and chlorite are of limited occurrence, whereas serpentine is usually relatively abundant.

Pyroxene-rich rocks are usually either Opx-dominant or Cpx-dominant (Table 1). Only one sample (CG-17A) has subequal amounts of Opx and Cpx. All contain some olivine, often less than 10%, but an appreciable number of samples have sufficient olivine to be called olivine metaclinopyroxenite, olivine metawebsterite, or olivine metaorthopyroxenite. Calcic amphibole is present in all but two pyroxene-rich samples, and frequently exceeds 5% of the mode. Serpentine is rarely present, and talc and chlorite are generally absent (but AD-21 is nearly half chlorite).

Amphibole-rich rocks from Chestnut Gap quarry contain both edenite and tremolite, which, as will be shown later, are derived from pyroxene-rich protoliths. For this reason we propose the name edenite-tremolite metapyroxenite for these rocks. Edenite-tremolite metapyroxenites have variable amounts of pyroxene (mostly relict Cpx), minor olivine and chlorite, and $\leq$ 1% chromite (Table 1). None contain talc, and only one sample (CG-2) has serpentine.

DESCRIPTION OF METAULTRAMAFIC ROCKS

Metadunite/Metaharzburgite

Metadunite is fine-grained and massive. It is gray-green on fresh surfaces and weathers to a brown color. In hand specimen the texture is granular, consisting of equant olivines with disseminated crystals of chromite. Relatively large, brown, vitreous Opx crystals are present in some rocks and tend to stand out in modest relief on weathered surfaces. With increased amounts of Opx, metadunites grade into olivine-rich metaharzburgites.

Olivine-rich rocks in thin section are variably textured, primarily in relation to the extent of hydration during metamorphism. Anhydrous rocks have a granoblastic polygonal texture with olivine grains often meeting in 120° triple junctions (Figure 3A). Opx, if present, occurs as

Table 1 Modal Abundances in Webster-Addie Metaultramafic Rocks.

Sample	Olivine	Chromite	Opx	Cpx	Calcic Amphibole	Talc	Chlorite	Serpentine	Comment
					Olivine-rich Rocks				
WA-1A	79	<1			2	7	3	9	Metadunite
WA-1B	80	2			<1		<1	17	Metadunite
WA-1C	93	<1			<1		Tr	5	Metadunite
WA-5	91	1			<1	<1		8	Metadunite
WA-7	72	1	4	Tr	3			20	Metadunite
WA-8C	56	<1	3	Tr	2			39	Serpentinized Metadunite
WA-9	34	1	1		2			61	Serpentinized Metadunite
WA-10	68	<1	11	Tr	5			15	Metaharzburgite
WA-11	69	1	2	Tr	<1			28	Metadunite
CC-2	84	<1	4		1		<1	10	Metadunite
CG-4	88	<1	6		3	2		1	Metadunite
CG-4S	59	1	37		3				Metaharzburgite
CG-8	91	1	Tr	Tr	<1			7	Metadunite
					Pyroxene-rich Rocks				
AD-7	21	<1		54	25				Ol Metaclinopyroxenite
AD-21	11	1		36			46	6	Ol Metaclinopyroxenite
WA-8B	2	<1	93	Tr	5				Metaorthopyroxenite
WA-8D	3	<1	90	Tr	6				Metaorthopyroxenite
WA-12	6	1	11	75	7				Ol Metawebsterite
WA-13	<1	<1	19	74	5				Metawebsterite
WA-16B	5	<1	21	65	8				Ol Metawebsterite
WA-16C	<1	<1	24	65	10				Metawebsterite
CG-1	<1	<1	88	1	9				Metaorthopyroxenite
CG-3B	3	1	1	51	36		4	2	Metaclinopyroxenite
CG-5	14	<1	1	54	29		2		Ol Metaclinopyroxenite
CG-5A	2	<1	92		6				Metaorthopyroxenite
CG-5B	14	Tr	77		8			<1	Ol Metaorthopyroxenite
CG-8S	4	<1	78		7	10	<1		Metaorthopyroxenite
CG-10A	1		5	93					Metaclinopyroxenite
CG-12B	7	<1	84	4	4				Ol Metaorthopyroxenite
CG-14A	4		70	19	3	4			Metawebsterite
CG-14B	<1		73	23	3				Metawebsterite
CG-17A	<1		49	41	7	3			Metawebsterite
CG-21	15	<1		52	32				Ol Metaclinopyroxenite
CG-22	30	5	58	3	3	<1	2		Ol Metaorthopyroxenite
CG-25	2	<1	70		26	<1	<1		Metaorthopyroxenite
CG-27A	1	<1	87	<1	11		<1		Metaorthopyroxenite

Table 1 Modal Abundances in Webster-Addie Metaultramafic Rocks (cont).

Amphibole-rich Rocks								
CG-2	1	1			89	1	8	Ed-Tr Metapyroxenite
CG-3C	<1	<1			98	1		Ed-Tr Metapyroxenite
CG-9	7	<1	3	28	52	9		Ed-Tr Metapyroxenite
CG-16				43	56	<1		Ed-Tr Metapyroxenite
CG-23	20	<1	1	6	71	1		Ed-Tr Metaperidotite
CG-28	3	1	3	13	80	<1		Ed-Tr Metapyroxenite

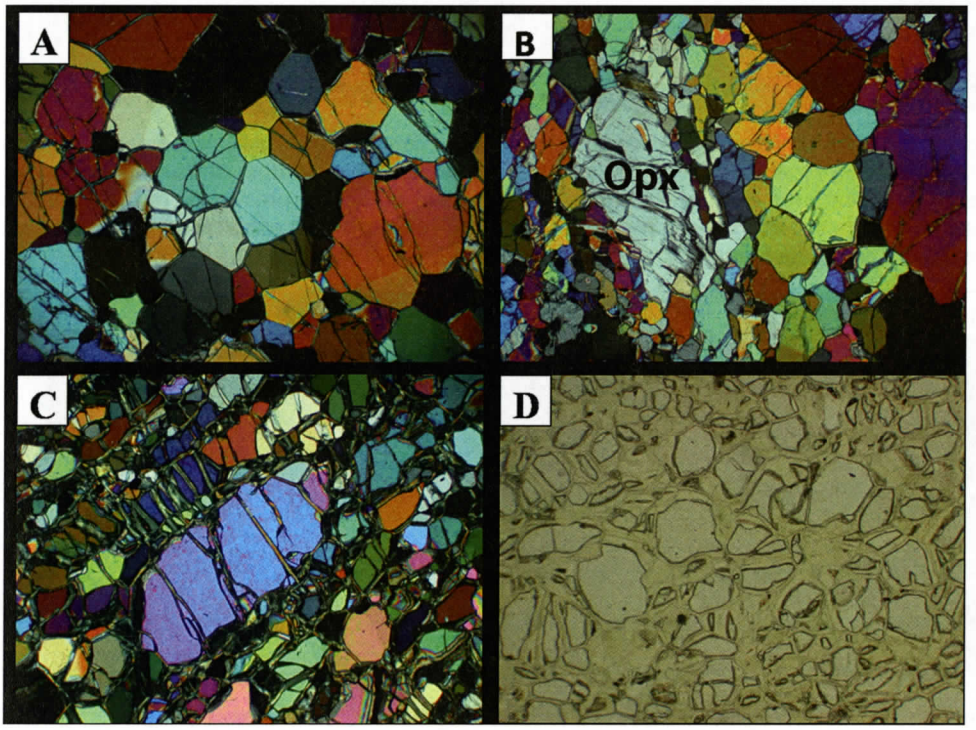

Figure 3. Photomicrographs (crossed nicols, except (D), which was taken in plane polarized light) of olivine-rich metaultramafic rocks. Long dimension of field of view is approximately 3 mm in each photo. A) Metadunite (WA-1C) showing granoblastic polygonal texture in olivine. Note strain banding in larger olivine crystal at right. B) Metadunite (CG-4) containing Opx (irregular crystal left of center). C) Serpentinized metadunite (WA-8C) with equigranular tabular texture, poorly developed banding, and minor serpentine development along fractures and grain boundaries. D) More extensively serpentinized metadunite (WA-9), in which olivine grains are wholly enclosed by serpentine.

larger, irregular crystals, that are typically subelongate (Figure 3B). Olivine in more hydrated samples shows incipient alteration to serpentine along internal cracks and grain boundaries (Figure 3C). In highly serpentinized metadunites, olivine grains are completely engulfed by serpentine (Figure 3D). Olivine grains range in size from a few tenths of a millimeter to a maximum of 3 mm; in most samples the average size is about 0.5 mm. A few metadunites exhibit a faint banding marked by layers of finer-grained olivine alternating with those of coarser olivine.

The habit of chromite is more varied and correlates with the presence or absence of chlorite. Where chlorite is absent, chromite occurs as subhedral to euhedral "clean" crystals (Lipin, 1984) that typically are brown to deep reddish

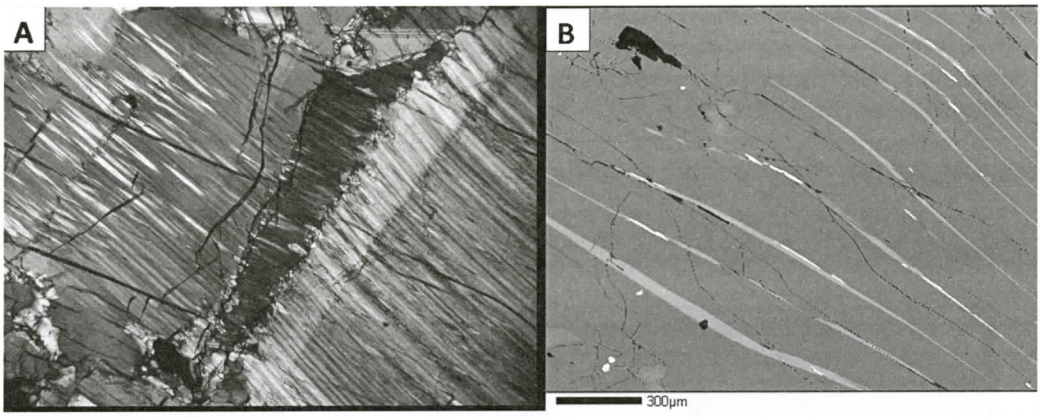

Figure 4. A) Photomicrograph (crossed nicols, long dimension ~ 3 mm) of metaorthopyroxenite (CG-1) showing strain banding in Opx porphyroclast and also bending of Cpx exsolution lamellae. B) Backscattered electron image (bar gives scale) of Opx porphyroclast in CG-1 containing exsolution lamellae of Cpx (slightly brighter) and Al-rich chromian spinel (brightest phase). Note bending of exsolution lamellae.

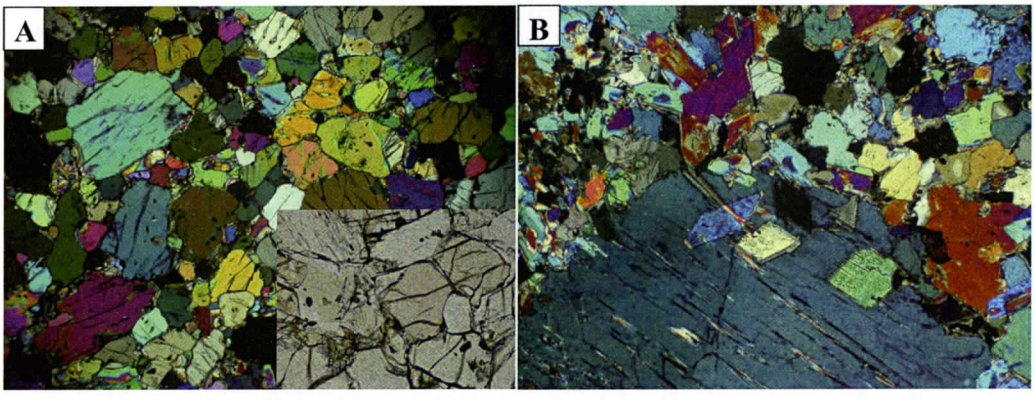

Figure 5. Photomicrographs (crossed nicols, long dimension ~ 3 mm) of Cpx-rich rocks. A) Metawebsterite (WA-12) consisting primarily of Cpx plus subordinate Opx. Inset (plane polarized light, higher magnification) illustrates pale pink pleochroism by which Opx can be distinguished from Cpx. Also note pale green color of associated edenite (at left). B) Metaclinopyroxenite (CG-3B) containing abundant calcic amphibole, shown here replacing a Cpx porphyroclast.

brown in transmitted light. In contrast, chromite in chlorite-bearing samples has a corona of chlorite and a "lattice" or poikiloblastic texture (Lipin, 1984) formed by chlorite-chromite intergrowths.

Metaorthopyroxenite

Metaorthopyroxenite occurs as small lenses or boudins enclosed in metadunite, and is considerably coarser-grained than the surrounding metadunite (Figure 2B). Brown or greenish brown, subequant Opx porphyroclasts are typically 2-5 mm in length, but may exceed 1 cm (largest observed was ~ 5 cm long). Smaller, deep green crystals of edenite are also visible in hand specimens. In thin section, orthopyroxene porphyroclasts locally show evidence of strain deformation, including undulatory extinction, kink bands, and bent exsolution lamellae (Figure 4A). Both Cpx and minor Al-rich spinel occur as exsolution lamellae (Figure 4B). Recrystallized Opx porphyroclasts have irregular, sutured margins and are rimmed by a fine-

Table 2 Whole-rock Geochemical Analyses of Webster-Addie Metaultramafic Rocks.

	Metadunite				Meta-orthopyroxenite	Metaclinopyroxenite/ Metawebsterite				Edenite-Tremolite/ Metapyroxenite
	WA-1A	WA-5	CC-2	CG-8	CG-1	CG-3B	CG-5	WA-12	WA-16B	CG-2
SiO_2	41.98	42.27	42.16	39.80	55.70	51.99	51.60	50.49	51.48	52.97
TiO_2	BDL	BDL	BDL	BDL	0.03	0.06	0.06	0.07	0.06	0.07
Al_2O_3	0.46	0.23	0.48	0.31	1.23	2.73	1.99	2.21	2.23	2.01
Cr_2O_3	0.35	0.43	0.37	1.12	0.50	0.46	0.41	0.45	0.38	1.10
FeO	7.84	7.66	7.49	8.74	6.13	4.05	4.33	5.23	5.48	2.80
MgO	44.56	45.69	45.84	47.23	32.93	20.34	21.05	20.69	20.91	25.39
MnO	0.11	0.10	0.10	0.11	0.13	0.08	0.10	0.11	0.12	0.05
NiO	0.31	0.37	0.31	0.30	0.10	0.03	0.03	0.04	0.05	0.11
CaO	0.50	0.35	0.51	0.46	2.06	17.24	19.05	19.45	18.40	11.48
Na_2O	0.04	0.01	0.02	0.01	0.06	0.33	0.29	0.16	0.18	0.38
LOI	3.0	2.0	1.9	1.0	0.3	2.1	1.2	1.2	0.75	3.4
Sum	99.15	99.11	99.18	99.08	99.17	99.41	100.11	100.10	100.04	99.76
Mg#	91.0	91.4	91.6	90.6	90.5	89.9	89.7	87.6	87.2	94.2

Mg# = Mg/(Mg+Fe) BDL = below detection limit

grained aggregate of recrystallized Opx and calcic amphibole, plus minor olivine and chromite. Chromite in metaorthopyroxenite is much finer-grained (typically < 0.2 mm) than in the enclosing olivine-rich rocks.

Metawebsterite/Metaclinopyroxenite

Metawebsterite and metaclinopyroxenite are fine-grained with a saccharoidal texture. Fresh surfaces are green and turn brown to gray-brown upon weathering. Cpx is the dominant mineral, but subordinate Opx is usually present (Table 1). Resistant veins of calcic amphibole, 1-5 mm thick, cut through metawebsterite at the Webster type locality. Thin sections reveal that the Cpx-rich rocks are populated by irregular, equant to subequant pyroxene crystals most of which are < 0.5 mm across (Figure 5A). Opx can usually be distinguished from Cpx by means of its characteristic pink pleochroism (Figure 5A, inset). The rocks are equigranular for the most part, but grade to porphryoclastic-textured rocks containing larger pyroxene crystals up to ≥ 3 mm long. The porphyroclasts frequently contain exsolved pyroxene plus deformational features similar to those found in metaorthopyroxenite (described above). Calcic amphiboles, both green-colored edenite and colorless tremolite, are common in metawebsterite and metaclinopyroxenite and may be quite abundant (Table 1). Frequently, the edenite is mantled by tremolite. In some samples (e.g., CG-3B), calcic amphibole replaces Cpx porphyroclasts (Figure 5B). Spinel crystals are brown to greenish brown, rounded to rod-shaped, and extremely small, usually between 0.05 and 0.1 mm in length. They occur both as inclusions or lamellae within silicate minerals and as individual crystals bounded by silicate grains.

Edenite-Tremolite Metapyroxenite

Numerous layers of fine-grained, gray-green amphibole-rich rocks are interlayered with metadunite at the Chestnut Gap quarry (Figure 3C). Similar layers were noted at the Addie quarry prior to its reclamation (Cronin, 1983; Peterson and others, 2006). The layers are commonly several centimeters thick, but may be as thin as a few millimeters. They contain varying proportions of calcic amphibole and Cpx, and grade from amphibole-bearing metaclinopyroxenite (Figure 5B) to nearly pure amphibole rocks. Edenite-tremolite metapyroxenite is the

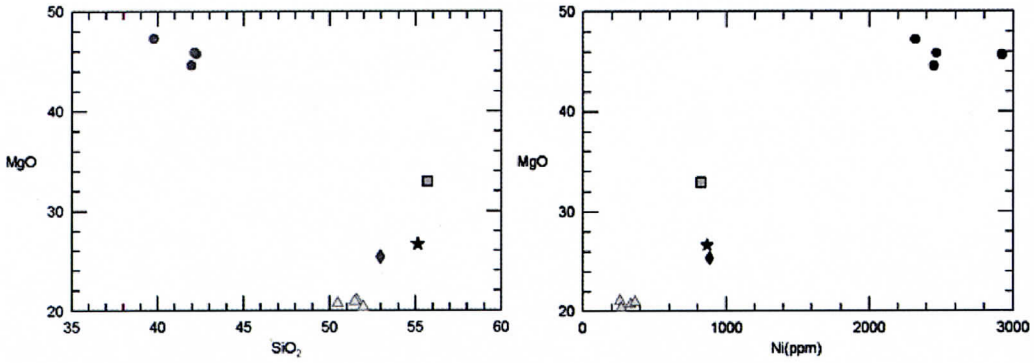

Figure 6. Plot of MgO vs SiO_2 (left) and MgO vs Ni (right) in Webster-Addie metaultramafic rocks. Symbols: circles, metadunites/metaharzburgites; square, metaorthopyroxenite; triangles, metawebsterites/metaclinopyroxenites; diamond, edenite-tremolite metapyroxenite. Star denotes analysis of websterite from type locality (Williams, 1890).

name we designate for metapyroxenites in which calcic amphibole is now the principal mineral. Both pale green edenite and colorless tremolite are present, and, where intergrown, tremolite invariably mantles edenite. As indicated in the preceding section, calcic amphibole originated at the expense of Cpx (Figure 5B).

WHOLE-ROCK GEOCHEMISTRY

Table 2 gives whole-rock analyses for representative samples of metaultramafic rocks from the Webster-Addie complex (additional analyses were reported by Madison (1968) and Ryan and others (2005)). Metadunites contain about 45 wt% MgO and have Mg-numbers (Mg# = 100 x Mg/(Mg + Fe)) of 91±1. Both CaO and Al_2O_3 are ≤ 0.5 wt%, while NiO is between 0.3 and 0.4 wt%. Metawebsterites and metaclinopyroxenites have the lowest MgO (20-21 wt%) and NiO (≤ 0.05 wt%), and Mg-numbers < 90. These Cpx-rich rocks contain 18±1 wt% CaO and ≥ 2 wt% Al_2O_3. Metaorthopyroxenite CG-1 has the highest silica content and its MgO (and Mg#) and NiO contents are intermediate between metadunite and the Cpx-rich rocks (Table 2; Figure 6). FeO, CaO, Na_2O, and Al_2O_3 are intermediate as well. Edenite-tremolite metapyroxenite CG-2 has CaO, MgO, and SiO_2 intermediate between Opx-rich CG-1 and the Cpx-rich rocks. This sample has the lowest FeO (and, consequently, the highest Mg#) of

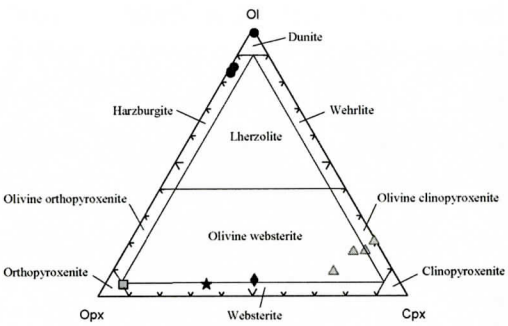

Figure 7. CIPW normative mineralogy plotted on ternary olivine-Opx-Cpx diagram. Ultramafic rock classification boundaries after IUGS (Streckeisen, 1973). Symbols: same as in Figure 6.

any rock analyzed. It plots closest to the type websterite analysis (star in Figure 6) given by Williams (1890) and reproduced in Pratt and Lewis (1905) and Hunter (1941).

CIPW norms were calculated (Kelsey, 1965) for each of the whole-rock analyses reported in Table 2 and plotted (Figure 7) on the IUGS classification diagram for ultramafic rocks (Streckeisen, 1973). The results reinforce the conclusion that metaultramafic rocks from the Webster-Addie complex fall mainly into three compositional types: olivine-rich, Opx-rich, and Cpx-rich. The normative mineralogy further suggests that (1) olivine-rich harzburgites may have been more common protoliths (relative to dunite) than indicated by the metamor-

Table 3 Electron Microprobe Analyses of Olivines, Webster-Addie Metaultramafic Rocks.

	Metadunite/Metaharzburgite					Metaorthopyroxenite	Metaclinopyroxenite/ Metawebsterite			
	WA-1B	WA-5	WA-10	CC-2	CG-8	CG-1	CG-3B	CG-5	WA-12	WA-16B
SiO_2	40.73	40.93	40.99	40.64	40.94	40.28	38.15	39.09	38.99	39.42
MgO	50.00	51.82	50.29	50.42	51.25	48.26	40.28	41.85	40.91	44.78
FeO	9.64	7.40	8.18	8.34	7.86	10.49	19.38	18.92	19.67	15.98
MnO	0.17	0.09	0.15	0.11	0.15	0.06	0.37	0.33	0.32	0.17
NiO	0.21	0.26	0.30	0.32	0.22	0.39	0.15	0.03	0.09	0.08
Total	100.75	100.50	99.91	99.83	100.42	99.48	98.33	100.22	99.98	100.43
Si	0.991	0.989	0.999	0.995	0.989	0.998	0.998	0.998	1.001	0.991
Mg	1.814	1.866	1.827	1.839	1.846	1.783	1.571	1.592	1.566	1.678
Fe	0.196	0.150	0.167	0.171	0.159	0.218	0.424	0.404	0.422	0.336
Mn	0.004	0.002	0.003	0.003	0.003	0.001	0.008	0.007	0.007	0.004
Ni	0.004	0.005	0.006	0.008	0.005	0.008	0.003	0.001	0.002	0.002
Sum	3.009	3.012	3.002	3.016	3.002	3.008	3.004	3.002	2.998	3.011
Fo	90.2	92.6	91.6	91.5	92.1	89.1	78.7	79.8	78.8	83.3

Table 4. Electron Microprobe Analyses of Pyroxenes, Webster-Addie Metaultramafic Rocks.

	Metadunite/Metaharzburgite					Metaorthopyroxenite			Metaclinopyroxenite/Metawebsterite					
	WA-7		WA-10		CC-2	CG-1		WA-8D	CG-3B	CG-5	WA-12		WA-16B	
	Opx	Cpx	Opx	Cpx	Opx	Opx	Cpx	Opx	Cpx	Cpx	Cpx	Opx	Cpx	Opx
SiO_2	56.48	54.12	57.00	54.51	56.28	56.91	54.72	57.36	53.24	53.48	52.82	54.96	52.97	54.08
Al_2O_3	2.23	1.55	1.72	0.89	1.39	1.21	0.98	1.00	2.29	1.67	2.32	2.22	2.16	3.25
Cr_2O_3	0.73	0.44	0.52	0.40	0.38	0.45	0.49	0.43	0.46	0.50	0.46	0.18	0.38	0.35
MgO	35.01	17.83	34.96	17.84	34.76	34.95	17.72	34.94	16.65	17.22	16.14	30.25	17.08	30.13
FeO	5.60	1.70	5.47	1.47	6.02	6.46	2.02	5.75	2.54	2.55	3.53	11.61	3.35	11.01
MnO	0.06	0.05	0.10	0.04	0.11	0.07	BDL	0.08	0.04	0.12	0.08	0.23	0.17	0.08
CaO	0.29	24.28	0.31	24.17	0.37	0.20	24.61	0.27	24.17	24.40	24.31	0.43	24.27	0.40
Na_2O	BDL	0.14	BDL	0.11	BDL	BDL	0.25	BDL	0.17	0.11	0.13	BDL	0.20	BDL
Total	100.40	100.11	100.08	99.43	99.31	100.25	100.79	99.83	99.56	100.05	99.79	99.88	100.58	99.30
Si	1.936	1.960	1.956	1.983	1.954	1.959	1.971	1.975	1.948	1.949	1.939	1.945	1.930	1.921
Al	0.090	0.066	0.070	0.038	0.057	0.049	0.042	0.041	0.099	0.072	0.100	0.092	0.083	0.136
Cr	0.020	0.013	0.014	0.012	0.011	0.012	0.014	0.012	0.013	0.014	0.013	0.005	0.011	0.010
Mg	1.789	0.962	1.789	0.968	1.799	1.793	0.951	1.794	0.907	0.935	0.882	1.596	0.926	1.594
Fe	0.161	0.052	0.157	0.045	0.175	0.186	0.061	0.166	0.078	0.078	0.108	0.344	0.102	0.327
Mn	0.002	0.002	0.003	0.001	0.003	0.002		0.002	0.001	0.004	0.003	0.007	0.005	0.003
Ca	0.011	0.942	0.012	0.942	0.014	0.007	0.950	0.010	0.946	0.952	0.955	0.016	0.946	0.015
Na		0.010		0.008			0.018		0.012	0.008	0.009		0.014	
Sum	4.009	4.007	4.001	3.997	4.013	4.008	4.007	4.000	4.004	4.012	4.009	4.005	4.027	4.006
Wo	0.5	48.2	0.6	48.2	0.7	0.4	48.4	0.5	49.0	48.5	49.1	0.8	47.9	0.8
En	91.3	49.2	91.4	49.5	90.5	90.3	48.5	91.1	47.0	47.6	45.3	81.6	46.9	82.3
Fs	8.2	2.6	8.0	2.3	8.8	9.4	3.1	8.4	4.0	3.9	5.6	17.6	5.2	16.9
Mg#	91.8	94.9	91.9	95.6	91.1	90.6	94.0	91.6	92.1	92.3	89.1	82.3	90.1	83.0

Mg# = Mg/(Mg+Fe) BDL = below detection limit

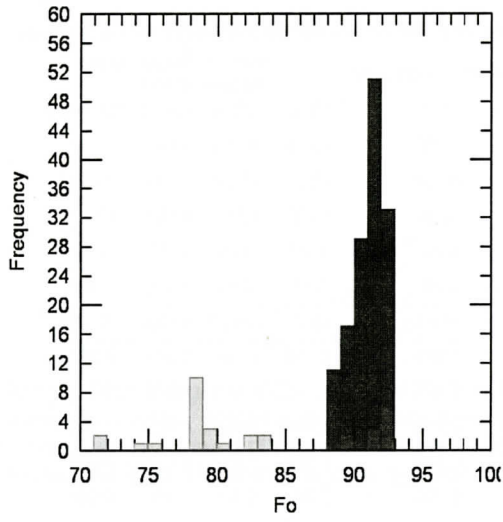

Figure 8. Histogram of olivine Fo in Webster-Addie metaultramafic rocks. Symbols: black, metadunites/metaharzburgites and metaorthopyroxenites; light gray, metawebsterites/metaclinopyroxenites.

phic mineral modes (Table 1), and (2) protoliths for most Cpx-rich rocks were probably olivine websterites or olivine clinopyroxenites. Interestingly, the normative mineralogy determined for edenite-tremolite metapyroxenite CG-2 is consistent with a websterite or olivine websterite protolith with subequal amounts of Opx and Cpx, a mineralogy similar to that of the type websterite (star, Figure 7).

MINERAL COMPOSITIONS

Representative electron microprobe mineral analyses of olivine, pyroxene, calcic amphibole, and spinel-group minerals are reported in Tables 3-6, respectively. Salient features of the mineral chemistry of the Webster-Addie metaultramafic rocks are summarized in Figs. 8-11. For the primary silicate minerals (olivine, Opx, Cpx), metamorphic recrystallization has resulted in extremely homogenized mineral compositions and crystals that are unzoned. In a given sample, individual minerals usually exhibit less than 1 mol% variation in Fo or Mg#. In some metawebsterites, there is greater (1-3 mol%) compositional variability within minerals. From the data in Tables 3 and 4 and the histograms in Figures 8 and 9 the following additional points emerge:

1. Olivine Fo and Opx Mg# are very similar, but Cpx Mg# is 3-7 mol% higher.

2. Mafic minerals in Cpx-rich rocks are more Fe-rich than in metaorthopyroxenites or metadunites (the latter are comparable). This is consistent with the lower Mg-numbers for metaclinopyroxenite and metawebsterite whole-rock analyses in Table 2.

As previously stated, calcic amphibole in Webster-Addie metaultramafic rocks typically consists of an edenite core rimmed by tremolite. Examination of the data in Table 5 shows that,

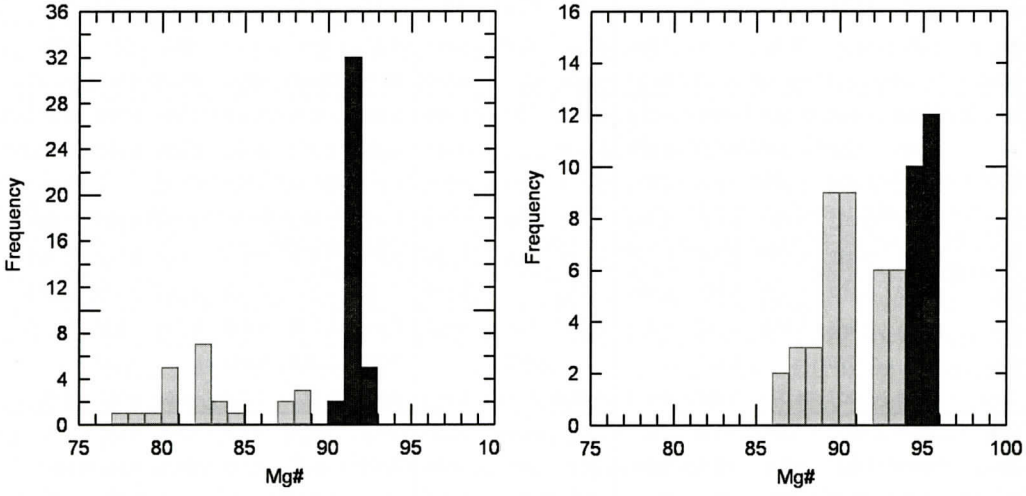

Figure 9. Histograms showing Mg# of Opx (left) and Cpx (right) in Webster-Addie metaultramafic rocks. Symbols: same as in Figure 8.

Table 5 Electron Microprobe Analyses of Amphiboles, Webster-Addie Metaultramafic Rocks

	Metadunite/Metaharzburgite				Meta-orthopyroxenite	Metaclinopyroxenite/ Metawebsterite				Edenite-Tremolite Metapyroxenite	
	WA-1A		WA-10		CG-1	WA-12		CG-3B		CG-2	
	edenite	tremolite	edenite	tremolite		edenite	tremolite	edenite	tremolite	edenite	tremolite
SiO_2	48.70	58.25	49.35	57.89	50.99	46.55	56.37	45.80	56.74	47.53	57.28
TiO_2	0.22	0.05	0.05	BDL	0.24	0.39	0.08	0.39	BDL	0.31	0.07
Al_2O_3	10.38	0.12	10.03	0.87	7.77	11.88	2.08	11.50	1.25	9.68	0.58
Cr_2O_3	1.20	BDL	1.75	0.27	1.78	0.83	0.18	0.89	0.13	1.02	0.16
MgO	19.25	24.06	19.50	23.96	20.40	17.24	21.62	18.34	22.77	19.82	23.40
FeO	2.48	1.78	2.54	1.51	2.76	5.97	3.33	4.78	3.37	2.55	1.49
MnO	BDL	0.05	BDL	0.05	0.06	0.06	0.05	0.07	BDL	0.05	0.05
CaO	12.05	13.00	12.41	13.21	12.85	12.95	13.90	12.31	13.08	13.38	13.79
Na_2O	2.15	0.16	1.85	0.21	1.62	1.98	0.20	2.74	0.41	2.16	0.15
Total	96.43	97.47	97.48	97.97	98.47	97.85	97.81	96.82	97.75	96.50	96.97
Si	6.861	7.962	6.885	7.878	7.052	6.600	7.769	6.551	7.814	6.748	7.890
Ti	0.023	0.005	0.005		0.025	0.042	0.008	0.042		0.033	0.007
Al	1.724	0.019	1.649	0.140	1.267	1.985	0.338	1.939	0.203	1.620	0.094
Cr	0.134		0.193	0.029	0.195	0.093	0.020	0.101	0.014	0.114	0.017
Mg	4.042	4.902	4.055	4.860	4.206	3.644	4.441	3.910	4.674	4.194	4.805
Fe	0.292	0.203	0.296	0.172	0.319	0.708	0.384	0.572	0.388	0.303	0.172
Mn		0.006		0.006	0.007	0.007	0.006	0.008		0.006	0.006
Ca	1.819	1.904	1.855	1.926	1.904	1.967	2.052	1.886	1.930	2.035	2.035
Na	0.587	0.042	0.500	0.055	0.434	0.544	0.053	0.760	0.109	0.595	0.040
Sum	15.481	15.044	15.389	15.066	15.409	15.591	15.071	15.768	15.132	15.649	15.067
Ca	29.6	27.2	29.9	27.7	29.6	31.1	29.8	29.6	27.6	30.8	28.3
Mg	65.7	69.9	65.3	69.9	65.4	57.7	64.6	61.4	66.8	64.2	69.0
Fe	4.7	2.9	4.8	2.5	5.0	11.2	5.6	9.0	5.5	5.0	2.7
Mg#	93.3	96.0	93.2	96.6	93.0	83.7	92.0	87.2	92.3	92.8	96.2

Mg# = Mg/(Mg+Fe) BDL = below detection limit

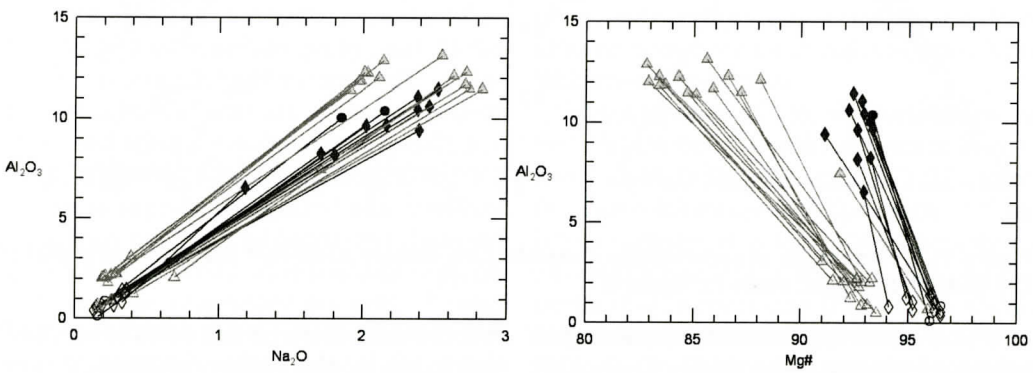

Figure 10. Composition of coexisting edenite (solid symbols) and tremolite (open symbols); lines connect core (edenite) and adjacent tremolite mantle. Symbols: same as Figure 6.

Table 6 Electron Microprobe Analyses of Spinel Group Minerals, Webster-Addie Metaultramafic Rocks

	Metadunite/Metaharzburgite					Metaortho pyroxenite		Metaclinopyroxenite/ Metawebsterite				
	WA-1B		WA-5	WA-10		CG-8	CG-1	CG-3B		WA-12	WA-13	WA-16B
	core	rim		core	rim							
SiO_2	0.03	0.02	BDL	0.03	0.04	0.04	0.04	0.05	BDL	0.03	0.03	0.08
TiO_2	0.21	0.31	BDL	BDL	BDL	0.25	0.15	BDL	2.24	0.12	0.09	BDL
Al_2O_3	13.12	5.03	6.75	19.96	27.29	10.31	15.69	49.43	0.42	42.11	52.96	49.89
Cr_2O_3	43.97	52.51	58.47	45.43	39.51	53.21	47.59	11.76	17.13	17.71	8.54	14.18
Fe_2O_3	10.57	9.84	4.54	3.16	2.19	6.19	4.04	3.03	46.20	5.34	1.84	2.10
FeO	25.05	26.86	22.79	20.80	19.50	22.62	24.54	21.14	31.27	23.55	22.91	18.36
MgO	5.67	3.65	6.51	9.11	10.94	7.17	6.04	11.43	0.76	9.57	10.89	13.68
Total	98.62	98.22	99.06	98.49	99.47	99.79	98.09	96.84	98.02	98.43	97.26	98.29
Si	0.001	0.001		0.001	0.001	0.001	0.001	0.001		0.001	0.001	0.002
Ti	0.006	0.008				0.006	0.004		0.065	0.003	0.002	
Al	0.528	0.214	0.276	0.760	0.987	0.411	0.625	1.671	0.019	1.463	1.765	1.643
Cr	1.188	1.500	1.605	1.161	0.959	1.423	1.271	0.267	0.522	0.413	0.191	0.313
Fe^{3+}	0.272	0.268	0.119	0.077	0.051	0.157	0.102	0.065	1.341	0.118	0.039	0.040
Fe^{2+}	0.716	0.812	0.662	0.562	0.501	0.640	0.693	0.508	1.009	0.580	0.542	0.433
Mg	0.289	0.197	0.337	0.439	0.501	0.362	0.304	0.489	0.044	0.420	0.459	0.569
Sum	3.000	3.000	2.999	3.000	3.000	3.000	3.000	3.001	3.000	2.998	2.999	3.000
Cr#	0.692	0.875	0.853	0.604	0.493	0.776	0.670	0.138	0.965	0.220	0.098	0.160
Mg#	0.288	0.195	0.338	0.438	0.500	0.361	0.305	0.491	0.042	0.420	0.459	0.570

Cr# = Cr/(Cr+Al); Mg# = Mg/(Mg+Fe) BDL = below detection limit

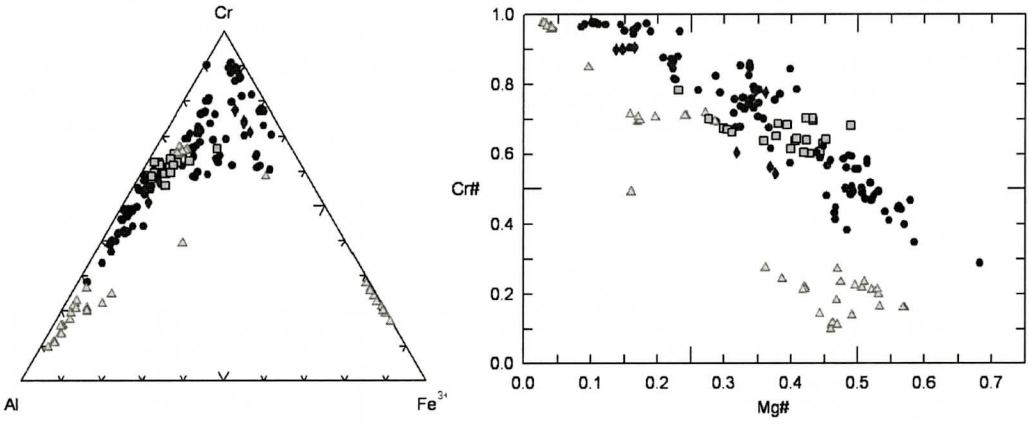

Figure 11. Composition of spinel-group minerals. Left, ternary Al-Cr-Fe^{3+} diagram; right, plot of Cr# vs Mg#. Symbols: same as Figure 6.

relative to coexisting tremolite, edenite is characterized by having higher Al_2O_3, Cr_2O_3, FeO, and Na_2O and lower SiO_2 and MgO (therefore, lower Mg#). Figure 10 graphically illustrates these relations. Note that amphiboles in Cpx-rich rocks are more Fe-rich (with lower Mg#) than in olivine-rich or Opx-rich rocks, thus reinforcing point (2) above.

In stark contrast to the associated silicates, spinel-group minerals exhibit tremendous com-

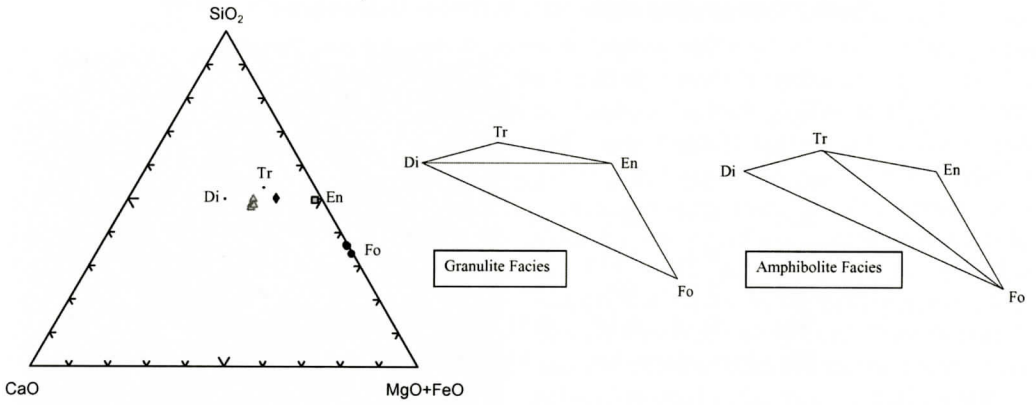

Figure 12. Plot of CaO-MgO-SiO_2 system (modified to include FeO) showing bulk-rock compositions of Webster-Addie samples (Table 2) with reference to end-member compositions of Cpx (Di), Opx (En), calcic amphibole (Tr) and olivine (Fo). Region bounded by Di-Tr-En-Fo is expanded at right to show chemography in granulite facies vs upper amphibolite facies (after Evans, 1977).

positional variability (Table 6, Figure 11). They include: (1) greenish brown, Al-rich spinels in metawebsterites; (2) reddish brown, intermediate Cr-Al spinels in chlorite-absent metadunites; (3) opaque, Cr-rich spinels in chlorite-bearing metadunites; and (4) chromian magnetite locally occurring with serpentine and in metaclinopyroxenite sample CG-3B. Furthermore, individual crystals may be zoned: usually, Cr/(Cr + Al) increases and Mg/(Mg + Fe) decreases from core to rim, but the reverse also occurs (Table 6). Progressive metamorphism is known to produce systematic changes in spinel compositions (Evans and Frost, 1975; Swanson and Raymond, this volume), with Al-poor spinels being characteristic of lower grade, hydrated assemblages, modest amounts of Al appearing at intermediate grades, and Al-rich spinels existing at high metamorphic grades. Complicating the story are the varied textural habits and mineral associations of spinels. Spinel in Webster-Addie metaultramafic rocks is present as large discrete grains (with or without associated chlorite), as inclusions (typically quite small) in olivine, as exsolutions in pyroxenes, and as secondary minerals formed through various metamorphic reactions. Differences in original tectonic setting and also in host rock compositions may also contribute to spinel compositional variability (Raymond and others, 2003; Swanson and others, 2006). For example, spinels in Cpx-rich rocks at Webster-Addie are more Fe-rich than spinels in metadunites (Figure 11).

METAMORPHISM OF CPX-RICH ROCKS

Recent studies have shown that Paleozoic metamorphism of olivine-rich metaultramafic rocks in the Blue Ridge Belt has involved a progressively retrograde sequence of metamorphic events marked by variable amounts of hydration (Abbott and Raymond, 1984; Swanson, 2001; Warner, 2001; Raymond, 2002, ch. 29; Raymond and others, 2003; Warner and Hepler, 2005). A similar history of retrograde metamorphism and accompanying hydration must have affected the pyroxene-rich rocks exposed in the Webster-Addie complex.

Metamorphism of Cpx-rich metaultramafic rocks is best modeled with reference to the system CaO-MgO-SiO_2 (Evans, 1977). The anhydrous protolith assemblage Cpx + Opx + olivine is here represented by the end-member compositions of diopside (Di), enstatite (En), and forsterite (Fo), respectively (Figure 12). Calcic amphibole, introduced by hydration accompanying metamorphism, is indicated by the end member, tremolite (Tr). Also plotted on this ternary diagram are the compositions of the samples analyzed in this study (Table 2). Note that

Table 7 Composition of Minerals in Olivine Metawebsterite, WA-12

	Cpx	Opx	Al-spinel	Olivine	Edenite	Tremolite
SiO_2	52.82	54.96	0.03	38.99	46.55	56.37
Al_2O_3	2.32	2.22	42.11	BDL	11.88	2.08
Cr_2O_3	0.46	0.18	17.71	BDL	0.83	0.18
FeO	3.53	11.61	28.50	19.67	5.97	3.33
MgO	16.14	30.25	9.57	40.91	17.24	21.62
CaO	24.31	0.43	BDL	BDL	12.95	13.90
Na_2O	0.13	BDL	NA	NA	1.98	0.20
Total	99.71	99.65	97.92	99.57	97.40	97.68

BDL = below detection limit NA = not analyzed

we have taken into account the Fe in the system by combining FeO with MgO. The bulk-rock compositions lie (as expected) in the Di + En + Fo field, with two samples (metaclinopyroxenite, CG-3B and edenite-tremolite metapyroxenite, CG-2) virtually plotting on the Di-En join.

As shown in Figure 12, the aforementioned Di-En join, which is stable under conditions of granulite grade metamorphism, is replaced by a tie line connecting Fo and Tr in the amphibolite facies (Evans, 1977). The corresponding metamorphic reaction (Bucher and Frey, 1994) is

$$5\ \text{En} + 2\ \text{Di} + H_2O \leftrightarrow \text{Fo} + \text{Tr} \quad (1)$$

As indicated by Bucher and Frey (1994), a more generalized reaction for the granulite facies to amphibolite facies transition in ultramafic rock is given by

$$\text{Opx} + \text{Cpx} + H_2O \leftrightarrow \text{Amphibole} + \text{Olivine} \quad (2)$$

Here, amphibole is a calcic amphibole that departs from the tremolite end-member composition (viz., edenite). Reaction (2) takes place at a higher temperature than reaction (1) and reflects the fact that the partitioning of "extra components" such as Al_2O_3 between Cpx and calcic amphibole results in a substantial increase in stability of the amphibole field towards higher temperatures (Evans, 1977; Bucher and Frey, 1994). Depending on the pressure, a difference of 35-50°C separates the above reactions, giving rise to an amphibolite-granulite facies transition zone characterized by the assemblage Cpx + Opx + olivine + calcic amphibole (Bucher and Frey, 1994). This assemblage, with the addition of small amounts of Al-rich spinel, is prevalent among the pyroxene-rich rocks sampled at Webster-Addie, and is the exclusive assemblage in samples (WA-12; WA-13; WA-16B,C) from the main metawebsterite body east of Webster (Table 1).

To more closely model the metamorphism of the Cpx-rich protolith rocks, we have listed in Table 7 the compositions of all minerals present in one sample (WA-12) from the main metawebsterite body. Although petrographic evidence indicates that calcic amphibole replaces Cpx (Figure 5B), it is apparent that clinopyroxene does not contain enough Na and Al to account for the modal amounts of edenite in the Webster-Addie rocks. Al-rich spinel, if involved in the edenite-forming reaction, can provide the necessary Al to form edenite. Yet, none of the protolith minerals contains sufficient Na_2O to form edenite, so that unless the original Cpx had a significant jadeite component (for which there is no evidence in the bulk rock chemistry), Na must have been added from elsewhere. Yang (2003) proposed that edenite could form from the recrystallization of clinopyroxene by the addition of a fluid enriched in Na. The metaultramafic rocks exposed in the quarries at Chestnut Gap and Addie are intruded by felsic pegmatite dikes (Ryan and others, 2005). These intrusions provide a likely source for metasomatic addition of Na, and we infer that they supplied the requisite Na to produce edenite. We therefore propose the following as a more complete reaction describing the conversion of Cpx to edenite:

$$\text{Cpx} + \text{Opx} + \text{Al-Cr spinel} + Na_2O\ (\text{fluid}) + H_2O \leftrightarrow \text{Edenite} + \text{Olivine} \quad (3)$$

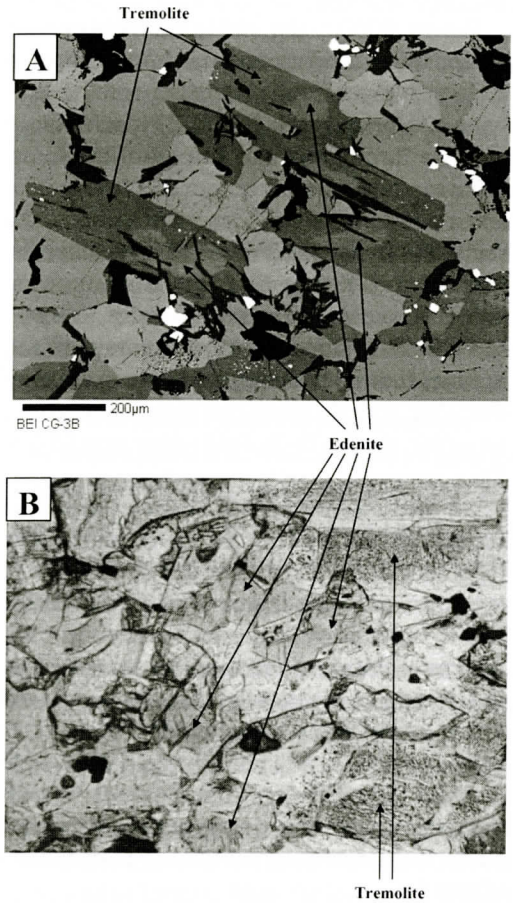

Figure 13. A) Backscattered electron image (bar gives scale) showing tremolite (darker) mantling edenite (metaclinopyroxenite, CG-3B). B) Photomicrograph (plane polarized light, long dimension ~ 1 mm) of calcic amphiboles in metaclinopyroxenite (CG-3B). Note abundance of minute, opaque spinel inclusions in tremolite versus lack thereof in associated edenite.

A reaction essentially equivalent to the above was postulated by Neal (1988) to account for the formation of pargasitic amphibole during metasomatism of spinel lherzolite xenoliths from the Solomon Islands. The amphibole in the lherzolite xenoliths is more sodic (3.4 – 4.8 wt% Na_2O) and slightly more aluminous than the edenite at Webster-Addie, but has comparable Mg#s, while the compositions of Cpx, Opx, and spinel are very similar.

Edenite was in turn partially retrograded to tremolite, as evidenced by tremolite rims surrounding edenite (Figure 13A). Replacement of edenite by tremolite releases Al_2O_3, Cr_2O_3, FeO and Na_2O (Table 7). The Al_2O_3, Cr_2O_3 and FeO combine (with some MgO) to form Cr-Al spinel. Petrographic evidence for this reaction is manifested by numerous tiny spinel inclusions that are typically present in tremolite (Figure 13B - the inclusions are too small to quantitatively analyze, but EDS spectra indicate they are chromite-rich spinels). Thus, the breakdown of edenite produces spinel, whereas spinel is consumed in the formation of edenite.

Conditions of Metamorphism

The absence of cummingtonite or anthophyllite in the olivine-rich metaultramafic rocks from the Webster-Addie complex provides a lower pressure limit for the metamorphism experienced by the Cpx-rich rocks under consideration. In the system $MgO\text{-}SiO_2\text{–}H_2O$, the upper pressure stability limit for anthophyllite coexisting with olivine (forsterite) is 7.7 ± 0.5 kb (Chernosky and others, 1985; Day and others, 1985). At higher pressures low-Ca amphibole is replaced by assemblages involving enstatite (Opx) and talc, as is reflected in the modes (Table 1) for olivine-rich rocks. The presence of Fe in amounts typical for ultramafic rock compositions extends the anthophyllite + olivine stability field to about 11 kb (Evans and Guggenheim, 1988). Thus, pressure during metamorphism of the Webster-Addie rocks must have exceeded 7.7 kb, and probably was at least 11 kb. For comparison, Quinn (1991) estimated that a peak pressure of 9 kb was reached during metamorphism of rocks from the surrounding Tallulah Falls Formation.

As noted earlier, the assemblage Cpx + Opx + olivine + calcic amphibole + Al-rich spinel found in the Cpx-rich rocks at Webster-Addie is characteristic of the amphibolite/granulite facies transition zone. At a pressure of 11 kb this assemblage is stable between temperatures of just under 800°C to an upper temperature limit of approximately 835°C, according to Figure 5.4 of Bucher and Frey (1994).

Metamorphism has produced exsolution la-

Table 8 Two-Pyroxene Temperatures for Webster-Addie Rocks.

Rock Type	Temperature
Metadunites	800°C ± 56°C
Metaharzburgite	798°C ± 62°C
Metaorthopyroxenites	821°C ± 37°C
Metawebsterites*	833°C ± 40°C

*Includes metaclinopyroxenite

Temperatures calculated after method of Wells (1977)

mellae in the pyroxenes, both Cpx exsolved from host Opx crystals (Figure 4A,B) and Opx exsolved from host Cpx crystals. Compositions of coexisting host and lamella allow estimation of metamorphic temperatures through application of the two-pyroxene geothermometer (Wells, 1977). The results (Table 8) yield temperatures ranging from 798°C to 833°C, with slightly higher temperatures recorded by pyroxene-rich rocks relative to metadunite and metaharzburgite. The two-pyroxene temperatures are thus in excellent agreement with temperatures estimated from the petrogenetic grid for ultramafic rock compositions (Figure 5.4 in Bucher and Frey, 1994). We therefore conclude that the Cpx-rich rocks experienced peak metamorphic conditions of 795-835°C at pressures at or just above 11 kb.

Over the temperature interval indicated above, the composition of calcic amphibole changes with decreasing temperature from an aluminous hornblende (edenite in our samples) to compositions approaching tremolite (Misch and Rice, 1975; Evans, 1977). The frequent presence of calcic amphiboles with edenite cores mantled by tremolite (Figure 13A) indicates that this reaction occurred, but did not go to completion. Possibly, some tremolite formed by partial replacement of edenite in a retrograde metamorphic event at a temperature below 800°C. Chlorite, which is present in less than a third of the pyroxene-rich samples, but in all the edenite-tremolite metapyroxenites, may have formed at this time, as it is stable to at least 800°C in ultramafic rock compositions (Bucher and Frey, 1994). Aluminum released by the breakdown of edenite could have promoted the growth of chlorite.

Below 800°C, the stable assemblage for compositions corresponding to the Cpx-rich rocks at Webster-Addie is Cpx + tremolite + olivine + chlorite (Evans, 1977). This assemblage persists throughout the amphibolite facies. Whereas talc appears at temperatures below about 670°C in olivine-rich compositions, the stable Fo-Tr tie line (Figure 12) precludes the formation of talc in Cpx-rich compositions. Talc is present in two metawebsterites, CG-14A and CG-17A (Table 1), but we attribute this to the fact that both samples contain more Opx than Cpx, with the result that their compositions lie within the Fo-Tr-Tc field rather than Di-Fo-Tr.

Serpentine (antigorite) becomes stable in metaultramafic rocks in the lower amphibolite to greenschist facies. Antigorite appears in metadunites when temperatures drop below 550°C (assemblage is olivine + tremolite + antigorite + chlorite), but formation of antigorite in Cpx-rich compositions does not occur until lower temperatures, when the Fo-Tr join is replaced by the Di-Atg join (Evans, 1977). Note that very few Webster-Addie Cpx-rich metaultramafic samples contain serpentine, in contrast to the extensively serpentinized metadunites (Table 1).

DISCUSSION

Nature of Protolith

The Webster-Addie complex is unique among metaultramafic bodies of the Blue Ridge Belt in that it contains a relatively large amount of Cpx-rich rocks. Based upon the normative data (Figure 7), olivine websterite and olivine clinopyroxenite appear to have been the dominant pyroxene-rich protolith rocks at Webster-Addie. We infer that the Cpx-rich rocks were derived from ultramafic cumulates formed in the lower (plutonic complex) portion of an ophiolite sequence (Coleman, 1977). Although stratigraphic position and relative volumes vary, ophiolite ultramafic cumulate complexes characteristically contain interlayered dunite, wehrlite, and various Cpx-rich cumulates

Table 9 Comparison to Cpx-rich Ophiolite Cumulate Rocks

	1	2	3	4
SiO_2	50.45	51.12	49.4	50.49-51.99
Al_2O_3	2.49	1.86	2.76	1.99-2.73
FeO	5.56	5.11	3.74	4.05-5.48
MgO	23.22	19.64	23.23	20.34-21.05
CaO	16.87	19.78	18.00	17.24-19.45
Na_2O	0.12	0.03	0.20	0.16-0.33
Cr (ppm)	2694	3229	4220	2624-3161
Ni	401	153	532	258-366
Mg#	88.2	87.3	91.7	87.2-89.9

Columns: 1 - Cpx-rich wehrlite, Bay of Islands ophiolite, Newfoundland (Komor et al., 1985); 2 - Olivine clinopyroxenite, Tekirova (Antalya) ophiolite, Turkey (Bağci et al., 2006); 3 - Cpx-ol adcumulate, Samail ophiolite, Oman (Smewing, 1981); 4 - Cpx-rich metaultramafic rocks, Webster-Addie (this paper). Mg# = Mg/(Mg+Fe)

(clinopyroxenite, olivine clinopyroxenite, websterite), together with minor chromitite layers (Coleman, 1977; Jackson and others, 1975; Elthon and others, 1982; Komor and others, 1985). The compositional similarity between Cpx-rich cumulates in ophiolites and the Cpx-rich metaultramafic rocks at Webster-Addie is indicated in Table 9. Note the low sodic content of the ophiolite cumulate rocks, which is consistent with the absence of a substantial jadeite component in the Cpx.

The interlayering of Cpx-rich or amphibole-rich rocks and metadunite observed at Chestnut Gap quarry (Figure 2A,C,D) very closely resembles the pervasive fine-scale layering displayed by ultramafic cumulates in the Bay of Islands ophiolite (Elthon and others, 1982). The layering at Bay of Islands is marked by sharp changes in mineralogy at a scale that can be less than a centimeter thick. Elthon and others (1982) also describe a coarser layering (termed megalenses) that is generally measured in hundreds of meters. This is comparable in scale at Webster-Addie to the main occurrence of metawebsterite near the town of Webster (Figure 1).

The whole-rock data (Table 2) reveal that the Cpx-rich metaultramafic rocks have lower Mg-numbers (87.2-89.9) than metadunite and metaorthopyroxenite (90.5-91.6). This is reflected in the compositions of olivine and pyroxene in the Webster-Addie complex, which are consistently more Fe-rich (lower Mg#) in metawebsterite and metaclinopyroxenite relative to metadunite, metaharzburgite and metaorthopyroxenite (Figures 8, 9). This relationship is consistent with mineral chemical data for ophiolites, as olivines and pyroxenes in Cpx-bearing ultramafic cumulate rocks are more Fe-rich than in the basal metamorphic dunites (Coleman, 1977). Thus, the field occurrence, whole-rock composition, and mineral chemistry of the Cpx-rich metaultramafic rocks at Webster-Addie are compatible with an origin as part of the ultramafic cumulate section of an ophiolite, now dismembered. After emplacement, the mineral compositions were buffered by the bulk rock compositions during metamorphism.

Rarity of Cpx-rich Metaultramafics

With the prominent exception of the Webster-Addie complex, clinopyroxene-bearing metaultramafic rocks are rare in the Blue Ridge Belt of western North Carolina and northern Georgia. In part this may be due to the fact that the metaultramafic bodies primarily were derived from the basal tectonite portions of dismembered ophiolites. As such, they are dominated by metadunite, but may also contain minor olivine-rich metaharzburgite. The Webster-Addie complex is unique in that, in part or in whole, it was derived from the overlying ultramafic cumulate section. Certainly, this accounts for the relative abundance of clinopyroxene in the Webster-Addie metaultramafic rocks.

A characteristic feature of the pyroxene-rich rocks at Webster-Addie is the presence of calcic amphibole. It is found in nearly all Cpx-rich rocks, in which it is frequently quite plentiful (Table 1), and it is the dominant mineral in edenite-tremolite metapyroxenites. Calcic amphibole is particularly common at Chestnut Gap quarry. There, gray-green rocks interlayered with metadunite (Figure 2C) contain varying

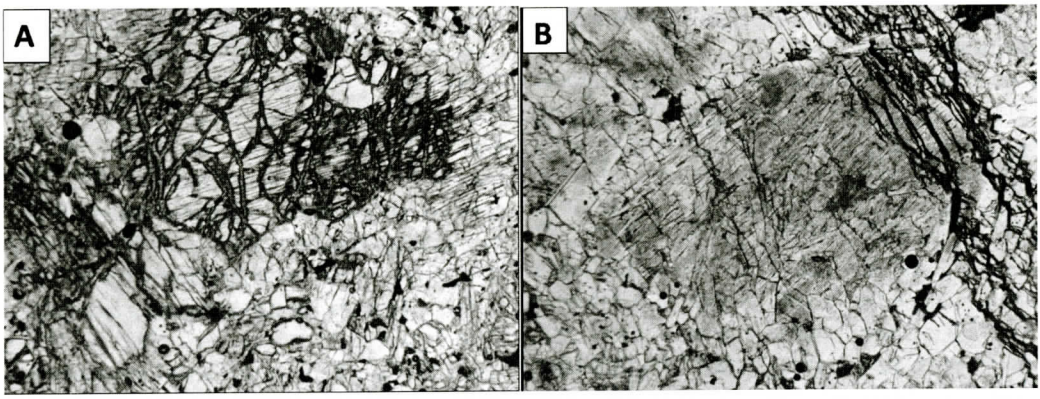

Figure 14. Photomicrographs (plane polarized light, long dimension ~ 3 mm) showing stages in calcic amphibole replacement of pyroxene. A) Cpx crystal in WA-16A partially replaced by calcic amphibole. Note that orientation of spinel lamellae in Cpx is retained in surrounding amphibole. B) Pyroxene completely replaced by calcic amphibole (edenite-tremolite metapyroxenite, CG-2). Outline of original pyroxene crystal is preserved by oriented spinel inclusions in the amphibole.

proportions of calcic amphibole and Cpx, and apparently grade from amphibole-bearing metawebsterite or metaclinopyroxenite to nearly pure amphibole rocks. In some thin sections, calcic amphibole clearly is replacing Cpx (Figure 5B). As shown in Figure 14A, Cpx porphyroclasts may contain spinel lamellae. In the process of Cpx being converted to calcic amphibole, the orientation of the spinel lamellae is retained in the surrounding amphibole. In those samples in which Cpx is no longer present (e.g., some edenite-tremolite metapyroxenites), the former outlines of individual Cpx crystals can be discerned by the abundance and orientation of spinel lamellae preserved in the replacing amphibole (Figure 14B). This texture makes a good case for the relict nature of the amphibole-rich rocks as former clinopyroxenites.

Whereas Blue Ridge metaultramafic bodies rarely contain Cpx, calcic amphibole is commonly present (Warner and others, 2006). For example, at nearby Dark Ridge, metadunites contain as much as 4% calcic amphibole in the mode, and associated metaharzburgites average between 7 and 8% modal calcic amphibole, with some samples having 10-15% (Warner and Hepler, 2005). Calcic amphibole occurs in more than half of the metadunite samples from Buck Creek examined by Warner (2001). Interestingly, calcic amphiboles at both Buck Creek and Dark Ridge typically are characterized by composite crystals consisting of edenite (or tremolitic hornblende) cores and tremolite rims, a relationship similar to that observed at Webster-Addie (Figure 13A). Unless calcium was added during hydration and metamorphism of the rocks (Scotford and Williams, 1983), a primary Ca-bearing mineral (presumably Cpx) must have been present in the ultramafic protoliths.

CONCLUSIONS

The Webster-Addie ultramafic complex consists primarily of metadunite, but, unique to metaultramafic bodies of the Blue Ridge Belt, also contains significant clinopyroxene-rich rocks (chiefly metawebsterite and olivine metaclinopyroxenite). The latter occur as layers and lenses in the metadunite, ranging in thickness from a few millimeters to tens of meters. Compositional and structural (layering) characteristics are similar to those found in the ultramafic cumulate portion of an ophiolite.

Metamorphism of the clinopyroxene-rich rocks has produced the assemblage clinopyroxene (Cpx) + orthopyroxene (Opx) + olivine + calcic amphibole + Al-rich spinel, which marks the transition between granulite and amphibolite facies metamorphism. Both Cpx and Opx show extensive exsolution related to metamorphic recrystallization. Two-pyroxene geothermometry combined with the absence of

cummingtonite/anthophyllite in associated metadunites indicates peak metamorphic conditions were 795-835°C at ~11 kb, typical of high-P granulite facies.

Various stages of replacement of Cpx by calcic amphibole exist. Initially, edenite formed at the expense of Cpx. Later, edenite was, in part, retrograde metamorphosed to tremolite, resulting in composite calcic amphibole crystals with edenite cores mantled by tremolite. A similar origin is proposed for calcic amphiboles found in other Blue Ridge metaultramafic bodies.

The appearance of mesh texture and vein serpentinite in associated metadunites and metaharzburgites indicate a late-stage greenschist facies metamorphism that affected the pyroxene-rich Webster-Addie rocks to a lesser extent. Thus, three stages of metamorphism – the highest granulite grade best represented by Cpx-rich rocks and two retrograde amphibolite and greenschist facies events represented by formation of tremolite and serpentine, respectively – mark the post-igneous history of the ultramafic rocks. Such a retrograde history is consistent with the Paleozoic metamorphic history of the Blue Ridge rocks as a whole (Adams and Trupe, 1997; Raymond and others, 2003).

ACKNOWLEDGMENTS

Chris Fleisher, University of Georgia, provided invaluable assistance in the microprobe analyses. Our long-time friend and colleague, Loren Raymond, has greatly contributed to our understanding of Blue Ridge metaultramafic rocks, and we are indebted to him for a careful review which has substantially improved this manuscript.

REFERENCES CITED

Abbott, R.N., Jr., and Raymond, L.A., 1984, The Ashe metamorphic suite, northwest North Carolina: Metamorphism and observations on geologic history: American Journal of Science, v. 284, p. 350-375.

Adams, M.G., and Trupe, C.H., 1997, Conditions of timing and metamorphism in the Blue Ridge Thrust Complex, northwestern North Carolina and eastern Tennessee, *in* Stewart, K.G., Adams, M.G., and Trupe, C.H., eds., Paleozoic structure, metamorphism, and tectonics of the Blue Ridge of western North Carolina: Carolina Geological Society Annual Field Trip Guidebook, p. 33-47.

Bağci, U., Parlak, O., and Höck, V., 2006, Geochemical character and tectonic environment of ultramafic to mafic cumulate rocks from the Tekirova (Antalya) ophiolite (southern Turkey): Geological Journal, v. 41, p. 193-219.

Bence, A.E., and Albee, A.L., 1968, Empirical correction factors for the electron microanalysis of silicates and oxides: Journal of Geology, v. 76, p. 382-403.

Berger, S., Cochrane, D., Simons, K., Savov, I., Ryan, J.G., and Peterson, V.L., 2001, Insights from rare-earth elements into the genesis of the Buck Creek Complex and other Blue Ridge ultramafic bodies: Southeastern Geology, v. 40, p. 201-212.

Boudier, F., and Nicolas, A., 1985, Harzburgite and lherzolite subtypes in ophiolitic and oceanic environments: Earth and Planetary Science Letters, v. 76, p. 84-92.

Bucher, K., and Frey, M., 1994, Petrogenesis of Metamorphic Rocks: Springer-Verlag, Berlin, 318 pp.

Chernosky, J.V., Jr., Day, H.W., and Caruso, L.J., 1985, Equilibria in the system MgO-SiO_2–H_2O: Experimental determination of the stability of mg-anthophyllite: American Mineralogist, v. 70, p. 223-236.

Coleman, R.G., 1977, Ophiolites – Ancient Oceanic Lithosphere?: Springer-Verlag, Berlin, 229 pp.

Cronin, T.P., 1983, Petrogenesis of the Webster-Addie ultramafic body, Jackson County, North Carolina [MS thesis]: Knoxville, University of Tennessee, 112 pp.

Day, H.W., Chernosky, J.V., and Kumin, H.J., 1985, Equilibria in the system MgO-SiO_2–H_2O: a thermodynamic analysis: American Mineralogist, v. 70, p. 237-248.

Elthon, D., Casey, J.F., and Komor, S., 1982, Mineral chemistry of ultramafic cumulates from the North Arm Massif of the Bay of Islands ophiolite: Evidence for high-pressure crystal fractionation of oceanic basalts: Journal of Geophysical Research, v. 87, p. 8717-8734.

Evans, B.W.,1977, Metamorphism of alpine peridotite and serpentinite: Annual Review of Earth Planetary Sciences, v. 5, p. 397-447.

Evans, B.W., and Frost, B.R., 1975, Chrome-spinel in progressive metamorphism – a preliminary analysis: Geochimica et Cosmochimica Acta, v. 39, p. 959-972.

Evans, B.W., and Guggenheim, S., 1988, Talc, pyrophyllite, and related minerals, *in* Bailey, S.W. ed., Hydrous Phyllosilicates, Mineralogical Society of America, Reviews in Mineralogy, v. 19, p. 225-294.

Hatcher, R.D., Jr., Hooper, R.J., Petty, S.M., and Willis, J.D., 1984, Structure and chemical petrology of three southern Appalachian mafic-ultramafic complexes and their bearing upon the tectonics of emplacement and origin of Appalachian ultramafic bodies: American Journal of Science, v. 284, p. 494-506.

Hess, H.H., 1955, Serpentines, orogeny, and epeirogeny: Geological Society of America Special Paper 62, p. 391-408.

Hunter, C.E., 1941, Forsterite olivine deposits of North Carolina and Georgia: North Carolina Department of Con-

servation and Development, Division of Mineral Resources Bulletin 41, 117 pp.

Hunter, C.E., Murdock, T.G., and MacCarthy, G.R., 1942, Chromite deposits of North Carolina: North Carolina Department of Conservation and Development, Division of Mineral Resources Bulletin 42, 39 pp.

Jackson, E.D., Green, H.W., and Moores, E.M., 1975, The Vourinos ophiolite, Greece: Cyclic units of lineated cumulates overlying harzburgite tectonite: Geological Society of America Bulletin, v. 86, p. 390-398.

Kelsey, C.H., 1965, Calculation of the C.I.P.W. norm: Mineralogical Magazine, v. 34, p. 276-282.

Komor, S.C., Elthon, D., and Casey, J.F., 1985, Mineralogic variations in a layered ultramafic cumulate sequence at the North Arm Mountain massif of the Bay of Islands ophiolite, Newfoundland: Journal of Geophysical Research, v. 90, p. 7705-7736.

Larrabee, D.M., 1966, Map showing distribution of ultramafic and intrusive mafic rocks from northern New Jersey to eastern Alabama: US Geological Survey Map, I-476.

Lipin, B.R., 1984, Chromite from the Blue Ridge province of North Carolina: American Journal of Science, v. 284, p. 507-529.

Madison, J.A., 1968, Petrology and geochemistry of the Webster-Addie ultramafic body, Jackson County, North Carolina [PhD thesis]: St Louis, Washington University, 139 pp.

McElhaney, M.S., and McSween, H.Y., Jr., 1983, Petrology of the Chunky Gal Mountain madic-ultramafic complex, North Carolina: Geological Society of America Bulletin, v. 94, p. 855-874.

McIlmoil, R.D., Ryan, J., and Ranson, W.R., 2002, The nature and origin of orthopyroxenite lenses and layers in dunites from the Chestnut Gap quarry, Sylva South quadrangle, Jackson County, NC: Geological Society of America, Abstracts with Programs, v. 34, no 2, p. A-81.

McSween, H.Y., Jr., and Hatcher, R.D., Jr., 1985, Ophiolites (?) of the southern Appalachian Blue Ridge, *in* Woodward, N.E., ed., Field trips in the southern Appalachians: University of Tennessee, Department of Geological Sciences, Studies in Geology, v. 9, p. 144-170.

Miller, R., III, 1951, The structure and petrology of the Webster-Addie ultrabasic ring, Jackson County, North Carolina [PhD thesis]: Princeton, Princeton University, 39 pp.

Miller, R., III, 1953, The Webster-Addie ultramafic ring, Jackson County, North Carolina, and secondary alteration of its chromite: American Mineralogist, v. 38, p. 1134-1147.

Misch, P., and Rice, J.M., 1975, Miscibility of tremolite and hornblende in progressive Skagit metamorphic suite, North Cascades, Washington: Journal of Petrology, v. 16, p. 1-21.

Misra, K.C., and Keller, F.B., 1978, Ultramafic bodies in the southern Appalachians: A review: American Journal of Science, v. 278, p. 389-418.

Murdock, T.G., and Hunter, C.E., 1946, The vermiculite deposits of North Carolina: North Carolina Department of Conservation and Development, Division of Mineral Resources Bulletin 50, 44 pp.

Neal, C.R., 1988, The origin and composition of metasomatic fluids and amphiboles beneath Malaita, Solomon Islands: Journal of Petrology, v. 29, p. 149-179.

Nicolas, A., and Boudier, F., 2003, Where ophiolites come from and what they tell us, *in* Dilek, Y., and Newcomb, S., eds., Ophiolite concept and the evolution of geological thought, Geological Society of America Special Paper 373, p. 137-152.

Peterson, V., Ryan, J., Yurkovich, S., Burr, J., and Kruse, S., 2006, The petrogenesis and tectonic implications of Blue Ridge mafic-ultramafic rocks: The Buck Creek and Carroll Knob complexes, and rocks of the Addie-Willets region, *in* Labotka, T.C., and Hatcher, R.D., Jr., eds., 2006 Southeastern Section meeting, Geological Society of America, field trip 5, p. 101-127.

Pike, J.E.N., 1968, Petrology and genesis of the Webster-Addie ultramafic body, Jackson County, North Carolina [MS thesis]: Ann Arbor, University of Michigan, 64 pp.

Pratt, J.H., and Lewis, J.V., 1905, Corundum and the peridotites of North Carolina: North Carolina Geological Survey, Volume I, 464 pp.

Quinn, M.J., 1991, Two lithotectonic boundaries in western North Carolina: Geological interpretation of a region surrounding Sylva, North Carolina [MS thesis]: Knoxville, University of Tennessee, 223 pp.

Raymond, L.A., 2002, Petrology: the Study of Igneous, Sedimentary, and Metamorphic Rocks (2nd ed): McGraw-Hill, Boston, 720 pp.

Raymond, L.A., and Abbott, R.N., 1997, Petrology and tectonic significance of ultramafic rocks near the Grandfather Mountain window in the Blue Ridge Belt, Toe terrane, western Piedmont zone, North Carolina, *in* Stewart, K.G., Adams, M.G., and Trupe, C.H., eds., Paleozoic structure, metamorphism, and tectonics of the Blue Ridge of western North Carolina: Carolina Geological Society Annual Field Trip Guidebook, p. 67-85.

Raymond, L.A., Love, A., and McCarter, R., 2001, Petrology of the Hoots ultramafic body, Blue Ridge Belt, northwestern North Carolina: Southeastern Geology, v. 40, p. 149-162.

Raymond, L.A., Swanson, S.E., Love, A.L., and Allan, J.F., 2003, Cr-spinel compositions, metadunite petrology, and the petrotectonic history of Blue Ridge ophiolites, southern Appalachian orogen, USA, *in* Dilek, Y., and Robinson, P.T., eds., Ophiolites in Earth History: Geological Society of London Special Publication 218, p. 253-278.

Raymond, L.A., and Warner, R.D., 2001, Preface (to Selected ultramafic and related rocks of the southern Appalachian orogen: Petrology and tectonic significance): Southeastern Geology, v. 40, p. i.

Ross, C.S., and Shannon, E.V., 1926, Nickeliferous vermiculite and serpentine from Webster, North Carolina:

American Mineralogist, v. 11, p. 90-93.

Ross, C.S., Shannon, E.V., and Gonyer, F.A., 1928, The origin of nickel silicates at Webster, North Carolina: Economic Geology, v. 23, p. 528-552.

Ross, C.S., Shannon, E.V., and Gonyer, F.A., 1929, Is chromite always a magmatic segregation product?: Economic Geology, v. 24, p. 641-645.

Ryan, J.G., Yurkovich, S., Peterson, V., Burr, J., and Kruse, S., 2005, Geology and petrogenesis of mafic and ultramafic rocks of the Willets-Addie area, central Blue Ridge, NC, *in* Hatcher, R.D., Jr., and Merschat, A.J., eds., Blue Ridge geology geotraverse east of the Great Smoky National Park, western North Carolina: North Carolina Geological Survey, Carolina Geological Society Annual Field Trip Guidebook, p. 91-98.

Scotford, D.M., and Williams, J.R., 1983, Petrology and geochemistry of metamorphosed ultramafic bodies in a portion of the Blue Ridge of North Carolina and Virginia: American Mineralogist, v. 68, p. 78-94.

Smewing, J.D., 1981, Mixing characteristics and compositional differences in mantle-derived melts beneath spreading axes: Evidence from cyclically layered rocks in the ophiolite of North Oman: Journal of Geophysical Research, v. 86, p. 2645-2659.

Streckeisen, A.L., 1973, Plutonic rocks, classification and nomenclature recommended by the IUGS subcommission on the systematics of igneous rocks: Geotimes, v. 18, p. 26-30.

Swanson, S.E., 1980, Petrology of the Rich Mountain ultramafic and associated rocks, Watauga County, North Carolina: Southeastern Geology, v. 21, p. 209-225.

Swanson, S.E., 2001, Ultramafic rocks of the Spruce Pine area, western North Carolina: a sensitive guide to fluid migration and metamorphism: Southeastern Geology, v. 40, p. 163-182.

Swanson, S.E., and Warner, R.D., 2001, Pyroxene-rich rocks of the Webster-Addie complex, western North Carolina: Geological Society of America, Abstracts with Programs, v. 33, No 7, p. A31.

Swanson, S.E., Warner, R.D., and Raymond, L.A., 2006, Chromite and other spinels from metaultrafic rocks in the Cartoogechaye Terrane of North Carolina: Geological Society of America, Abstracts with Programs, v. 38, No 3, p. 80-81.

Swanson, S.E., Raymond, L.A., Warner, R.D., Ryan, J.G., Yurkovich, S.P., and Peterson, V.L., 2005, Petrotectonics of mafic and ultramafic rocks in Blue Ridge terranes of western North Carolina and northern Georgia, *in* Hatcher, R.D., Jr., and Merschat, A.J., eds., Blue Ridge geology geotraverse east of the Great Smoky National Park, western North Carolina: North Carolina Geological Survey, Carolina Geological Society Annual Field Trip Guidebook, p. 73-90.

Warner, R.D., 2001, Mineralogy and petrology of metaultramafic rocks at Buck Creek, North Carolina: Southeastern Geology, v. 40, p. 183-200.

Warner, R.D., and Hepler, C.W., 2005, Petrology of the Dark Ridge metaultramafic body, North Carolina, *in* Hatcher, R.D., Jr., and Merschat, A.J., eds., Blue Ridge geology geotraverse east of the Great Smoky National Park, western North Carolina: North Carolina Geological Survey, Carolina Geological Society Annual Field Trip Guidebook, p. 99-112.

Warner, R.D., and Swanson, S.E., 2000, Mineralogy and petrology of ultramafic rocks from the Webster-Addie area: a preliminary assessment: Geological Society of America, Abstracts with Programs, v. 32, No 2, p. 80-81.

Warner, R.D., Swanson, S.E., and Raymond, L.A., 2006, Where are the Cpx-bearing rocks in Blue Ridge metaultramafic rock bodies?: Insights from the Webster-Addie complex, NC: Geological Society of America, Abstracts with Programs, v. 38, No 7, p. 562.

Wells, P.R.A., 1977, Pyroxene thermometry in simple and complex systems: Contributions to Mineralogy and Petrology, v. 62, p. 129-139.

Williams, G.H., 1890, The non-feldspathic intrusive rocks of Maryland and the course of their alteration: American Geologist, v. 6, p. 35-50.

Yang, J.-J., 2003, Relict edenite in a garnet lherzolite from the Chinese Su-Lu UHP metamorphic terrane: Implications for metamorphic history: American Mineralogist, v. 88, p. 180-188.

SOUTHEASTERN GEOLOGY
V. 47, No.3, August 2010, p. 147-172

PETROGENESIS OF CHROMITE IN METAULTRAMAFIC ROCKS OF THE SPRUCE PINE AREA, NORTH CAROLINA

SAMUEL E. SWANSON

Department of Geology
University of Georgia
Athens, GA 30602-2501

LOREN A. RAYMOND

Department of Geology
Appalachian State University
Boone, NC 30602

ABSTRACT

Chromian spinels record petrogenetic processes in their chemistry. To date, no systematic study of Cr-spinel chemical changes in a polymetamorphic setting has demonstrated a high- to low-grade progression of changes through a facies series. Here, we analyze the retrograde metamorphism of ultramafic rocks, in the Blue Ridge Belt of the southern Appalachian Orogen, that followed a retrograde path from eclogite to low greenschist facies conditions. Over this range of metamorphic grades, the chromian spinels of high olivine, eclogite/upper amphibolite facies rocks (metadunites) that are aluminous, low Ti chromites of moderate magnesium and chrome number, change to iron-enriched, low Al, low Mg number, higher Cr number spinels (chromian magnetites) with approximately one percent TiO_2 in moderate to low olivine rocks of the lower amphibolite facies. Under lower grade greenschist facies conditions in hydrous analogues of the olivine rocks C serpentinites C the spinels are Al, Mg, and Ti deficient end member magnetites. The spinel chemical changes accompany a four stage, retrogressive, hydrous metamorphic path through P,T space. Initial igneous spinel chemistries, perhaps reflected by core chemistries of the highest grade spinels, suggest a suprasubduction zone or subarc petrogenetic setting. Metamorphism of spinel-bearing metaultramafic rocks would require introduction of chromium, if the spinels were to follow a duplicate, but prograde path to higher grade chemistries.

INTRODUCTION

Chromian spinel is a important recorder of petrogenetic processes in mafic and ultramafic igneous systems (e.g. Irvine, 1967; Gole et al,1987, Dick and Bullen, 1984; Roeder, 1994; Barnes, 1998; Barnes and Roeder, 2001; Kamenetsky et al, 2001). Chromian spinels are also known to recrystallize during serpentinization of ultramafic rocks at the lowest grades of metamorphism (Evans and Frost, 1975) and several studies document the recrystallization of chromian spinel at various metamorphic grades (e.g., Medaris, 1975; Barnes, 2000). Some studies note the lack of textural equilibrium in chromite with rims of chromian magnetite on chromite cores (e.g., Ulmer, 1974; Bliss and MacLean, 1975, Hoffman and Walker, 1978). Here, we evaluate the compositional response of chromian spinel to polyphase metamorphism and evaluate this mineral phase as a recorder of the petrogenetic history of ultramafic rocks from the Blue Ridge of North Carolina.

Previous studies of Blue Ridge Belt ultramafic rocks from the Spruce Pine area (e.g., Swanson, 1981; Raymond, 1995; Swanson, 2001; Raymond et al., 2003a) and the enclosing schists and gneisses (Butler, 1972; Adams and Trupe., 1997) documented multiple metamorphic events under a variety of conditions including rare, relict eclogite facies, wide-spread amphibolite facies, and minor greenschist facies conditions. In the Blue Ridge metaultra-

Table1 Modal data for metaperidotites (volume percent)

Sample #	olivine	opx[1]	crsp[1]	chlorite	tremolite	cumm[1]	talc	serp[1]	other
97BR7A	tr		2.7	95.7		0.3	1.3		tr carb[1]
MSP37D			2.7	25.3			72.0		
MSP37E			0.7	42.3		8.0	49.0		
MSP16B1			1.7	11.0	8.3	40.0	39.0		
MSP16C3			0.7	34.3		33.3	31.7		
DB71A	82.3	3.3	tr	11.8		1.3		1.3	
DB72A	81.9		0.7	5.3	2.0	1.3	1.0	0.7	
DB134B	91.7		1.8	1.2	tr			5.3	
DB150	79.3		16.7	2.0	tr		1.0	1.0	
DB151	63.0		1.0	28.7	3.0		3.3	0.7	0.3 antig[1]
DB153	82.7	3.0	2.0	1.7	tr	4.7	4.6	1.3	
DB154A	85.6		3.3	2.2				8.9	
F2A	84.0	9.0	tr	3.0	0.7			3.3	
F19	36.0	11.7	3.3	5.0		0.3	0.7	34.7	8.3 mag[1]
F21			35.7	48.7		15.6			
F84-5	72.3	9.3	1.0	4.0	tr	tr		13.3	
F84-7	45.7	21.7	3.7	3.0	tr		0.7	25.3	
F84-8	57.0	tr	0.3	tr	39.3	tr-w	1.0	0.3	2.0 mag[1]
F84-10	41.7	m	1.7	1.0	27.3		0.3	tr	28.0 mag[1]
HC2A	98.0		tr	0.7	0.7			0.7	
HC5	96.3		0.3	0.7	0.3		tr	1.7	
HC7	53.0	29.0	tr	9.3	3.0	4.0	1.3	0.3	
HC11	41.3	20.7	0.7	6.3	20.3	7.7		3.0	
MC6	59.0		0.7	0.3	0.3			39.6	
NA4	46.3		0.3	7.0		45.3	1.0		
ND2	88.7		0.7	tr			2.0	8.3	tr mag[1],antig[1]
ND6	65.7	3.0	1.7	2.0			17.7	10.0	tr antig[1]
ND8	83.3		3.0	0.3	0.7		2.0	7.3	3.3 mag[1]
ND20	82.7		6.0	tr	tr			11.3	0.3 mag[1]
ND22	66.7	2.7	tr	tr	tr		2.7	27.7	0.3 mag[1]
NDCr	81.7		8.0	tr			1.0	9.3	
NV2			0.7	7.3	14.0	76.0			
NV4	1.0		tr	20.0	tr cores	73.7	3.7		
PGC3	50.0	3.3	0.7	1.7	1.3		1.0	42.0	
SE19	71.2	8.0	tr	4.7	0.4			12.8	
SP1	48.3		1.3	2.7		6.0	10.3	28.3	0.3 antig[1]
SP2	31.0		5.0	2.3	3.3	4.6	5.0	48.8	

Table1 cont., Modal data for metaperidotites (volume percent)

MSP52F	52.0		6.0	tr		tr	0.7	38.3
W1			8.3	45.3	5.3	41.1		
W3	32.7		5.0	4.3				58.0
W4	36.0		1.7	5.3				57.0
W8			12.0	5.3		82.7		
W9			38.0	38.7				23.3
MSP57HH	31.7	31.3	5.3	4.0	tr		17.0	10.7

[1] opx = enstatite, crsp = chromite (+magnetite+ilmenite), cumm/antho = low-Ca amphibole, serp = serpentine, carb = magnesite, antig = antigorite

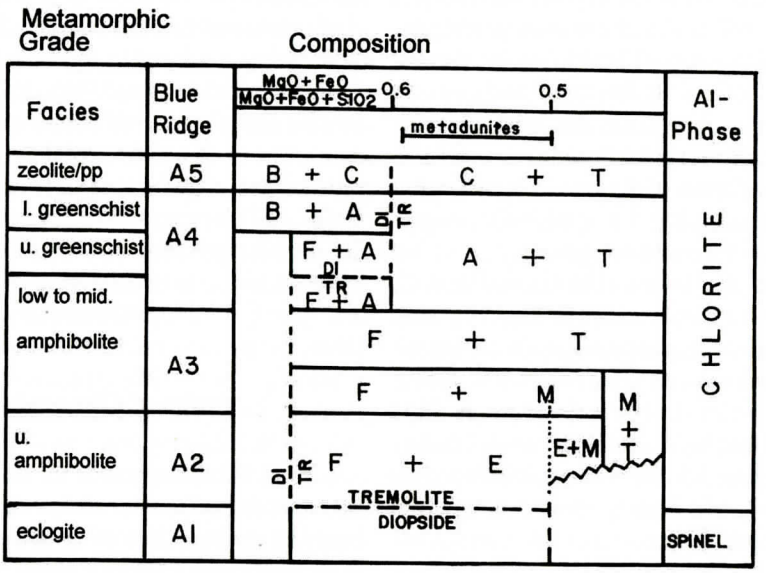

Figure 1. Relation of mineral associations in Spruce Pine metadunites to mineral assemblages in metaultramafic rocks at various metamorphic grades in the Alps (modified from Trommsdorff and Evans, 1974). The range of composition of Spruce Pine metadunites (shown on the figure) is based on data from Hunter (1941), Carpenter and Chen (1978), and Sharpe (1979). (A = antigorite, B = brucite, C = chrysotile, Di = diopside, E = enstatite, F = forsterite, M = magnesiocummingtonite/anthophyllite, T = talc, Tr = tremolite).

mafic rocks Raymond (1995; 2002) and Raymond and Abbott (1997) documented five mineral associations (A1 to A5, Figs. 1, 2) related to retrograde hydration and recrystallization spanning this range of conditions. The associations range from high grade, olivine-rich assemblages (A1 = olivine + chromite ± ortho- and clinopyroxene; A2 = olivine + chromite ± ortho- and clinopyroxene ± tremolite ± chlorite) to lower grade assemblages containing amphiboles with moderate amounts to little or no relict olivine (A3 = ± chlorite ± anthophyllite ± tremolite ± magnesite ± talc ± magnetite). Low grade serpentine-bearing associations are distinguished based on the serpentine mineralogy, but include some monomineralic veins of other minerals (A4 = ± serpentine [antigorite] ± talc ± chlorite ± magnetite ± tremolite; A5 = serpentine [± chrysotile ± lizardite] ± magnetite ± talc ± chlorite ± tremolite ± opal ± or a variety of other low temperature phases (e.g., Tien, 1977). Typically, lower grade associations overprint higher grade associations in the same sample (Table 1). Garnet and phlogopite, originally included in the A3 association (Raymond, 1995) are restricted to metasomatic reaction

zones between ultramafic rocks and the enclosing country rock or intruding granitoids (Kulp and Brobst, 1954; Swanson, 1981), and are not otherwise observed within the metaultramafic bodies.

The relation between the five associations and the well-established sequence of index minerals in metaultramafic rocks from the Alps (Trommsdorff and Evans, 1974) is illustrated in Figure 1. Bulk compositions of metadunites from the Spruce Pine district are higher in silica (ratio of (MgO+FeO) to ($MgO+FeO+SiO_2$) is between 0.5 to 0.6) than the brucite-bearing assemblages of the Alps (Fig. 1), but the mineral associations defined by Raymond and coworkers generally correspond to the index minerals identified by Trommsdorff and Evans (1974). The A3 association of Raymond locally contains both talc and low-Ca amphibole (magnesiocummingtonite and/or anthophyllite), but Trommsdorff and Evans (1974) show low-Ca amphibole as a stable phase at higher grades than the talc-bearing assemblages (for appropriate bulk compositions). Talc commonly replaces low-Ca amphibole in the Spruce Pine metadunites and here we divide the A3 assemblage into upper A3 (low-Ca amphibole stable) and lower A3 (talc-bearing, low-Ca amphibole deficient) subdivisions.

Petrogenesis of Blue Ridge Ultramafic Rocks

The origin and tectonic significance of the Blue Ridge metaultramafic rocks remain debatable (Misra and Keller, 1978; Raymond and Warner, 2001; Raymond et al. 2003a). A polyphase history of deformation and recrystallization, recorded in Blue Ridge rocks, resulted in recrystallization of the ultramafic rocks. This complex history makes interpretation of igneous heritage and petrotectonics very difficult (Butler, 1972; Hatcher et al. 1984; Abbott and Raymond, 1984; McSween et al. 1989; Adams and Trupe, 1997; Stewart et al. 1997; Swanson et al. 2005). Some workers suggested ophiolitic origins for the ultramafic rocks based on the association with mafic rocks and the general tectonic setting (Abbott and Raymond, 1984; McSween and Hatcher, 1985) and there is some support for this idea in the geochemistry of the rocks (Hatcher et al., 1984; Misra and Conte, 1991; Tenthoery et al. 1996; Berger et al. 2001; Raymond et al. 2003a). The isolated occurrence of ultramafic rocks, often without any obvious stratigraphic or structural connection with spatially associated mafic rocks, however, makes such a determination problematic.

One intriguing proposal for the origin of the Blue Ridge ultramafic rocks is the idea that the ultramafic rocks formed as the result of prograde metamorphism of serpentinites that were presumably emplaced tectonically in the orogen (Carpenter and Phyfer, 1969). Dehydration reactions associated with the progressive metamorphism of ultramafic protoliths are relatively well known experimentally (see summary by Evans, 1977; Spear, 1993; O'Hanley, 1996) and the ultimate products of such reactions are anhydrous rocks composed of olivine, pyroxene and spinel; similar to ultramafic igneous protoliths.

Role of Chromite

Lipin (1984) supported the deserpentinization hypothesis for Blue Ridge ultramafic rocks based on compositions of Cr-spinels. Cr-spinels in metaultramafic rocks occur as accessory grains and massive layers and pods of chromitite. Earlier, Carpenter and Fletcher (1979) reported that accessory chromite grains were chemically homogeneous and at least partially in equilibrium with olivine. They calculated olivine-chromite temperatures in the range of 700° to 1000° C for accessory chromite grains with olivine. Lipin (1984) found a similar, but lower, range of temperatures (600° to 700° C), but he noted that some of the accessory chromite grains were chemically zoned from Mg-rich cores to more Fe-rich rims. Both of these studies report that chromite from chromitite is higher in Mg than accessory chromite. Lipin (1984) also showed that accessory chromite followed a metamorphic compositional trend identified by Evans and Frost (1975). The compositions of chromitite spinels overlap the metamorphic trend, but some of the analyses

plot outside the metamorphic trend and in the range defined by chromite from igneous rocks from stratiform ultramafic bodies (Lipin, 1984).

The occurrence of "metamorphic" chromite as accessory grains with Fe-rich rims indicated to Lipin (1984) that at least some of the ultramafic rocks were serpentinites at one time *prior* to the crystallization of the olivine currently present in the metadunites. Lipin, in support of the deserpentinization hypothesis he favored, argued that the Fe-rich rims formed during serpentinization and were preserved during progressive recrystallization of serpentine to olivine.

Some accessory chromite from the Blue Ridge metaultramafic bodies is zoned with respect to Ti or has elevated levels of Ti. This observation led to the contrasting hypothesis that the metadunites represent restite sublithospheric melt channels and olivine from a suprasubduction zone setting (Raymond and Allan, 2001; Raymond et al, 2003a).

Raymond et al (2003a) speculated that a more thorough analysis of the Cr-spinel compositions might resolve the different petrotectonic arguments and issues and provide information on the petrogenesis of the metaultramafic rocks, while giving a clearer view of chemical changes in Cr-spinels during metamorphism. The purposes of this paper are: (1) to track chromite compositions in relation to the mineral assemblages of metaultramafic rocks in the Spruce Pine area of the Gossan Lead thrust block of western North Carolina and (2) further clarify the histories of the Cr-spinels and their host rocks. Several of the metaultramafic bodies studied by Lipin (1984) are in the Gossan Lead thrust block of the Spruce Pine area. Segregated and accessory chromite occurs in the Spruce Pine metaultramafic rocks and some of the chromite grains are zoned (Lipin, 1984). Results of our detailed analysis should guide future studies of both chromitite petrogenesis and petrotectonics in the Southern Appalachian Orogen.

SPRUCE PINE METAULTRAMAFIC ROCKS

Rocks of the Spruce Pine Mining District (Fig. 3) are part of the Gossan Lead thrust block, the structurally highest thrust sheet in the northern part of the Blue Ridge Belt of western North Carolina (Raymond, 1998). Rocks of the Gossan Lead thrust block are part of the Tugaloo Terrane of Hatcher et al (2005, 2007), an exoctic terrane composed of metasediments, interlayered amphibolite, small bodies of ultramafic rock and a few mafic - ultramafic complexes accreted during the Taconic Orogeny

Metaultramafic rocks occur in the Tugaloo Terrane as pods and lenses enclosed in pelitic schists, amphibolites, and gneisses of the Ashe Metamorphic Suite (Abbott and Raymond, 1984; Raymond and Abbott, 1997; Swanson et al, 2005). Contacts between the metaultramafic rocks and the host rocks are generally conformable and are commonly marked by a metasomatic reaction zone between the Si-poor, Mg-rich ultramafic rocks and the relatively Si-rich, Mg-poor surrounding rocks. This zone is composed of variable proportions of tremolite, talc, chlorite, low-Ca amphibole, and vermiculite (altered Mg-rich mica) all of which, except for the vermiculite, occur in the metaultramafic rocks. Minerals in the contact zone are coarse-grained and are consistent with formation during regional amphibolite-grade metamorphism. Conformable contacts, mineralogy, textures, composition, the small size of many of the bodies, lack of intrusive relations, and the absence of evidence of contact metamorphism indicate that the ultramafic rocks are of the Alpine-type (Raymond, 2002,Ch. 29).

Numerous studies of Blue Ridge metaultramafic rocks are available in the literature and much of this earlier work is summarized by Misra and Keller (1978). Larrabee (1966) provides a detailed compilation of the distribution of the ultramafic and related rocks and Raymond (1995, ch. 31) reviews the metamorphic history of the ultramafic rocks.

Mineral assemblages in the Spruce Pine metaultramafic rocks are quite variable (Tables 1

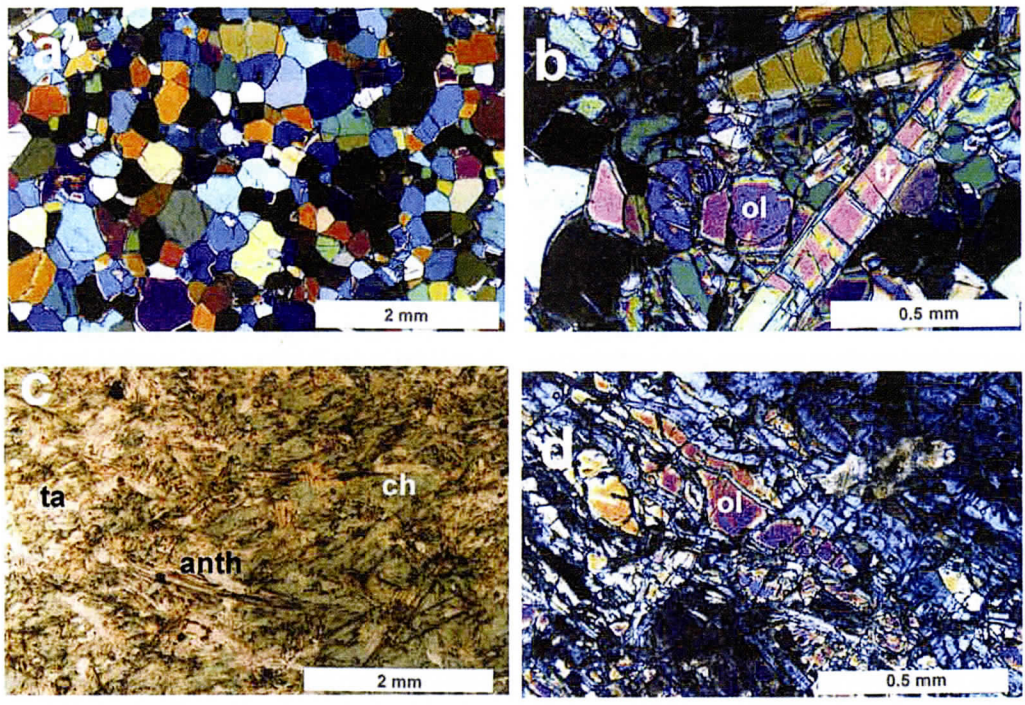

Figure 2. Textures in metaultramafic rocks. (a) A2, olivine-rich metadunite, (b) upper A3, olivine metadunite with magnesiocummingtonite coronas on tremolite (tr), (c) lower A3, anthophyllite (anth) - talc (ta) - chlorite (ch) schist, (d) antigorite in A4 assemblage replacing relict A3 olivine (ol).

and 2), reflecting multiple periods of recrystallization. Rock types range from metadunites and metaharzburgites (mainly along the northern edge of the Gossan Lead Block, Fig. 3) to amphibole schists, amphibole-talc-chlorite schists, and serpentinites (in the vicinity of the town of Spruce Pine, Fig. 3).

Despite the variable degrees of hydration and recrystallization, two points are clear: 1) all of the ultramafic bodies studied here are dominated by equilibrium mineral assemblages consistent with amphibolite facies metamorphism (A2, A3); and 2) the degree of hydration within individual bodies is variable on a local (hand sample or outcrop) scale. Also of note is the observation that many of the higher-grade olivine-rich bodies (with A2 and upper A3 assemblages) occur near the structural base of the Gossan Lead thrust sheet block (Swanson, 2001).

Mg-rich metadunites are the most common host for FeCr-oxides discussed in this paper. Enclosing schists and gneisses of the Ashe Metamorphic Suite reflect amphibolite (and locally eclogite) grade metamorphic conditions (Willard and Adams, 1994; Adams et al, 1995; Adams and Trupe, 1997; Page et al, 2003). Possible pre-metamorphic relicts in the metaultramafic rocks include brown grains of enstatite (brown color is due to very-fine-grained inclusions of rod-like chromite; Swanson et al., 2007), and mineralogic layering defined by pyroxene and chromite. As we show below, chemically the olivine-spinel mineralogy indicates that the (A2) metamorphic mineral assemblages in the metadunites reflect the same amphibolite A1 conditions as the schists and gneisses of the Ashe Metamorphic Suite group (Raymond 1995; 2002; Raymond and Abbott, 1997; Swanson, 2001). Although local areas of rock contain apparent A1 assemblages (representing the eclogite facies), the chemical compositions of the minerals are compatible with A2 assemblages (and conditions). Later retrograde assemblages (A3-A5), reflect variable de-

Table 2. Mineral Associations in Spruce Pine Metaultramafic Rocks (modified from Raymond and Abbott, 1997).

Association A1 (A1)	olivine ± enstatite + chromite
Association A2 (A2)	olivine ± enstatite + chromite + chlorite ± tremolite
Association A3 (A3)	± olivine ± tremolite ± magnesiocummingtonite ± anthophyllite ± chlorite ± talc ± magnesite ± magnetite
Association A4 (A4)	± antigorite ± tremolite ± chlorite ± talc ± magnesite ± magnetite
Association A5 (A5)	± lizardite ± chrysotile ± tremolite ± chlorite ± talc ± magnetite

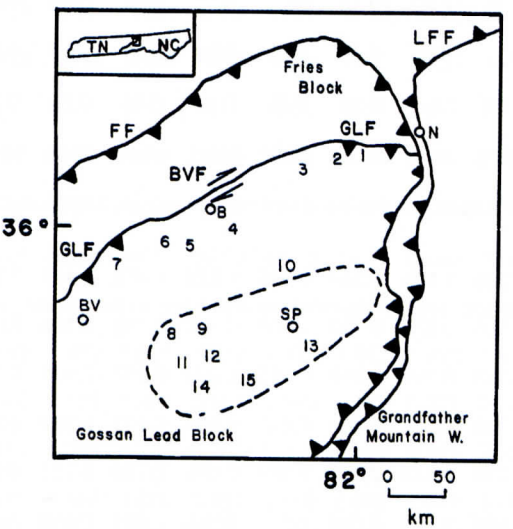

Figure 3. Generalized structural map showing the location of bodies of metaultramafic rocks in the Spruce Pine area of western North Carolina discussed in this paper (based on Raymond, 1998; Trupe et al., 2003). Barbed lines are thrust faults. Bodies include 1 = Frank (F), 2 = Senia (SE), 3 = Henson Creek (HC), 4 = Mine Creek (MC), 5 = Pleasant Grove Church (PGC), 6 = Woody (W), 7 = Day Book (DB), 8 = Newdale Anthophyllite (NA), 9 = Newdale Dunite (ND), 10 = Normanville (NV), 11 = Blue Rock Mine (BRM), 12 = Blue Rock Road (BRR), Grassy Creek 13 = (GC), 14 = Blue Rock Quarry (BRQ), and 15 = Crabtree Creek (CTC). The dashed line represents the approximate outcrop area of the larger granitoid stocks in the Spruce Pine Plutonic Suite (taken from Brobst, 1962). Communities include B = Bakersville, BV = Burnsville, SP = Spruce Pine, and N = Newland. The Burnsville Fault (BVF) is an Acadian dextral strike-slip fault that reactivated the general zone of the Taconic (?) Gossan Lead Fault (GLF), a thrust fault. Other thrust faults are the Fries Fault (FF) and the Linville Falls Fault (LFF).

grees of hydration and recrystallization of the metadunites under lower amphibolite and greenschist facies conditions.

Silicate Minerals

Olivine and, more rarely, enstatite occur in several textural settings within the Spruce Pine metaultramafic rocks. Both minerals occur as clear, fine-grained neoblasts defining an equigranular granoblastic-polygonal texture (Fig. 2a). Porphyroclasts of olivine occur as coarser grains showing evidence of strain and deformation (kink bands, deformation of the grain) and are replaced along their margins by a fine-grained mosaic of neoblastic olivine. De-

Table 3. Compositions of selected accessory chromite grains from rocks with high olivine content

Texture	intergranular										intragranular	
sample	DB 71A		DB 72A		DB 150		DB 153		HC 15		DB 153	
core/rim	c	r	c	r	c	r	c	r	c	r	c	c
Cr_2O_3	50.61	46.44	45.62	46.68	60.02	55.28	47.10	49.78	61.19	61.10	45.59	51.24
Al_2O_3	12.00	3.91	15.58	2.36	7.47	3.24	3.03	2.47	2.28	2.08	1.46	2.39
Fe_2O_3	5.92	18.19	7.66	18.60	1.71	10.92	17.49	15.45	4.72	6.53	16.52	13.56
MgO	7.67	4.97	7.78	3.61	8.64	6.72	4.31	3.96	6.77	6.29	3.29	3.91
FeO	21.38	24.44	22.23	26.15	19.14	21.63	24.77	25.22	20.60	22.10	25.79	25.13
NiO	nd	0.05	0.03	0.14	nd	0.12	0.04	0.08	nd	0.05	0.07	0.09
SiO_2	nd	nd	0.09	0.04	0.02	0.04	0.01	0.02	0.02	0.04	0.07	0.06
TiO_2	0.03	0.28	nd	0.31	0.05	0.17	0.11	0.05	0.01	0.02	0.07	0.02
total	97.61	98.28	98.99	97.89	97.05	98.12	98.86	97.03	95.59	98.21	95.86	96.40
	Number of cations on the basis of 4 oxygen atoms, normalized to 3 cation											
Cr	1.365	1.325	1.195	1.362	1.646	1.559	1.375	1.457	1.770	1.732	1.455	1.509
Al	0.482	0.166	0.609	0.103	0.306	0.136	0.132	0.108	0.099	0.088	0.065	0.105
Fe^{+3}	0.151	0.494	0.191	0.516	0.045	0.293	0.486	0.431	0.130	0.176	0.471	0.380
Mg	0.390	0.268	0.385	0.199	0.447	0.357	0.237	0.219	0.369	0.337	0.186	0.217
Fe^{+2}	0.610	0.738	0.616	0.807	0.555	0.645	0.765	0.781	0.630	0.663	0.817	0.783
Ni	nd	0.002	0.001	0.004	nd	0.003	0.001	0.002	nd	0.002	0.002	0.003
Si	nd	nd	0.003	0.001	0.001	0.001	0.001	0.001	0.001	0.001	0.003	0.002
Ti	0.001	0.008	nd	0.009	0.001	0.005	0.003	0.001	0.001	0.001	0.002	0.001
Cr/Cr+Al	0.739	0.889	0.663	0.930	0.843	0.920	0.912	0.931	0.947	0.952	0.957	0.935
$Al/Cr+Al+Fe^{+3}$	0.24	0.08	0.30	0.05	0.15	0.07	0.07	0.05	0.05	0.04	0.03	0.05
$Fe^{+3}/Cr+Al+Fe^{+3}$	0.08	0.25	0.10	0.26	0.02	0.15	0.24	0.22	0.07	0.09	0.24	0.19
$Cr/Cr+Al+Fe^{+3}$	0.68	0.67	0.60	0.69	0.83	0.78	0.69	0.73	0.88	0.87	0.73	0.76
$Mg/Mg+Fe^{+2}$	0.390	0.266	0.234	0.198	0.446	0.364	0.237	0.219	0.369	0.337	0.185	0.217

nd = not determined

spite the apparent textural disequilibrium, there is no difference between olivine porphyroclast and neoblast chemistry within a given thin section (Swanson, 2001). Enstatite also occurs as deformed porphyroclasts, sometimes with very-fine-grained rod-like inclusions of chromite that color the enstatite brown (Swanson et al., 2007). In a few localities, lenses and veins of metaorthopyroxenite occur in metadunite (Raymond et al., 2001; Swanson, 2001).

Recent studies of mineral assemblages in the Spruce Pine metaultramafic rocks (Swanson,

Table 4. Compositions of segregated chromite grains from chromitite pods or from chromite-rich layers hosted by rocks with high olivine content

	podiform				layer structure					
sample	**DB73**		**DB74B**		**DB154B**		**DB154D**		**HC15**	
core/rim	**c**	**r**	**c**	**r**	**c**	**r**	**c**	**r**	**c**	**r**
Cr_2O_3	57.28	53.48	60.89	59.12	55.91	61.40	54.01	56.01	55.06	52.58
Al_2O_3	9.25	4.38	7.12	3.48	11.56	4.13	9.24	4.42	9.93	4.01
Fe_2O_3	4.51	12.37	3.41	8.36	4.64	6.63	6.41	9.81	5.03	13.50
MgO	10.34	8.60	10.31	8.72	11.60	11.76	10.70	9.10	8.78	6.80
FeO	17.21	18.95	16.96	18.65	13.06	14.09	16.03	18.10	19.74	21.57
NiO	nd	nd	nd	nd	0.06	0.04	nd	nd	0.03	0.10
SiO_2	nd	nd	nd	nd	0.03	0.01	0.02	nd	nd	nd
TiO_2	0.03	0.23	0.03	0.10	0.12	0.11	0.08	0.19	0.09	0.04
total	98.64	98.03	98.72	98.53	98.73	98.17	96.49	97.62	98.66	98.60
Number of cations on the basis on 4 oxygen atoms, normalized to 3 cations										
Cr	1.519	1.482	1.628	1.632	1,437	1.657	1.458	1.550	1.472	1.472
Al	0.366	0.181	0.284	0.143	0.443	0.166	0.372	0.182	0.396	0.167
Fe^{+3}	0.114	0.326	0.087	0.220	0.113	0.170	0.165	0.258	0.128	0.360
Mg	0.517	0.449	0.520	0.454	0.580	0.660	0.545	0.475	0.443	0.359
Fe^{+2}	0.483	0.555	0.480	0.545	0.355	0.402	0.458	0.530	0.558	0.639
Ni	nd	nd	nd	nd	0.002	0.001	nd	nd	0.001	0.003
Si	nd	nd	nd	nd	0.001	0.000	0.001	nd	nd	nd
Ti	0.001	0.006	0.001	0.003	0.003	0.003	0.002	0.005	0.002	0.001
Cr/Cr+Al	0.806	0.891	0.852	0.919	0.764	0.909	0.797	0.895	0.788	0.898
$Al/Cr+Al+Fe^{+3}$	0.18	0.09	0.14	0.07	0.22	0.08	0.19	0.09	0.20	0.08
$Fe^{+3}/Cr+Al+Fe^{+3}$	0.06	0.16	0.04	0.11	0.06	0.09	0.08	0.13	0.06	0.18
$Cr/Cr+Al+Fe^{+3}$	0.76	0.75	0.81	0.82	0.72	0.83	0.73	0.78	0.74	0.74
$Mg/Mg+Fe^{+2}$	0.517	0.447	0.520	0.454	0.621	0.598	0.543	0.473	0.442	0.360

nd = not determined

Table 5. Compositions of selected accessory chromite and Cr-spinel grains from rocks with moderate olivine content

sample	F848		ND6		PGC3		GC52F	
core/rim	c	r	c	r	c	r	c	r
Cr_2O_3	28.09	17.29	52.44	51.05	54.86	49.85	56.20	38.55
Al_2O_3	0.60	0.29	9.99	6.82	2.37	3.40	6.81	0.68
Fe_2O_3	39.24	51.06	6.78	10.56	10.65	14.16	5.54	28.65
MgO	2.99	2.05	7.55	5.55	4.38	4.47	5.33	3.30
FeO	25.97	27.58	21.47	23.93	24.81	25.01	24.49	26.68
NiO	0.19	0.31	0.04	0.04	nd	0.08	0.05	0.19
SiO_2	0.02	0.07	0.04	0.03	0.05	0.23	0.02	0.07
TiO_2	0.12	0.03	0.02	0.09	0.08	0.11	0.09	0.50
total	97.22	98.68	98.33	98.07	97.20	97.31	98.53	98.62
	Number of cations on the basis of 4 oxygen atoms, normalized to 3 cations							
Cr	0.844	0.52	1.419	1.428	1.595	1.441	1.565	1.139
Al	0.027	0.013	0.403	0.285	0.103	0.147	0.283	0.030
Fe^{+3}	1.122	1.460	0.175	0.281	0.295	0.390	0.147	0.799
Mg	0.170	0.116	0.385	0.293	0.240	0.244	0.280	0.183
Fe^{+2}	0.825	0.877	0.615	0.708	0.763	0.765	0.721	0.828
Ni	0.006	0.009	0.001	0.001	nd	0.002	0.001	0.006
Si	0.001	0.003	0.001	0.002	0.002	0.008	0.001	0.002
Ti	0.003	0.001	0.02	0.09	0.002	0.003	0.002	0.014
Cr/Cr+Al	0.969	0.976	0.779	0.834	0.939	0.908	0.847	0.975
$Al/Cr+Al+Fe^{+3}$	0.02	0.01	0.20	0.14	0.05	0.07	0.14	0.02
$Fe^{+3}/Cr+Al+Fe^{+3}$	0.56	0.73	0.09	0.14	0.15	0.20	0.07	0.41
$Cr/Cr+Al+Fe^{+3}$	0.42	0.26	0.71	0.72	0.80	0.73	0.79	0.57
$Mg/Mg+Fe^{+2}$	0.170	0.117	0.385	0.293	0.239	0.242	0.280	0.181

nd = not determined

2001) require additional modifications to the A1 to A5 mineral associations. The most important change is the recognition of olivine as a stable phase in the A3 association (Table 2). Veins of talc + chlorite contain subhedral grains of olivine, tremolite, magnesiocummingtonite - anthophyllite, antigorite, and magnesite with olivine (Swanson, 1981), indicating that olivine is part of the A3 assemblage. The overall range of olivine composition is small, Fo 88 to 97, but there is a sympathetic variation in the compositions of olivine with that of enstatite, tremolite,

Table 6. Compositions of selected segregated chrome spinel grains from rocks without (low) olivine

sample	BRM7A		NV4		F21		W9	
core/rim	c	r	c	r	c	r	c	r
Cr_2O_3	24.19	5.74	26.37	30.41	51.74	39.97	26.60	26.91
Al_2O_3	0.37	0.07	0.62	0.68	6.16	0.57	0.99	1.03
Fe_2O_3	43.78	63.28	37.71	33.09	10.18	27.12	41.43	40.70
MgO	1.70	0.89	0.57	0.45	4.09	2.56	3.79	3.68
FeO	29.18	29.76	31.32	31.37	26.30	27.81	25.80	25.86
NiO	0.24	0.29	0.16	0.10	nd	nd	0.43	0.41
SiO_2	0.09	0.02	0.06	0.06	nd	nd	nd	nd
TiO_2	0.49	0.21	1.40	1.57	0.14	0.51	0.58	0.59
total	100.04	100.26	98.21	98.13	98.62	98.55	99.59	99.20
Number of cations on the basis of 4 oxygen atoms, normalized to 3 cations								
Cr	0.716	0.173	0.799	0.921	1.460	1.183	0.776	0.788
Al	0.016	0.003	0.028	0.031	0.259	0.025	0.043	0.045
Fe^{+3}	1.234	1.811	1.088	0.954	0.273	0.764	1.150	1.134
Mg	0.095	0.050	0.033	0.026	0.218	0.143	0.207	0.203
Fe^{+2}	0.914	0.947	1.004	0.018	0.785	0.871	0.796	0.801
Ni	0.007	0.009	0.005	0.003	nd	nd	0.013	0.012
Si	0.003	0.001	0.002	0.002	nd	nd	nd	nd
Ti	0.014	0.006	0.040	0.045	0.004	0.014	0.016	0.017
Cr/Cr+Al	0.978	0.981	0.966	0.968	0.849	0.979	0.947	0.946
$Al/Cr+Al+Fe^{+3}$	0.01	0.00	0.02	0.02	0.13	0.01	0.02	0.02
$Fe^{+3}/Cr+Al+Fe^{+3}$	0.63	0.91	0.56	0.50	0.14	0.39	0.58	0.58
$Cr/Cr+Al+Fe^{+3}$	0.36	0.09	0.42	0.48	0.73	0.60	0.21	0.20
$Mg/Mg+Fe^{+2}$	0.094	0.050	0.031	0.024	0.217	0.141	0.394	0.401

nd = not detected

magnesiocummingtonite, and talc. Only the serpentine minerals do not show any systematic variation in composition with olivine (Swanson, 2001). Thus, textural and compositional data support inclusion of olivine as a phase in the A-3 association.

Metamorphic Grade or Mineral Assemblages

Chemical equilibrium among the various metamorphic minerals (Swanson, 2001) occurs on the scale of a thin section. Equigranular oliv-

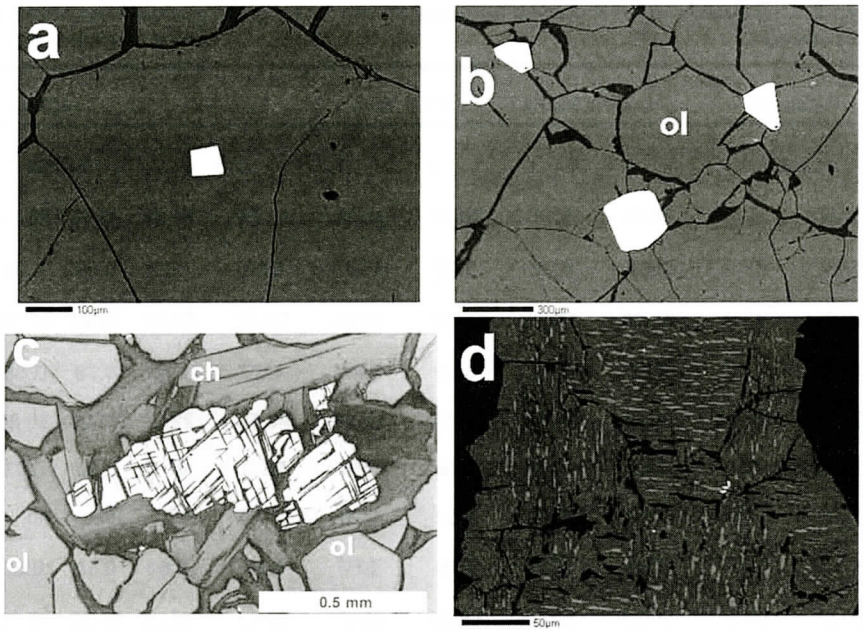

Figure 4. Back-scattered electron images showing representative textures and structures of spinels. (a) chromite included in olivine, (b) intergranular chromite in metadunite, (c) trellis texture in chromite with chlorite intergrown along the octahedral crystallographic planes in the spinel, (d) exsolved magnetite (brighter) in ilmenite. ol = olivine, ch = chlorite.

ine fabrics form dominant textures in higher grade rocks (A2, upper A3) and are in chemical and textural equilibrium with accessory chlorite and tremolite. Talc commonly forms large ragged grains in the olivine fabric (lower A3), but it too, is in chemical equilibrium with the olivine (Swanson, 2001). Chlorite occurs as coronas on chromite and as isolated grains in the silicate fabric, where it is associated with olivine, enstatite, amphiboles, and talc. In A2 assemblages, chlorite is a chromian clinochlore (McCormick, 1975; Swanson, 1981). In Spruce Pine rocks, chlorite occurs both between neoblasts of olivine and as inclusions in the porphyroclasts of olivine and enstatite. In the A3 to A4 rocks, chlorite is interleaved with talc and amphibole (Fig 2c). Chlorite compositions within thin section-scale domains are uniform and show no variation with textural setting (corona on Cr-spinel vs isolated grains within the olivine+enstatite fabric vs inclusions in olivine and enstatite.). Serpentine occurs as antigorite coronas (association A4, Fig. 2d) on chlorite and olivine (Swanson et al. 1985). Antigorite also forms a mesh-work texture replacing and enclosing olivine in rocks of A2, A3, and olivine ghosts in A4 mineral associations. In the A5 association, chrysotile forms vein-fillings that replace other silicate minerals.

FECR OXIDES

Oxide mineralogy varies with silicate mineral assemblages in the Spruce Pine metaultramafic rocks. Chromite is the common opaque mineral in more olivine-rich rocks of A2 and A3 associations, whereas chromian magnetite (as separate grains or as coronas on chromite) is more common in rocks with major modal amphibole and/or talc. Amphibole-chlorite-talc schists contain isolated grains of magnetite with or without ilmenite at Blue Rock Road (BRR) and Blue Rock Quarry (BRQ) (Fig. 3). Nearly pure end-member magnetite occurs in association with serpentine minerals in the A4 and A5 mineral associations.

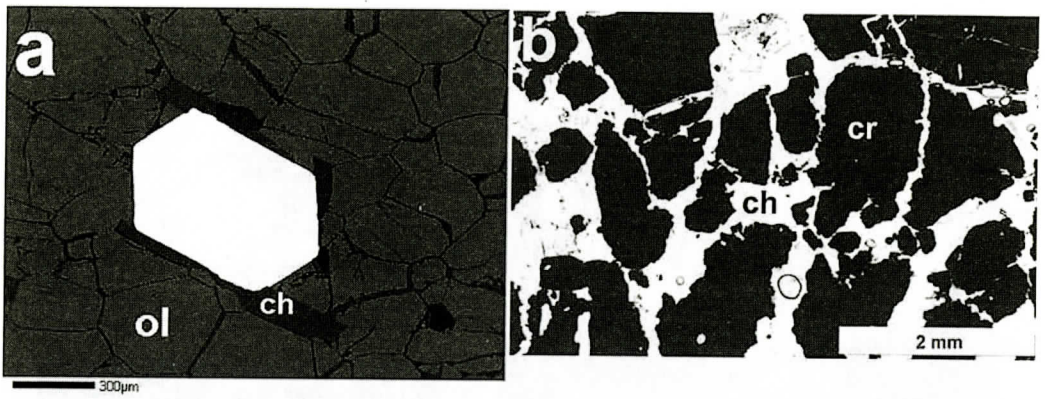

Figure 5. Chlorite coronas on Cr-spinel. (a)back scattered electron image of intergranular chromite in metadunite, (b) transmitted light image of segregated chromitite. ol = olivine, ch = chlorite, cr = chromite.

Chromite Textures

Accessory chromite is typically fine-grained and ranges from euhedral to anhedral (Fig. 4). Chromite occurs as euhedral grains in olivine (Fig. 4a), but is commonly interstitial to the olivine neoblasts (Fig. 4b). A corona of chlorite typically surrounds interstitial chromite grains in association A2 and A3 rocks (Fig. 5a), whereas chromite included in olivine lacks chlorite rims (Fig. 4 a). Chromite in segregated chromitite is medium- to coarse-grained, is usually anhedral (Figs, 5b), and is often rimmed by chlorite. A few chromite grains are visibly zoned from a more reflective outer rim to an inner, less reflective core; however, most of the chromite found to be zoned by microprobe analyses shows no optical evidence of the zoning in polished sections. The most Al-rich chromite is dark reddish brown in plane polarized light.

A few accessory chromite grains show a trellis-like texture with chlorite intergrowth along the {111} plane of the spinel (Fig. 4c). Lipin (1986) termed this textural variety "lattice chromite". The trellis texture resembles the exsolution textures of spinels (e.g. Haggerty, 1991). Lattice texture does not occur in chromite included within olivine grains. Some ilmenite grains show exsolution of magnetite (Fig. 4d).

Chromite-rich segregations (Fig. 6) occur in both the olivine-bearing and olivine-absent rocks and rock bodies. Segregations include thin, discontinuous layers of chromite grains; thicker, more continuous layers of chromitite (mined at Day Book during WWI: Hunter et al., 1942); and pods of chromitite (Fig. 6a). Thin chromite layers from the Frank body are enclosed in a matrix of chlorite and tremolite. Small pods of chromian magnetite in the Woody body are surrounded by a mantle of chlorite.

Chromite Compositions

Spinel compositions were analyzed on a JEOL 8600 Superprobe at the University of Georgia. Natural and synthetic minerals were used as standards. Spinel compositions are represented by six end-members involving one divalent cation (Mg or Fe^{+2}) and the trivalent cations Al, Cr, or Fe^{+3}. Microprobe analyses reported total Fe as Fe^{+2}; Fe^{+3} was calculated based on stoichometry.

Representative spinel analyses are given in Tables 3-6. Chromium contents of the Spruce Pine spinels are quite variable, ranging from less than 1 to over 61 weight percent Cr_2O_3 (Tables 3-6). Aluminum ranges from 0 to almost 16 weight percent and total Fe (as FeO) ranges from 16 to 87 weight percent. Magnesium and Al correlate positively with one another, but MgO has a smaller range (MgO varies from 0.1 to over 9 weight percent). Recalculation of total

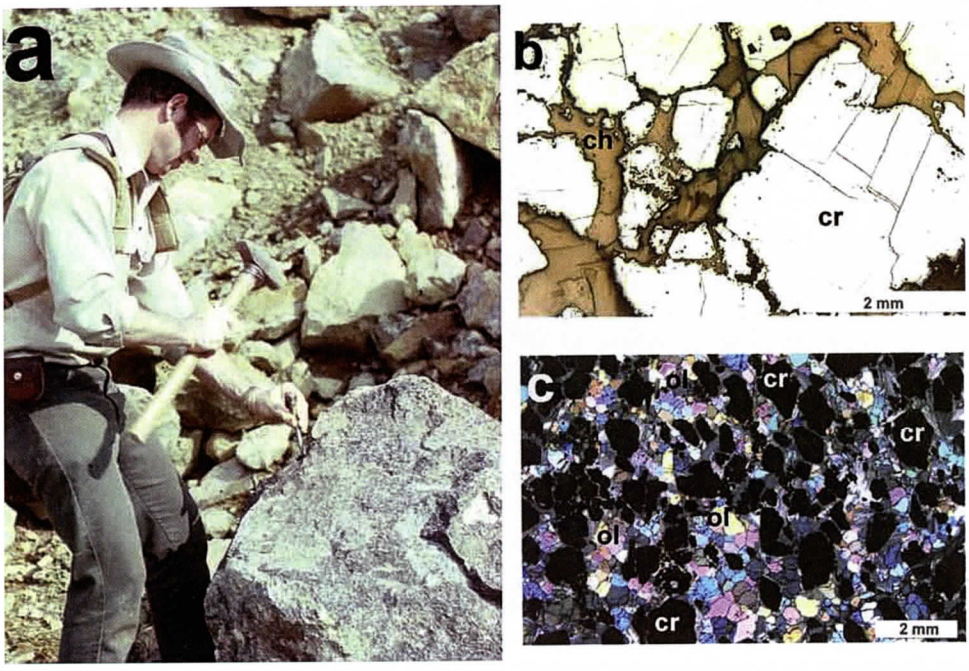

Figure 6. Segregated chromite. (a) one of the authors (LAR) tries to sample a pod of segregated chromite at Day Book, (b) reflected light image of segregated chromite from pod in (a), (c) transmitted light image of chromitite with interstitial olivine. ch = chlorite, cr = chromite, ol = olivine.

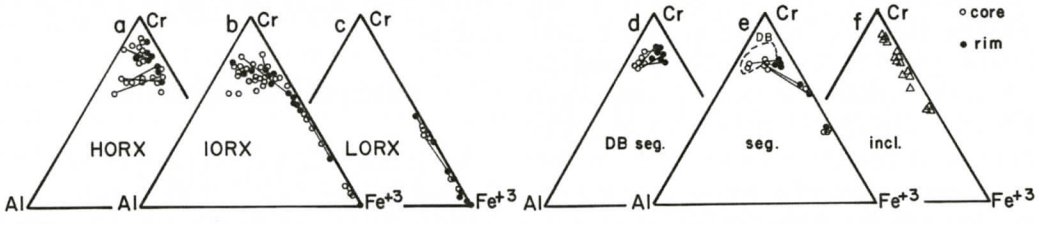

Figure 7. Triangular plots of trivalent components in spinels. (a) high-olivine (HORX, > 80 modal percent olivine,) A2 rocks, (b) intermediate-olivine (IORX, 20 to 80 modal percent olivine) upper A3 rocks, (c) low-olivine (< 20 percent modal olivine) lower A3 rocks; (d) segregated chromites from the Day Book body, (e) segregated spinels from other bodies (showing field for Day Book (DB) data), and (f) spinel included in olivine. Tie lines connect core and rim analyses from the representative grains. Note these same grains and tie lines are reproduced in subsequent figures.

Fe based on spinel stoichiometry (3 cations, 8 positive charges) results in Fe^{+3} values ranging from 20% to 66% of the total Fe. The recalculations result in analysis totals near 100% in lower-Cr spinels, but totals for higher-Cr chromites are often low, on the order of 98%, but sometimes as low as 96%. Some trace elements (Mn, V, Zn) are present in the chromites in amounts up to several tenths of a weight percent each, but these components were not routinely analyzed and thus are not included in the reported totals. This may account in part for the low totals. However, the correspondence of low totals with high Cr contents suggest a problem with the Cr calibration, but attempts to use alternative standards (different Cr-spinels) for Cr yield similar results. Trace amounts of Ni and Ti are present in most spinels. Chromian magnetites contain up to 3 wt% TiO_2.

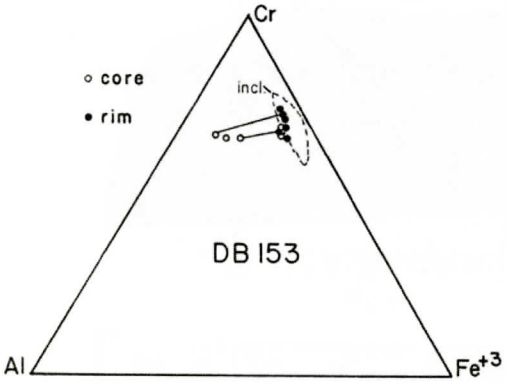

Figure 8. Composition of intergranular chromite compared to the field (dashed line) defined by chromite included in olivine in a typical metadunite sample (DB153).

RESULTS

Ternary plots of spinel trivalent cations (Fig. 7) show an almost continuous array of compositions from chromite to chromian magnetite to magnetite. Chromite is typically found in olivine-rich rocks of A2 and upper A3. Chromite typically contains at least 5 weight percent Al_2O_3 (Tables 3 and 4), but individual grains may be zoned with more Al-rich cores and Al-poor rims of chromian magnetite (Figs. 7a and 7b). Chromian magnetite or magnetite is the oxide phase in the A3 associations with little or no olivine. (Fig. 7c). Zoning in chromian magnetites is from chrome-rich cores to more Fe-rich rims (Figures 7b and 7c). Chromian magnetites contain at most a few weight percent Al_2O_3, but typically Al_2O_3 is less than one weight percent (Tables 3-6). Some of the chromian magnetites show continuous zoning from higher-Cr cores to low Cr, Fe^{+3}-rich rims near end-member magnetite (Figs. 7b and 7c). Pods and layers of chromitite occur in olivine-rich rocks in the Day Book and Henson Creek bodies (Fig.6) and these chromites are zoned from Al-rich cores to more Al-poor rims (Fig. 7d). Chromite grains in chromitite with hydrated assemblages of chlorite (Fig. 6b), talc and/or amphibole are zoned from chromite cores to chromian magnetite rims (core-rim analyses, Fig.7e). Thin stringers of unzoned chromian magnetite grains are found in A3 amphibole-talc-chlorite schists from the Frank and Woody bodies. Compositions of these unzoned spinels are low Al chromian magnetites, similar to the rims of segregated chromite grains from Day Book and Henson Creek (Figures 7d and 7e).

Small (5 to 25 mm) spinel grains included within olivine (Fig. 4a) are chromian magnetites (Fig. 7f). These included grains are unzoned and have the same composition as rims of zoned accessory chromites within a given sample (Fig. 8).

Spinel in metachromitites has different compositions than the adjacent accessory chromites in metadunites, reflecting the differences in bulk compositions (metachromitites vs. metadunites). The chromitite layer represented in Figure 9 contains interstitial chlorite and olivine (Fig. 6b, 6c). The larger chromite grains in the layer (e.g. samples DB 154B and DB154D, Table 3) are moderately zoned with more Al-rich cores (9-12 wt.% Al_2O_3) and lower Al rims (3-7 wt.% Al_2O_3). Some smaller, subhedral grains (neoblasts?) in the layer are unzoned and have compositions similar to the rims on the larger grains. Accessory chromite in the metadunite that hosts the chromitite layer (Fig. 9) is lower in Al (cores 3-9 wt.% Al_2O_3, rims 3-4 wt.% Al_2O_3). Interstitial olivine in chromitite is more Mg-rich than the immediately adjacent olivine of the host metadunite (Swanson, 2001). That trend is illustrated in Figure 9 where olivine in the metadunite, outside the chromitite layer, is lower in Mg than interstitial olivine in the chromitite layer. A similar trend is found in the chromite; chromite in the layer is higher in Mg than the accessory chromite outside the layer (Figure 9). Warner and Helper (2005) found a similar relationship at the Dark Ridge metaultramafic body.

The effect of host mineral assemblage (olivine vs. an assemblage of talc + chlorite + amphibole or serpentine) on spinel compositions, evident in Figure 7, is also apparent in their Fe/Mg contents (Figure 10a). For olivine-rich rocks, bulk compositions are high in Mg and the spinels reflect this. Chromite from olivine-rich rocks (Fig.10a) is generally more Mg-rich (Tables 3, 5, and 6) than spinels in rocks with less

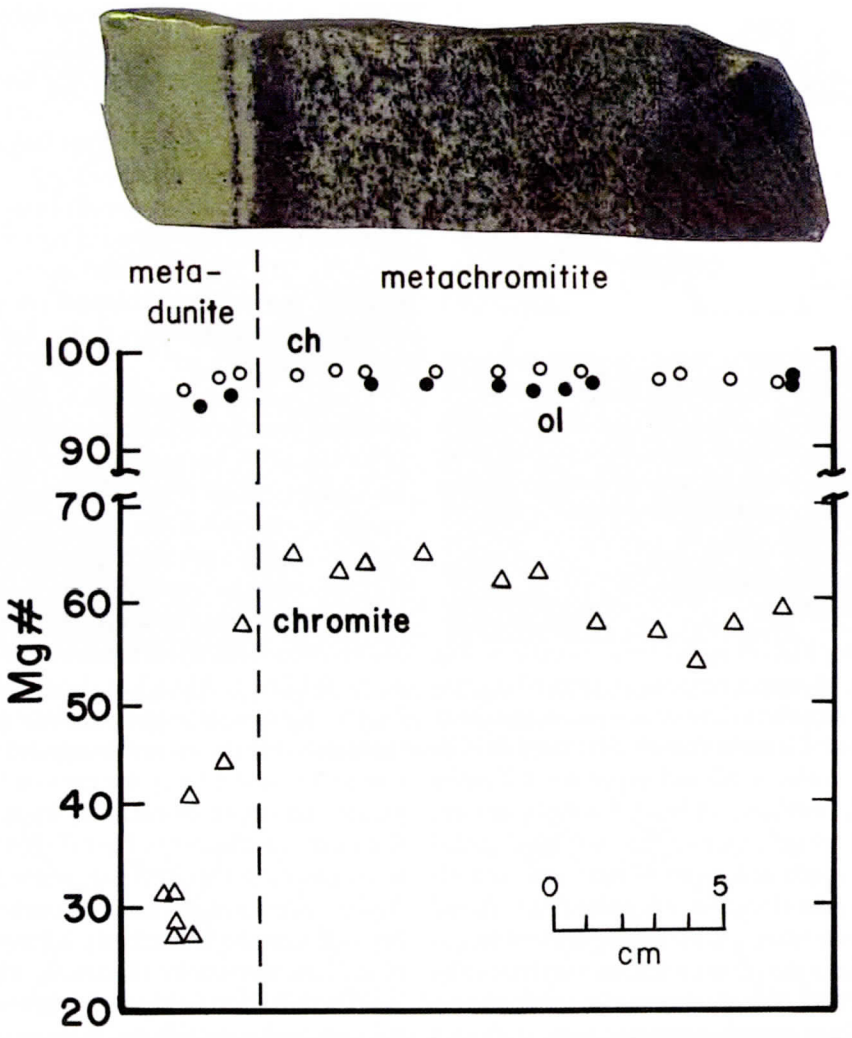

Figure 9. Slab of a metachromitite layer from Day Book. Variation in Mg# (= Mg/Mg+Fe +2) for chromite rims and interstitial olivine (ol) and chlorite (ch) across the layer. Compositions of trivalent components for these same analyses are shown in Figure 7d. Lower Mg#s characterize all of the minerals in the metadunite relative to the metachromitite. olivine = filled circles, chlorite = open circles.

olivine (Figs. 10b and 10c). Rocks composed of variable amounts of chlorite, talc, and amphibole have variable amounts of Fe and Mg (e.g., Scotford and Williams, 1983) and spinels compositions reflect these variations. A few spinel analyses from amphibole - chlorite - talc rocks have elevated Mg and Cr contents, but most of these spinels are lower in Mg (Fig. 10b). Spinels with elevated Mg and Cr contents are typically zoned from more Cr- and Mg-rich cores to Fe-rich rims (Figs. 10a and 10b). Spinels included in olivine are low in Mg and Al (Fig. 10f), similar to many of the accessory spinels in rocks lacking olivine (Fig. 10b), but they are not as low in Mg and Al as chromian magnetites from the chlorite talc schists (Fig. 10c).

Titanium contents of the accessory and segregated chromites from olivine-bearing A2 and A3 assemblages are generally low - less than 0.1 weight percent (Tables 3-6). The recrystallization of olivine in A2 and upper A3 assemblages to olivine in a more hydrated lower A3 or

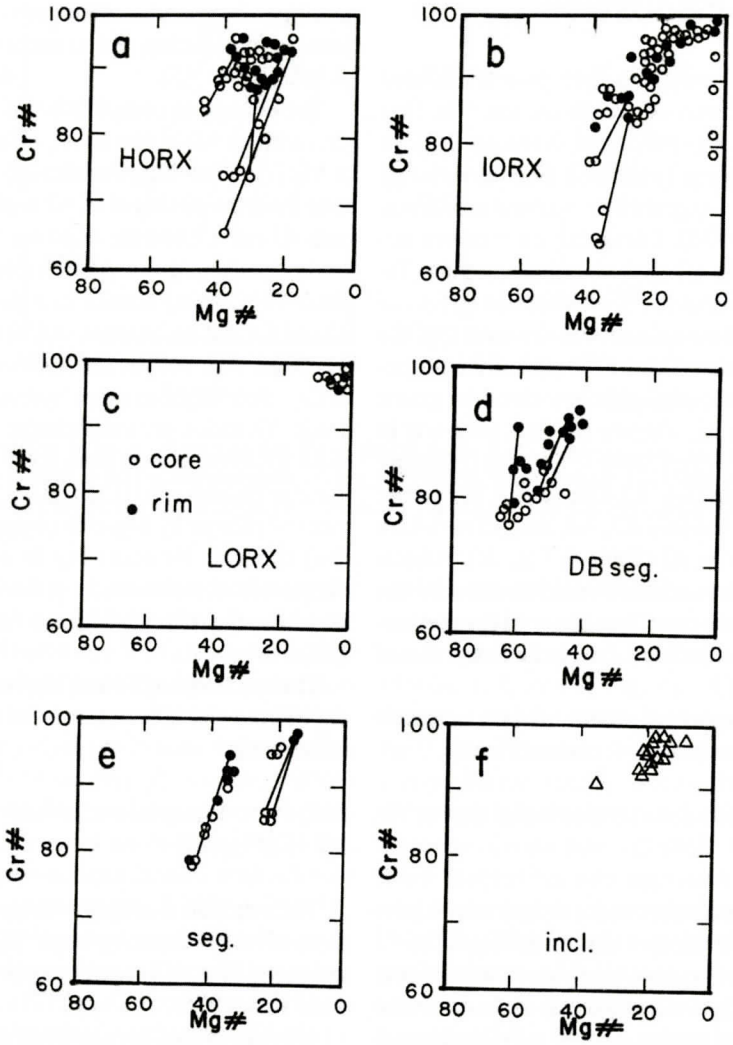

Figure 10 Plots of divalent vs trivalent components (Cr# = Cr/Cr+Al; Mg# = Mg/Mg+Fe+2) in spinels. From (a) HORX, (b) IORX, (c) LORX metaultramafic rocks; (d) segregated chromites from Day Book, (e) other segregated spinels showing field for Day Book data, and (f) chromite included in olivine. Tie lines and labels as in Figure 7.

A4 assemblage results in an increase in the magnetite component of the spinel in response to the formation of Fe-poor hydrous silicate phases. As the magnetite component of the spinel increases, the Ti content goes up also, resulting in an inverse correlation of Ti with Cr and Al (Tables 3 and 6).

Magnetite and ilmenite occur as individual unzoned grains in the lower A3 chlorite-talc schists of the Blue Rock Road body (Fig. 1). Compositions of the grains are near end-member ilmenite and magnetite. Both the magnetite and ilmenite occur in the lower A3 chlorite schist that forms the outer margin of the Blue Rock Mine body (Fig. 3) and in some of the amphibole-chlorite-talc schists. The ilmenite grains commonly show exsolution (Fig. 4d) of a titianomagnetite phase. Near end-member magnetite forms rims on the exsolved ilmenite grains and also forms fine-grained neoblasts in the talc and chlorite.

DISCUSSION

The low-Al spinel compositions are related to recrystallization of the chromites. The first stage of this recrystallization is the removal of Al to form chlorite (transition from association A1 to A2), as suggested by numerous workers (e.g.,Ulmer, 1974). Chromian clinochlore occurs in virtually all of the studied samples (Table 2). The formation of chlorite affected virtually all of the spinels, but the extent of the reaction was variable. In A2 and olivine-bearing A3 rocks, the cores of many chromite grains remain high in Al, whereas the rims are lower in Al and higher in Fe (Table 4, Fig. 7a) reflecting incomplete reaction. Chromite and magnetite formed in olivine-free A3, A4, and A5 rocks are uniformly low in Al (Table 6, Fig. 7c), reflecting complete reaction. The Al content of the chromite is the controlling factor in the production of chlorite and one may write a reaction of the type:

(R1) chromite + olivine + hydrous fluid = chromian clinochlore + ferroan chromite.

Continued hydration leads to a reaction of the type:

(R2) ferroan chromite + hydrous fluid = chromian clinochlore + chromian magnetite

The formation of silicate phases with higher Mg# (e.g., talc and antigorite) at lower metamorphic grades (lower A3 and A4) is accompanied by the growth of progressively more Fe-rich spinel (chromian magnetite and magnetite). The magnetite may form as rims on ferroan chromite or as discrete neoblasts. Various authors (Ulmer, 1974; Bliss and McClean, 1975; Hoffman and Walker, 1978) commented on the formation of magnetite and relate this to serpentinization. In the Spruce Pine metaultramafic rocks, the formation of chromian magnetite may be related to the formation of a late-stage mesh-work fabric antigorite between olivine grains. Spinels included in olivine (Figure 7f) do not show such Fe-enriched compositions, suggesting growth prior to the formation of serpentine. Inclusion of these grains in olivine is further evidence of crystallization above the stability of serpentine. Chromian magnetite appears to form during replacement of amphiboles by talc (lower A3).

The change in composition of the spinel begins with an initial loss of Al, followed by a loss of Mg (with resulting enrichment in Fe). Chromite from the olivine-rich A2 rocks is highest in both Al and Cr and these grains display typical zoning patterns from Al-rich cores to Al-poor rims. This zoning results in a decrease in both Al and Cr, but an increase in Cr# (Cr# = Cr/Cr+Al) (Figs. 10a, 10b) as the Al is lowered relative to Cr. Spinels from more hydrated, e. g. lower grade A3 rocks, are consistently low in Al and show a zoning pattern from more Mg-rich cores to more Fe-rich rims (Figs. 10,11). The replacement of olivine by Mg-rich phases (talc, tremolite) releases Fe resulting in an increase in magnetite component in spinel and a corresponding decrease in Mg and Mg# (Figs. 10a, 10b).

The exchange of Fe and Mg between coexisting olivine and chromite can be represented by the reaction

(R3) Mg-spinel + Fe^{+2} olivine = Mg-olivine + Fe^{+2} spinel

The reaction is strongly temperature dependent; olivine becoming more Mg-rich and spinel more Fe-rich at lower temperatures (Evans and Frost, 1975).

Olivine in the Spruce Pine metaultramafic rocks is unzoned and uniform in composition at the scale of a thin section (Swanson, 2001). The spinel, however, is zoned in most of the rocks. Use of the olivine-spinel geothermometer requires a determination of spinel compositions that are in equilibrium with the olivine. Previous work in the Spruce Pine metaultramafic rocks (Swanson, 2001) showed that olivine was in equilibrium with a variety of phases, including chlorite. Given that the Al-poor rims of the accessory spinels are related to the formation of chlorite, it is reasonable to assume the spinel rims are in equilibrium with the olivine. Figure 11 shows the variation of rim compositions of accessory and segregated chromite compositions in olivine-rich rocks in equilibrium with

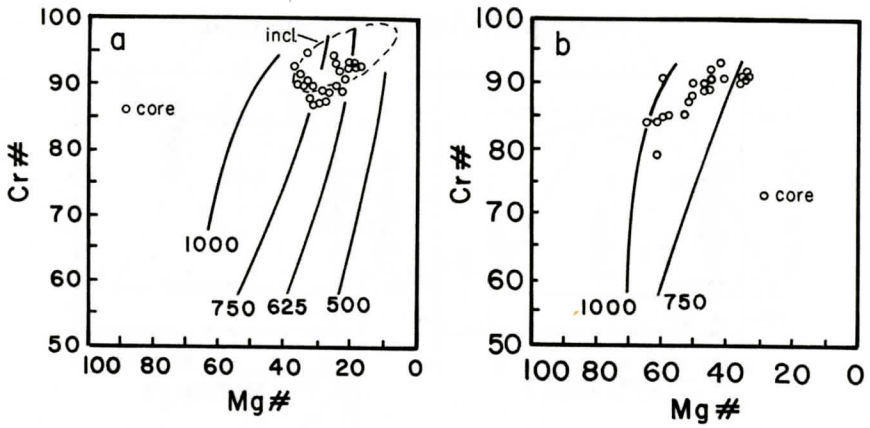

Figure 11. Variation in Cr-Al (Cr#) and Mg-Fe+2 (Mg#) in rims of (a) accessory and (b) segregated chromite from HORX (> 80 modal percent olivine, A2 rocks). Also shown are isotherms (°C) based on olivine-spinel thermometer of Sack and Ghiorso (1991) for the olivine compositions of Fo 91 (a) and Fo 94 (b).

olivine at various temperatures. Isotherms for Fo91, a average composition for olivine in the metadunites (Swanson, 2001) are shown in Figure 11a for olivine-spinel equilibration temperatures over the range of 600 to 900°C. Segregated chromites are in equilibrium with a more Mg-rich olivine (Fig. 8; Swanson, 2001) and Fo94 olivine was used to construct the isotherms for segregated chromites (Fig. 11b). Segregated spinels equilibrated with olivine over a temperature range of 700 to 1000°C, largely overlapping the temperature range of the accessory chromites. The olivine-spinel temperatures reflect metamorphic conditions. Lower temperatures reflect the amphibolite facies regional metamorphism prevalent in the area (Butler, 1972; Abbott and Raymond, 1984; Willard and Adams, 1994). Higher temperatures may record earlier, higher grade metamorphic events postulated for some of the enclosing rocks (Willard and Adams, 1994; Adams et al., 1995; Waters et al. 2000; Page et al. 2003, 2005).

Petrogenesis of Chromite

Chromite (and the enclosing silicate mineral assemblages) in the Spruce Pine ultramafic rocks largely recrystallized during retrograde cooling following peak regional metamorphism (Raymond and Abbott, 1997; Swanson, 2001). Metadunite bodies from the Spruce Pine area contain the A3, talc and/or low-Ca amphibole-bearing association and, less commonly, A2 assemblages lacking talc and low-Ca amphibole (Tables 1, 2, and 3; Fig. 3). Chromites from these A2 and A3 rocks, in part, show a similar range in composition (Figs.7a, 7b). Some of this compositional overlap is probably due to relic A2 spinels inherited in A3 assemblages. Spinels from the olivine-poor A3 rocks range to chromian magnetites and approach end-member magnetite, i.e. they are spinels with lower Cr (Fig. 7b). Chromian magnetites have higher Cr#'s and lower Mg#'s than any of the A2 spinels (Figs.10a and 10b). Zoning in the spinels from the olivine-bearing A3 rocks shows depletion in Cr and Mg at relatively constant Al values from the cores to the rims (Figs. 7b, 10b), which differs from the Al zoning in the spinels from the A2 rocks (Figs. 7a, 10a).

Rocks lacking olivine include talc-chlorite schists (lower grades of A3) and serpentinites (A4, A5). FeCr oxides in these rocks range from chromian magnetites to magnetite (Fig. 7c) and overlap the range of chromian magnetites from A3 (Fig. 7b). The magnetites are uniformly low in Al and are lower in overall Cr than most of the oxide minerals in the A3 rocks (Fig. 8b and 8c). Cores of chromian magnetites are generally higher in Cr than the rims, but the range of zoning decreases as the spinels approach end-member magnetite (Fig.7).

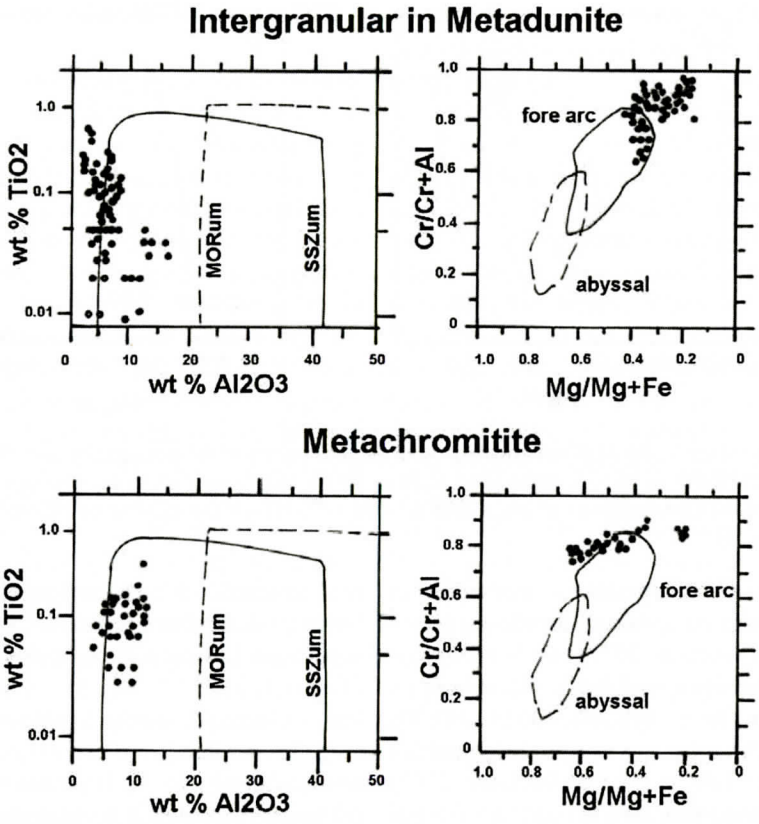

Figure 12. Core compositions of intergranular chromite from olivine-rich metadunite and metachromite. Also shown are the discriminate fields for suprasubduction zone (SSZum) and midocean ridge (MORum) peridotites (from Kamenetsky et al., 2001) and from abyssal and fore arc type ophiolites (their Types II and III, Dick and Bullen, 1984).

Lipin (1984) found low-Al chromite grains included in olivine and he thought these formed in a serpentinite that was recrystallized to metadunite during prograde metamorphism. Low-Al chromite grains included in olivine similar in composition to those reported by Lipin were found in this study (Fig.7f). Compositions of the included chromites are similar to rim compositions of accessory chromites in the olivine matrix (Fig. 8) and yield olivine-spinel temperatures of 500 to 600°C (Fig. 11a), temperatures too high, however, for the crustal formation of serpentine.

The compositions of chromite included in olivine appear to be related to the recrystallization of chromite during the early growth of Cr-chlorite (Fig. 8). This suggests that the spinels included in olivines are neoblasts that nucleated and grew during the formation of Cr-chlorite and were later incorporated into recrystallizing olivine. This is consistent with the observation that olivine and chlorite are in chemical equilibrium within a given sample (Swanson, 2001).

The changes in chromite composition toward magnetite with lower metamorphic grade is a well-known trend and is widely reported in studies of metaultramafic rocks (e.g., Ulmer, 1974; Bliss and MacLean, 1975; Hoffman and Walker, 1978). Spinels found in serpentinites are typically near magnetite in composition (O'Hanley, 1996) and lack the elevated Cr contents found in the intragranular chromites and chromian magnetites (Fig. 8). Recrystallization of the Spruce Pine spinels during retrograde metamorphism drove compositions toward magnetite (Figs. 7b and 6c), characteristic of

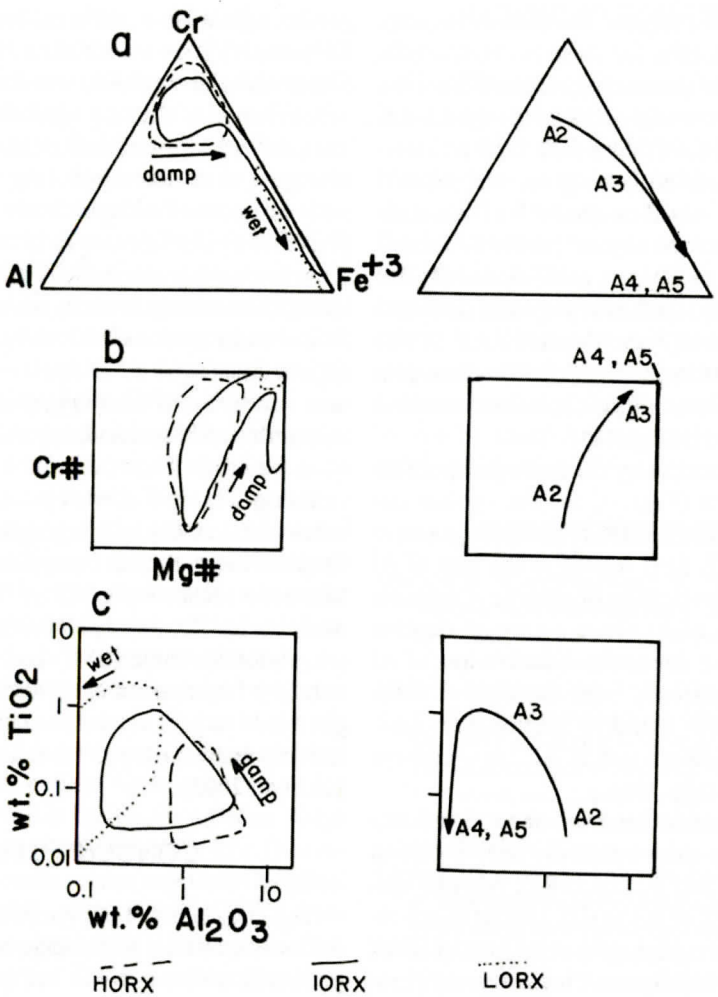

Figure 13. Chemical trends in spinel compositions related to retrograde metamorphic events. a. Cr-Al-Fe+3 trends (data from Fig. 6). Initial hydration (damp) results in loss of Al from A2 to A3 associations is related to formation of chlorite at the expense of chromite to form chromian magnetite. Then loss of Cr during continued hydration produces magnetite in A3 -A5 associations. b. Loss of Mg and Al during retrograde metamorphism (data from Fig. 10). Initial hydration results in an increase in Cr# (Cr# = Cr/Cr+Al) and a decrease in Mg# (Mg# = Mg/Mg+Fe+2) related to Mg and Al loss during formation of chlorite. c. Increase in Ti with decreases in Al during progressive hydration from A2 to A3 associations. Subsequent loss of Ti in A4 and A5 is related to formation of low temperature end member magnetite during serpentinization. Fields are for spinels from high olivine (HORX), moderate olivine (IORX) and low olivine (LORX) rocks. A2 to A5 represent the upper amphibolite (A2) to lower amphibolite (A3) to greenschist facies (A4, A5).

serpentinites (Figs. 7b and 7c) of the low grade A4 and A5 metamorphic associations representing the final stages of Blue Ridge metamorphism (Fig.7c).

Chromite Petrotectonics

Core compositions of the most Al-rich Spruce Pine chromite grains formed with olivine rich assemblages (A1, A2 or the olivine-rich part of A3 assemblages and represent the best

hope of trying to decipher the ultimate heritage of igneous protoliths for these metaultramafic rocks. Cores of accessory chromites from the Spruce Pine ultramafic rocks have high Cr #'s, generally above 0.6 (Tables 4-6). Dick and Bullen (1984) identified three groups of Alpine-type peridotites based on the Cr # of chromian spinel. Spinels from abyssal peridotite formed at oceanic ridges (Type I of Dick and Bullen 1984) have Cr# < 0.60, while spinels from arc-related peridotites (Type III of Dick and Bullen 1984) are higher in Cr (Cr# > 0.60). Based on these criteria, Spruce Pine chromites resemble arc-related spinels (Fig. 12).

Most of the accessory chromite grains coexist with chlorite (Figs. 4, 5). The typical decrease in Al from the cores of chromite grains to the rim (Figs. 7, 8) is related to the loss of Al during the crystallization of chlorite. Compositional profiles of Al show a gradual decline from core to rim due to the diffusive loss of Al to chlorite. Apparently even the cores of chromite grains from hydrated assemblages (A3, A4, and A5) suffered loss of Al due to chlorite crystallization (Fig. 13a).

Spinels in peridotites from abyssal and arc-related settings show relatively little variation in Mg# (Dick and Bullen,1984). Abyssal spinels have Mg#'s of 0.8 to 0.6, similar to arc-related peridotites with Mg#'s of 0.75 to 0.5 (Dick and Bullen, 1984). Spruce Pine accessory chromites show slight zoning in Mg#'s from higher cores to lower rims (Fig. 9), but the magnitude of the zoning is less than the Cr# zoning. Arai and Ishimaru (2008) summarized peridotite chromite compositions from fore arc settings of SSZ and found these spinels had Cr#'s ranging from 0.40 to 0.80, slightly overlapping the range of spinels from the Dick and Bullen abyssal peridotites (Fig. 12). Core compositions of Spruce Pine accessory chromite grains have lower Mg#'s than spinels from arc-related peridotites, but there is some overlap (Fig. 12). Low Mg#'s result from the crystallization of Mg-rich silicates (talc, antigorite) in the lower grades of A3 and A4. Segregated chromites show similar patterns of Al and Mg zoning to accessory spinels (Figs.7 and 10).

Ti and Al in spinels can be used to distinguish magmatism in different tectonic settings Kamenetsky et al. (2001). The work of Kamenetsky et al. (2001) was based mainly on volcanic rocks, but they also identified spinel compositions for peridotites at convergent or divergent plate boundaries (Fig. 12). Ti contents of Spruce Pine spinels are generally low (Tables 4-6). An increase in Ti content is found with increasing magnetite component of the spinels, commonly in rocks with little or no olivine (lower grades of A3, A4, A5; e.g. Table 6). Increases in Ti in the Spruce Pine spinels is thus a measure of the changes in metamorphic mineral assemblages and, apparently, is unrelated to the original igneous protolith.

Using the least altered subgrains (Al-rich cores of accessory and segregated chromites), Spruce Pine chromite compositions suggest a subduction-related origin (Fig. 12) for the ultramafic rocks. The fact that the data plot in the suprasubduction zone (SSZ) and arc fields was noted by Raymond et al. (2003b). Such an origin would require a reassessment of Blue Ridge tectonic models (Raymond et al. 2003a; Swanson et al. 2005).

CONCLUSIONS

The spinels in the Spruce Pine metaultramafic rocks exhibit a wide range of compositions primarily related to the complex history of metamorphism and recrystallization since their emplacement into the crust. Early-formed, high grade aluminous, low Ti chromite compositions are preserved in chromite cores, whereas rims and recrystallized grains reflect retrograde metamorphism. The series of metamorphic events affecting the Cr-spinel bearing rocks resulted in lower Al, Mg, and Cr contents and higher Ti and Fe oxide phases. Early-formed chromite was recrystallized during the formation of chromian chlorite. Later formation of talc, amphibole, and serpentine accompanied further recrystallization of the spinels, reducing both Al and Cr contents, and ultimately Ti content. Magnetite is the stable spinel at the lowest grades. Spinel compositions show regular changes in response to the fluid-facilitated, retrograde metamorphism that affected all of the

Spruce Pine rocks. Initial recrystallization of chromite at temperatures in the 600° C to 1000° C range (consistent with metamorphic conditions in surrounding rocks (Adams and Trupe, 1997) accompanies the moderate hydration of the highest grade olivine+chromite±enstatite assemblage to form the chlorite and tremolite-bearing assemblages (Fig. 13). This hydration (depicted by the "damp" trend on Figure 13) produced chlorite at the expense of high Al chromite and produced chromite higher in Cr#, Fe, and Ti, but lower in Al. Continued cooling and more extensive hydration added amphibole (tremolite/magnesiocummingtonite/anthophyllite) and talc to the olivine-rich assemblage to form association A3 (Fig. 13). The chromite lost Al as the amount of hydration increased ("wet" trend on Figure 13). Extensive, low temperature (300-500° C) hydration of some rocks produced abundant antigorite and low-Al, low-Ti, low Mg spinels that are chromian magnetites or magnetites (associations A3 to A4 and A5, Fig. 14).

The higher Al, low Ti, low Cr number spinel cores record the earliest retrograde event (A2, Fig. 14) preserved in the history of Blue Ridge ultramafic rocks. If the higher-Al, low Ti chromites and chromite cores represent original products of igneous crystallization, their compositions are consistent with formation in ultramafic rocks formed above a subduction zone rather than those associated with the MOR environment. Yet the fact that the largely anhydrous, olivine-rich rocks seem to fit into a five-stage (A1 to A5, Fig. 3, Table 2) metamorphic history casts doubt on their utility in deciphering that premetamorphic history (e.g., Minarik et al. 2003). Knowledge of that history may be limited to what can be learned through petrotectonic analysis (e. g. Swanson et al. 2005).

The change in FeCr-spinel chemistry during metamorphism from eclogite or granulite facies to greenschist facies conditions parallels phase assemblage changes in the metaultramafic rocks. Consequently, those chemical changes in the spinels can be used along with other data to identify and characterize the metamorphic grades of geologic terranes containing metaultramafic rocks.

ACKNOWLEDGEMENTS

Electron microprobe analyses were done at the University of Georgia under the direction of Chris Fleisher. His help made this study possible. Support for the study was provided by the University of Georgia and the Department of Geology. Helpful reviews of a earlier version of this manuscript by Steve Barnes and Hugh Rollinson greatly improved this paper. More recently, Rich Warner, Jeff Chaumba and Frank Stapor reviewed the paper and their comments are incorporated in the current version. A timely review by Mark Adams is responsible for the timely publication of this paper.

REFERENCES CITED

Abbott, R. N., Jr., and Raymond, L. A., 1984. The Ashe metamorphic suite northwest North Carolina: Metamorphism and observations on geologic history. American Journal of Science, v. 284, p. 350-375.

Adams, M.G., Stewart, K.G., Trupe, C.H., and Willard, R.A., 1995. Tectonic significance of high-pressure metamorphic rocks and dextral strike-slip faulting along the Taconic suture,.*in*: J. P. Hibbard, C. R. van Stall, and P. A. Cawood, eds., Current Perspectives in the Appalachian-Caledonian Orogen. Geological Association of Canada Special Paper 41, p. 21-42.

Adams, M. G., and Trupe, C.H.,1997. Conditions and timing of metamorphism in the Blue Ridge thrust complex, northwestern North Carolina and eastern Tennessee. *in* K. G. Stewart, M. G. Adams, and C. H. Trupe, eds., Paleozoic Structure, Metamorphism, and the Tectonics of the Blue Ridge of Western North Carolina. Carolina Geological Society 1997 Field Trip Guidebook, p. 33-47.

Arai, S., and Ishimaru, S., 2008. Insights into petrological characteristics of the lithosphere of mantle wedge beneath arcs through peridotite xenoliths: a review, Journal of Petrology, v. 49, p. 665-695.

Barnes, S. J.,1998. Chromite in komatiites, I. Magmatic controls on crystallization and composition. Journal of Petrology, v. 39, p. 1689-1720.

Barnes, S.J., 2000. Chromite in komatiites, II. Modification during greenschist to mid-amphibolite facies metamorphism. Journal of Petrology, v. 41, p. 387-409.

Barnes, S. J., and Roeder, P. L., 2001. The range of spinel compositions in terrestrial mafic and ultramafic rocks. Journal of Petrology, v. 42, p. 2279-2302.

Berger, S., Cochrane, D., Simons, K., Savov, I., Ryan, J.G., Peterson, V.L., and Schijf, J., 2001. Insights from rare earth elements into the genesis of the Buck Creek complex and other Blue Ridge ultramafic bodies. Southeastern Geology, v. 40, p. 201-212.

Bliss, N. W., and MacLean, W. H., 1975. The paragenesis of zoned chromite from central Manitoba. Geochimica et Cosmochimica Acta, v. 39. p. 973-990.

Brobst, D.A.,1962. Geology of the Spruce Pine District, Avery, Mitchell, and Yancey Counties, North Carolina. U.S. Geological Survey Bulletin 1122-A.

Butler, J. R., 1972. Age of Paleozoic metamorphism in the Carolinas, Georgia, and Tennessee southern Appalachians. American Journal of Science, v. 272, p. 319-333. Carpenter, R.R., and Phyfer, D.W., 1969. Proposed origin for the alpine type ultramafics of the Appalachians. Geological Society of America Abstracts with Program, v. 1, p. 261-263.

Carpenter, R.R., and Phyfer, D.W., 1975. Olivine compositions from southern Appalachian ultramafics. Southeastern Geology, v. 16, p. 169-172.

Carpenter, R.R., and Chen, H. S., 1978. Petrology and bulk rock geochemistry of the Frank ultramafic body, Avery County, N. C. And associated other ultramafic rock bodies of the southern Appalachians. Southeastern Geology, v. 20, p. 21-25.

Carpenter, R. R., and Fletcher, J. S., 1979. Chromite paragenesis in alpine-type ultramafic rocks of the southern Appalachians. Southeastern Geology, v. 20, p. 161-172.

Conrad, S. G., Wilson, W. F., Allen, E. P., and Wright, T. J., 1963. Anthophyllite asbestos in North Carolina. North Carolina Division of Mineral Resources Bulletin 77, 66p.

Dick, H.J.B., and Bullen, T., 1984. Chromian spinel as a petrogenetic indicator in abyssal and alpine-type peridotites and spatially associated lavas. Contributions to Mineralogy and Petrology, v. 86, p. 54-76.

Evans, B. W., 1977. Metamorphism of Alpine peridotite and serpentine. Annual Reviews of Earth and Planetary Sciences, v. 5, p. 397-447.

Evans, B. W., and Frost, B.R., 1975. Chrome-spinel in progressive metamorphisms - a preliminary analysis. Geochimica et Cosmochimica Acta, v. 39. p. 959-972.

Evans, B. W., Ghiorso, M. S., Yang, H, and Medenbach, O., 2001. Thermodynamics of the amphiboles; anthophyllite-ferroanthophyllite and the ortho-clino phase loop. American Mineralogist, v. 86, p. 640-651.

Haggerty, S.E,.1991. Oxide mineralogy in the upper mantle, *in*: D. H. Lindsley., ed., Oxide Minerals: Petrologic and Magnetic Significance. Reviews in Mineralogy, v. 25, p. 355-416.

Hatcher, R, D., Jr., Hooper, R. J., Petty, S. M., and Willis, J.D., 1984. Structure and chemical petrology of three southern Appalachian mafic-ultramafic complexes and their bearing upon the tectonics of emplacement and origin of Appalachian ultramafic bodies. American Journal of Science, v. 284, p. 484-506.

Hatcher, R. D., Jr., Merschat A. J., and Thigpen, J. R., 2005. Blue Ridge primer, *in* R. D. Hatcher Jr., and A. J. Merschat, eds., Blue Ridge Geology Geotraverse East of the Great Smoky Mountains National Park, Western North Carolina. Carolina Geological Society Annual Field Trip Guide, p. 1-24.

Hatcher, R. D. Jr., Bream, B. R., and Merschat, A. J., 2007. Tectonic map of the southern Appalachians: A tale of three orogens and a complete Wilson cycle, *in* R. D. Hatcher, Jr., M. P. Carlson, J. H. McBride, and J. R. Martínez, eds., 4-D Framework of Continental Crust. Geological Society of America Memoir 200, p. 595-632.

Hoffman, M.A., and Walker, D.1978. Textural and chemical variations of olivine and chrome spinel in the east Dover ultramafic bodies, south-central Vermont. Geological Society of America Bulletin, v. 89, p. 699-710.Hunter, C. E., 1941. Fosteritic olivine deposits of North Carolina and Georgia. North Carolina Division of Mineral Resources Bulletin 41, 117p.

Hunter, C.E., Murdock, T.G., and McCarthy, G.R., 1942. Chromite deposits of North Carolina, and Georgia. North Carolina Division of Mineral Resources Bulletin 42, 39p.

Irvine, T.N., 1967. Chromian spinel as a petrogenetic indicator. Part 2., Petrologic applications. Canadian Journal of Earth Science, v. 4, p. 71-103.

Kamenetsky, V. S., Crawford, A. J., and Meffre, S., 2001. Factors controlling chemistry of magmatic spinel: an empirical study of associated olivine, Cr-spinel and melt inclusions from primitive rocks. Journal of Petrology, v. 42, p. 655-671.

Kulp, J. L., and Brobst, D. A., 1954. Notes on the dunite and geochemistry of vermiculite at the Day Book Dunite deposit, Yancey County, North Carolina. Economic Geology, v. 49, p. 211-220.

Larrabee, D.M., 1966. Map showing distribution of ultramafic and intrusive mafic rocks from northern New Jersey to eastern Alabama. U.S. Geological Survey Miscellaneous Geologic Investigation Map I-476, 1:500,000.

Lipin, B.R., 1984. Chromite from the Blue Ridge Province of North Carolina. American Journal of Science, v. 284, p. 507-529.

Leblanc, M., 1987. Chromite in oceanic arc environments: New Caledonia, *in*, C. W. Stowe, ed., Evolution of Chromium Ore Fields. Van Nostrand Reinhold Co., New York, p. 265-296.

McCormick, G.R., 1975. A chemical study of kämmererite, Day Book Body, Yancey County, North Carolina. American Mineralogist, v. 60, p. 924-927.

McSween, H.Y., Jr., and Hatcher, R.D., Jr., 1985. Ophiolites (?) Of the southern Appalachian Blue Ridge, *in,* N. E.Woodward, ed., Field Trips in the Southern Appalachians. Univ. Tennessee, Department of Geological Sciences Studies in Geology, v. 9, p. 144-170.

McSween, H. Y., Jr., Abbott, R.N., Jr., and Raymond, L.A.,1989. Metamorphic conditions in the Ashe metamorphic Suite, North Carolina Blue Ridge. Geology, v. 17, p. 1140-1143.

Medaris, L. G., Jr., 1975. Coexisting spinel and silicates in alpine peridotites of the granulite facies. Geochimica et Cosmochimica Acta, v. 39. p. 947-958.

Minarik, W. G., Gale, A.and Booker, C., 2003. Provenance of Appalachian ophiolite chromites using osmium iso-

topes. EOS, Transaction of the American Geophysical Union, v. 84, no. 46, p. 897, abstract # (V11E-G-04).

Misra, K.C., and Keller, F.B.,1978. Ultramafic bodies in the southern Appalachians: A review. American Journal of Science, v. 278, p. 389-418.

Misra, K. C., and Conte, J.A., 1991. Amphibolites of the Ashe and Alligator back Formations, North Carolina. Geological Society of America, v. 103, p. 737-750.

Murdock, T. G., and Hunter, C. E., 1946. The vermiculite deposits of North Carolina.North Carolina Division of Mineral Resources Bulletin 50, 44p.

O'Hanley, H.S., 1996. Serpentinites: Records of tectonic and petrologic history. Oxford Monographs on Geology and Geophysics 34.

Page, F.Z., Essene, E. J., and Mukasa, S.B., 2003. Prograde and retorgrade history of eclogites from the astern Blue Ridge, North Carolina, USA. Journal of Metamorphic Geology, v. 21, p. 685-698.

Page, F.Z., Essene, E. J., and Mukasa, S.B., 2005. Quartz exsolution in clinopyroxene is not proof of ultrahigh pressures: Evidence from eclogites from the Eastern Blue Ridge, Southern Appalachians, U. S. A. American Mineralogist, v. 90, p. 1092-1099.

Pratt, J.H., and Lewis, J.V., 1905. Corundum and the Peridotites of North Carolina. North Carolina Division of Mineral Resources Bulletin 1, 440 p.

Raymond, L.A., 1995. Petrology: The Study of Igneous, Sedimentary and Metamorphic Rocks. W.C. Brown, Dubuque, Iowa.

Raymond, L. A.,1998. Geology of the Blue Ridge belt of northwestern North Carolina, *in* H. H. Mills, E. A. Cowan, K. C. Seramur, L. A. Raymond, J. B. Allison, and L. L. Acker, eds., Deposits and Landforms on the Piedmont Slopes of Roan, Rich, and Snake Mountains, Northwestern North Carolina and Northeastern Tennessee. Southern Friends of the Pleistocene 1998 Field Trip Guidebook, p. 1-8.

Raymond, L. A. 2002. Petrology: The Study of Igneous, Sedimentary and Metamorphic Rocks, 2nd ed.). W. C. Brown, Dubuque, Iowa.

Raymond, L. A., and Abbott, R. N., 1997. Petrology and tectonic significance of ultramafic rocks near the Grandfather Mountain Window in the Blue Ridge belt, Toe Terrane, western Piedmont zone, North Carolina, *in* P K. G. Stewart, M. G. Adams, and C. H. Trupe eds., Paleozoic Structure, Metamorphism, and the tectonics of the Blue Ridge of Western North Carolina. Carolina Geological Society 1997 Field Trip Guidebook, p. 87-101.

Raymond, L. A., Love, A., and McCarter, R., 2001. Petrology of the Hoots ultramafic body, Blue Ridge Belt, northwestern North Carolina. Southeastern Geology, v. 40, p. 149-162.

Raymond, L. A., and Allan, J.F., 2001. Spinel compositions as clues to the origin and tectonic significance of metadunite bodies in the Blue Ridge Belt of the Southern Appalachian Orogen. Geological Society of America Abstracts with Program, v. 33, p. A-227.

Raymond, L. A., Swanson, S. E., Allan, J.F., and Love, A.B., 2003a. Cr-Spinel compositions, metadunite petrology, and the petrotectonic history of the Blue Ridge ophiolites, southern Appalachian Orogen, USA, *in* Y. Dilek, and P. T. Bobinson, eds., Ophiolites in Earth History. Geological Society Special Publication 218, p. 253-277.

Raymond, L. A., Love, A.B., and Swanson, S.E. 2003b. Challenges presented by the Ashe Metamorphic Suite for reconstructing the tectonic history of the western North Carolina section of the Southern Appalachian Orogen. Geological Society of America Abstracts with Program, v. 35, p. 20.

Roeder, P. L., 1994. Chromite: From the fiery rain of chondrules to the Kilauea Iki lava lake. Canadian Mineralogist, v. 32, p. 729-746.

Sack, R.O., and Ghiorvso, M.S., 1991. Chromite as a petrogenetic indicator, *in* D. H. Lindsley, ed., Oxide minerals: Petrologic and magnetic significance. Reviews in Mineralogy, v. 25, p. 827-847.

Sharpe, R D., 1979. Petrology, geochemistry, and metamorphic history of the Henson Creek dunite, Mitchell County, North Carolina. M.S.Thesis, University of Georgia.

Spear,F.S., 1993. Metamorphic Phase Equilibria and Pressure-Temperature-Time Path. Mineralogical Society of America, Washington, D.C.

Stewart, K.G., Adams, M.G., and Trupe, C.H. 1997. Paleozoic structural evolution of the Blue Ridge thrust complex, western North Carolina, *in* K. G. Stewart, M. G. Adams, and C. H. Trupe eds., Paleozoic Structure, Metamorphism, and the Tectonics of the Blue Ridge of Western North Carolina. Carolina Geological Society 1997 Field Trip Guidebook, p. 21-31.

Swanson, S., E.,1980. Petrology of the Rich Mountain ultramafic bodies and associated rocks, Watauga County, North Carolina. Southeastern Geology, v. 21, p. 209-225.

Swanson, S., E.,1981. Mineralogy and petrology of the Day Book dunite and associated rocks, western North Carolina: Southeastern Geology, v. 22, p. 53-77.

Swanson, S., E., 1995, Alteration and metamorphism of ultramafic rocks in the Blue Ridge of Georgia, North Carolina, and Virginia. Geological Society of America Abstracts with Program, v. 27, p. 91.

Swanson, S., E., 1997, Mineral compositions from ultramafic rocks from the Spruce Pine Thrust Sheet, Western North Carolina. Geological Society of America Abstracts with Program, v. 29, p. 72.

Swanson, S., E., 2001, Ultramafic rocks of the Spruce Pine area, western North Carolina: a sensitive guide to fluid migration and metamorphism: Southeastern Geology, v. 40, p. 163-182.

Swanson, S., E. Naney, M. T., and Sturnick, M. A., 1985. Polyphase metamorphism in the Blue Ridge of western North Carolina: Evidence from the Day Book dunite. Geological Society of America Abstracts with Program, v. 17, p. 138.

Swanson, S. E., Raymond, L. A., Warner, R. D., Ryan, J., Yurkovich, S., and Petersen, V., 2005, Petrotectonics of mafic and ultramafic rocks in the Blue Ridge terranes of western North Carolina and northern Georgia, *in* R. D. Hatcher, Jr., and A. J. Merschat, eds., Blue Ridge Geology Geotraverse East of the Great Smoky Mountains National Park, Western North Carolina. Carolina Geological Society 2005 Field Trip Guidebook, p. 73-90.

Swanson, S., E., Warner, R. D., and Raymond, L. A., 2007, All enstatite is not created equal: a tale of orthopyroxene in metadunites of the eastern Blue Ridge of North Carolina and Georgia. Geological Society of America Abstracts with Program, v. 39, p. 27.

Tien, P., 1977. Carbonate minerals from a dunite mine, Yancey County, North Carolina. Geological Society of America Abstracts with Program, v. 9, p. 190.

Trommsdorff, V., and Evans, B. W., 1974. Alpine metamorphism of peridotitic rocks. Schweizerische Mineralogische und Petrographische Mitteilungen, v. 54, p. 333-352.

Trupe, C.H., Stewart, K.G., Adams, M.G., Waters, C.L., Miller, B.V., and Hewitt, L.K. 2003. The Burnsville fault: Evidence for the timing and kinematics of southern Appalachian Acadian dextral transform tectonics. Geological Society of America Bulletin v. 115, p. 1365-1376.

Turner, A. V. Swanson, S. E, and Roden, M. F., 1998. Mineralogical and geochemical comparison of two Native American soapstone quarries. Geological Society of America Abstracts with Program, v. 30, p. 17.

Ulmer, G.C., 1974. Alteration of chromite during serpentinization in the Pennsylvania-Maryland district. American Mineralogist, v. 59, p. 1236-1241.

Warner, R.D., 2001. Mineralogy and petrology of metaultramafic rocks at Buck Creek, North Carolina. Southeastern Geology, v. 40, p. 183-200.

Warters, C.L., Hewitt, L.K., Stewart, K.G., and Miller, B.V. 2000. Tectonothermal evolution of the Ashe Metamorphic Suite south of the Grandfather Mountain Window, NC. Geological Society of America Abstracts with Program, v. 32, p. A-81.

Willard, R.A., and Adams, M.G., 1994. Newly discovered eclogite in the southern Appalachian orogen, northwestern North Carolina. Earth and Planetary Science Letters, v. 123, p. 61-70.

ERATTA, VOL 47, NO. 2: THE HOLOCENE DEPOSITIONAL HISTORY OF THOUSAND ACRE MARSH (GEORGETOWN COUNTY, SC, USA) FROM CORRELATION OF GROUND PENETRATING RADAR WITH SUBSURFACE STRATIGRAPHY

A. SPRINGER

Department of Geological Sciences
University of South Carolina
Columbia, SC 29208
aspringer@geol.sc.edu

CAMELIA KNAPP

Department of Geological Sciences
University of South Carolina
Columbia, SC 29208

PAUL T. GAYES

Center for Marine and Wetland Studies
Department of Marine Science
Coastal Carolina University
Conway, SC 29526

LEONARD R. GARDNER

Department of Geological Sciences
University of South Carolina
Columbia, SC 29208

Page 98. Figure 3. Delete "**see figure 3"**
Page 100. Figure 8 is missing. See Below.

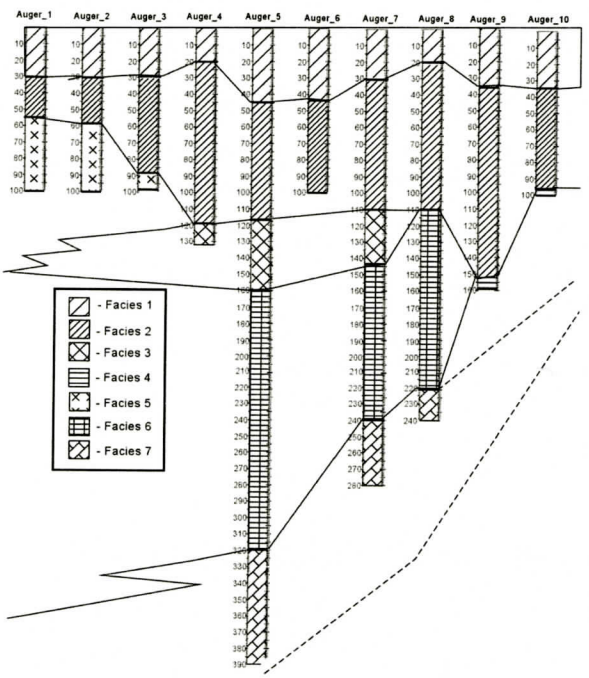

Figure 8. Lithology of auger cores from field and lab analyses.